Comparison of Continuous and Discontinuous Modelling for Computational Rock Mechanics

by

Therese Scheldt

This thesis has been submitted

to

Department of Geology and Mineral Resources Engineering
Norwegian University of Science and Technology

in partial fulfilment of the requirements for
the Norwegian academic degree

DOKTOR INGENIØR

December 2002

URN:NBN:no-3362

URN:NBN:no-3362

Abstract

Computational rock mechanics becomes more and more popular. New programs are constantly under development, and the modelling process has become a natural part of the planning process for many caverns and tunnels, as well as for the mining and petroleum industry.

There are two main categories of numerical methods in rock mechanics: Continuous modelling, where the rock mass is treated as a continuous medium and only a limited number of discontinuities may be included, and discontinuous modelling, where the rock mass is modelled as a system of individual blocks interacting along their boundaries.

When to use continuous modelling in preference to discontinuous modelling and vice versa, is an important question that has been discussed for a long time.

For this purpose, in this work continuous and discontinuous modelling is applied in order to analyze the stability of the Gjøvik Olympic Mountain Hall. The large span cavern (62m) was built in connection with the XVII Winter Olympic Games 1994 at Lillehammer, and is a unique case study because of the large amount of available input data from a comprehensive stress and deformation monitoring program carried out during and after the excavation, as well as thorough pre-investigations. Phase^2, a two-dimensional non-linear finite element program, and the Discontinuous Deformation Analysis (DDA) are used as representative tools for continuous and discontinuous modelling, respectively. DDA is both a theory and a computer program. The modelling procedure is similar to the distinct element modelling, while it more closely parallels the finite element method with respect to: i) Minimizing the total potential energy to establish equilibrium equations, ii) Choosing displacements as unknowns of the simultaneous equations and iii) Adding stiffness, mass and loading submatrices to the coefficient matrix of the simultaneous equation.

In general, the decision to use either continuous or discontinuous modelling should be based on data from the geological field mapping process. Mapping techniques which remove subjectivity from the results, for example scanline/area mapping or semi-automatic mapping, are recommended. If the rock mass is basically free of discontinuities, or if the discontinuities are very closely spaced in comparison to the dimensions of the problem to be analysed, continuous modelling is preferable. If large deformations including slip, rotation and separation are dominant, as for rock slope stability problems, discontinuous modelling may be selected. If the problem

to be analysed cannot be classified within one of the two groups, the quality of required input parameters and the purpose of the modelling should be taken into consideration.

For underground hard rock problems as the Gjøvik Olympic Mountain Hall, continuous modelling is strongly recommended. Today's mapping techniques are not good enough to give satisfactory information about the required and most crucial input for discontinuous modelling, namely the joint pattern, and the process for implementation of measured discontinuities into a numerical model is based on too many approximations. In addition, the discontinuous modelling process is very time consuming. A fast and high capacity computer is required.

Crucial input parameters for continuous modelling are strength and deformability parameters of the rock mass, and estimation of these parameters is dependent on the selected failure criterion, usually either Mohr-Coulomb or Hoek-Brown.

The magnitude of in-situ stresses, particularly the horizontal stresses, may have crucial influence on the general stability, and independent of whether continuous or discontinuous modelling is selected, in-situ stress measurements are strongly recommended in order to estimate a reasonably correct stress level for the problem to be analysed.

It is very difficult to estimate reliable input parameters for numerical modelling and a critical evaluation of the analysis results is absolutely recommended. Thus, analysis results should be considered as valuable additional input to field observations, in-situ and laboratory measurements, and experience rather than a precise answer for the given problem.

Acknowledgements

This work is carried out as a part of the Strategic Institute Program “Computational Mechanics in Civil Engineering” (CMC), and funded by a scholarship from the Norwegian Research Council and by teaching assistance at the Department of Geology and Mineral Resources Engineering, NTNU.

I am grateful to the following individuals for their support and assistance:

Professor Arne Myrvang, my supervisor (Department of Geology and Mineral Resources Engineering), for introducing me to the field of rock mechanics and for valuable recommendations along the way.

Professor Ming Lu, my co-supervisor (SINTEF and Department of Geology and Mineral Resources Engineering) for taking the initiative to this work as a part of the CMC project. His expertise and experience on numerical modelling have been invaluable and sources to inspiration and many discussions of great value, and his enthusiasm and thoughtful guidance were of great encouragement.

Professor Yuzo Ohnishi, Graduate School of Engineering Systems, Kyoto University, Japan, for inviting me to Kyoto University for six months, and for hosting and good advising during my stay.

Senior Manager Dr.Eng. Takeshi Sasaki, Kajima Corporations, Japan and Ph.D. Student Jianhong Wu, Kyoto University, Japan, for good advices concerning improvements and modifications in DDA.

Friends and colleagues at the Department of Geology and Mineral Resources Engineering, especially Anne-Irene Johannessen for sketching some of the figures and Kristin Holmøy for several useful discussions.

Eivind Grøv and his colleagues at O.T. Blindheim AS. Their inspiration during my project and diploma work in 1998 is a contributing factor to this work.

I also want to express my thanks to The Norwegian Rock Mechanics Group (NBG), The Norwegian Tunneling Association (NFF), Det Norske Veritas (DNV), Moss Høiere Allmenskoles Fond and Sasakawafondet for scholarships in connection with my stay at Kyoto University. Finally, I want to thank my parents for support and encouragement through many years.

URN:NBN:no-3362

Abstract I
Acknowledgements III

CHAPTER 1 Introduction 1

1.1 General 1
1.2 Scope of work 2
1.3 Thesis Organization 2

CHAPTER 2 Review of Numerical Methods in Rock Mechanics 5

2.1 Introduction 5
2.2 Finite Element Method 6
2.2.1 Introduction 6
2.2.2 Finite Elements 7
2.2.3 Shape Functions 8
2.2.4 Coordinate Transformation 9
2.2.5 Strain Displacement Relations 11
2.2.6 Stress Strain Relations 12
2.2.7 Local Stiffness Matrix 12
2.2.8 Global Stiffness Matrix 13
2.2.9 Some Relevant FEM Computer Programs 14
2.3 Boundary Element Method (BEM) 14
2.4 Discrete Element Method (DEM) 15
2.4.1 Introduction 15
2.4.2 The Concept of the Discrete Element Method 16
2.4.3 Some Relevant DEM Computer Programs 17
2.5 Summary 17

CHAPTER 3 Existing Mapping Techniques for Discontinuities 19

3.1 Introduction 19
3.2 Discontinuities 21
3.3 Discontinuity Data Collection 23
3.3.1 Introduction 23
3.3.2 Borehole Sampling 23
3.3.3 Measurements at Exposed Rock Face 27
3.3.4 Geotechnical Logging Chart 36
3.3.5 Geophysical Techniques 37
3.3.6 Semi-automatic Mapping 38
3.4 Application of Statistical Analysis 41
3.4.1 Poisson Process 43

3.4.2 The Central Limit Theorem 43
3.4.3 Sampling Bias and Mean Orientation 44
3.5 Implementation in modelling 45
3.6 Summary 46

CHAPTER 4 Theory of the Discontinuous Deformation Analysis 49

4.1 Introduction 49
4.2 Basic Theory 50
4.2.1 Block Deformations and Displacement Variables 50
4.2.2 Simultaneous Equilibrium Equations 53
4.2.3 Strain Energy Pe and Stiffness Matrix of Blocks 54
4.2.4 Displacements Constraints 56
4.2.5 Point Loading 59
4.2.6 Volume Loading 60
4.2.7 Initial Stress 62
4.2.8 Block System Kinematics 64
4.3 Summary 70

CHAPTER 5 Discontinuous Modelling -
DDA and Gjøvik Olympic Mountain Hall 71

5.1 Introduction 71
5.2 DDA as a Representative Tool for Discontinuous Modelling 72
5.3 Review of Existing Computer Programs Based on the DDA Method 72
5.3.1 DDA Programs 74
5.3.2 The Kyoto Version 77
5.3.3 Latest Developments in DDA 79
5.4 Gjøvik Olympic Mountain Hall 81
5.5 Geology 81
5.6 Discontinuous Modelling 82
5.6.1 Implementing measured discontinuities in a numerical model 83
5.6.2 In-situ Stresses and Boundary Conditions 92
5.6.3 Intact and Jointed Rock Parameters 92
5.6.4 Stage Excavation 92
5.7 Analysis Results and Discussion of Results 93
5.8 Strengths and Limitations of Discontinuous Modelling with DDA 97
5.9 Summary 99

CHAPTER 6 Continuous Modelling - Phase^2 and Gjøvik Olympic Mountain Hall 101

6.1 Introduction 101
6.2 Phase^2 102
6.3 Continuous modelling 103
6.3.1 Implementing Measured Strength Parameters in Modelling 103
6.3.2 In-situ Rock Stress 112
6.3.3 Finite Element Mesh, Boundary Conditions and Construction Sequence 112
6.4 Analysis Results and Discussion of Results 114
6.4.1 Mohr-Coulomb Analyses 115
6.4.2 Hoek-Brown Analyses 120
6.4.3 Comparison of Analysis Results and Field Measurements 122
6.5 Strengths and Limitations of Continuous Modelling with Phase^2 123
6.6 Summary 123

CHAPTER 7 Conclusions and Practical Guidelines for Numerical Modelling 127

7.1 Conclusions 127
7.1.1 Continuous modelling 127
7.1.2 Discontinuous modelling 128
7.1.3 Final Conclusions 129
7.2 Practical Guidelines for Numerical Modelling 130

References 135

URN:NBN:no-3362

CHAPTER 1 *Introduction*

1.1 General

This thesis is a part of the Norwegian Research Council Strategic Institute Program (SIP) “Computational Mechanics in Civil Engineering”, carried out by SINTEF Civil and Environmental Engineering and counterparts at The Norwegian University of Science and Technology, running from 1998 - 2002.

Due to rapid advancements in computer technology, the use of numerical methods in engineering sciences has become more and more popular during the last four decades. The field of rock mechanics is no exception, and the most commonly used programs are based on the finite element method (FEM) and the discrete element method (DEM), continuous and discontinuous modelling, respectively. In continuous models, the rock mass is modelled as a continuous medium and only a limited number of discontinuities may be included. On the other hand, in discontinuous models the rock mass is modelled as a system of individual blocks interacting along their boundaries.

The procedure of numerical modelling may be summarized in the following points: i) Definition of analysis type, material type and parameters, and in-situ stresses, ii) Pre-processing, iii) Model verification and calibration, iv) Computation, v) Post-processing and finally vi) Analysis of results and reporting.

Typical rock mechanics problems to be solved by using numerical modelling are stress and displacement calculations around underground openings, rock slope stability, and water and heat flow. A common problem for numerical modelling, independent of method and software, is to obtain reliable input parameters.

1.2 Scope of work

Numerical modelling has for some considerable time been used as a practical tool for stability analysis and design studies for both soft and hard rocks within the field of rock engineering. However, there are several elements of uncertainty connected to this use, and the experiences are mixed.

Thus, the background and motivation for this study is to produce some guidelines and recommendations for the practical use of numerical modelling in rock engineering. The results from this work may hopefully increase the average level of knowledge about this topic, and contribute to its rational use. Main questions to be answered are: i) When to use continuous modelling in preference to discontinuous modelling, ii) How to estimate required and reliable input parameters for the model, and iii) How to implement discontinuities measured by geological field mapping into a numerical model.

The study is limited to underground projects, and parallel analyses of a large span cavern are carried out with continuous and discontinuous software, represented by Phase^2 and the Discontinuous Deformation Analysis (DDA), respectively.

Gjøvik Olympic Mountain Hall, built for the XVIII Winter Olympic Games at Lillehammer, is a unique case study because of the large amount of available input data from a comprehensive stress and deformation monitoring program carried out during and after the excavation. In addition, thorough pre-investigations consisting of geological field mapping, mapping in nearby caverns, core drilling, refraction seismics and seismic tomography, in situ stress measurements and laboratory testing were carried out.

1.3 Thesis Organization

Chapter 2 gives a review of numerical methods in rock mechanics with emphasis on the Finite Element Method and the Discrete Element Method, which is an important part of this work. Basic theory and some relevant computer programs are presented.

The biggest challenge for discontinuous modelling is to create a reliable model of the jointed rock mass. Thus, Chapter 3 gives a summary of existing mapping techniques for discontinuities. It starts with a definition of discontinuities and is followed by a discussion of the validity of the different methods: Borehole sampling, measurements at exposed rock faces, geophysical techniques and so-called semi-automatic methods. Finally, how to implement the measured discontinuities into a numerical model is mentioned. This is exampled and discussed more detailed in Chapter 5.

DDA, which is both a theory and a program, is selected as a representative tool for the discontinuous modelling. The modelling procedure is similar to the distinct element modelling procedure, while it more closely parallels the finite element method with respect to: i) Minimizing the total potential energy to establish equilibrium equations, ii) Choosing displacements as unknowns of the simultaneous equations and iii) Adding stiffness, mass and loading submatrices to the coefficient matrix of the simultaneous equation. The theory of DDA is presented in Chapter 4, which is mainly based on Shi (1989), while Chapter 5 demonstrates the practical use of DDA. The author has mainly made use of programs based on the Kyoto-20020206 source code. In order to increase the applicability and to make the program more user friendly, some improvements and modifications are carried out in the programs. A total of 5 different joint models are generated, analysed and discussed.

Chapter 6 focuses on continuous modelling. Phase^2 is selected as a representative tool and more than 50 analyses are carried out in terms of Mohr-Coulomb and Hoek-Brown failure criteria. Different horizontal in-situ stress situations and strength parameter models are presented. The analysis results are compared with field measurements.

Chapter 7 includes conclusions, and some practical guidelines for the numerical modelling process based on the experience from this study are presented.

URN:NBN:no-3362

CHAPTER 2

Review of Numerical Methods in Rock Mechanics

2.1 Introduction

In empirical methods, analysis is based purely on experience and comparison, while analytical analysis is based on calculation or modelling. Numerical methods belong to the latter group and consist mainly of continuous and discontinuous models. In continuous models the rock mass is modelled as a continuous medium, where only a limited number of discontinuities is included, and in discontinuous models the rock mass is modelled as a system of individual blocks interacting along their boundaries.

A rock mass differs from other engineering materials by widespread contents of discontinuities. Whether or not these discontinuities should be allowed for, is a primary decision to be made for a particular rock mechanics problem. If the answer is yes, the further question is how, explicitly or implicitly? According to Brown (1987) the fundamental consideration in selecting a model, is the relation between the discontinuity spacing and the size of the problem (the domain).

Figure 2.1 shows a general classification of numerical methods for rock mass analysis. There are mainly two categories of numerical methods in rock mechanics: Continuous models and discontinuous models.

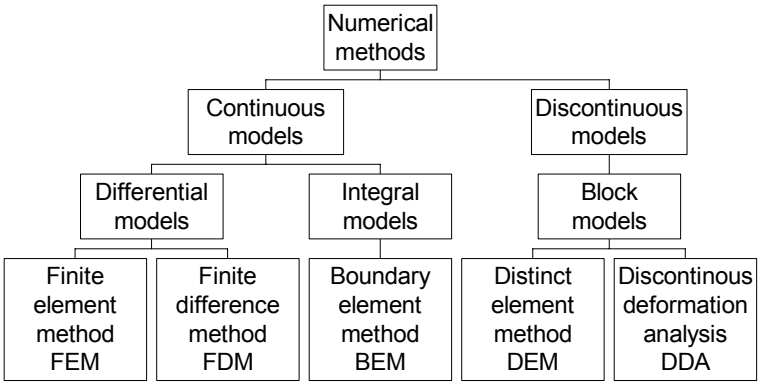

FIGURE 2.1 Numerical methods for rock mass analysis

Three of the methods mentioned above, have mainly been used in rock mechanics to model the response of rock masses to loading and unloading. These are the Finite Element Method FEM (FEM), the Boundary Element Method (BEM) and the Discrete Element Method (DEM), which covers the Distinct Element Method and the Discontinuous Deformation Analysis. All methods are approximate methods, i.e. they give an approximate solution to the problem, as described below.

2.2 Finite Element Method

2.2.1 Introduction

The finite element method had its birth in the aerospace industry in the early 1950s and was first presented in a publication by Turner (Pande et al, 1990). The method has developed to become the most popular numerical method in many branches of engineering, and the field of rock mechanics is no exception.

The fundamental concept of the finite element method is to divide the defined problem (the domain) into smaller elements, which are connected to each other at certain points called nodes. The elements may have various shapes, and the total number of elements and nodes to be used in a particularly problem will depend on

the desired accuracy of the results, costs of computing and of course the effort in data preparation. Theoretically, each of the elements may have different material properties. Stresses are calculated at one or more points inside each of the elements while displacements are arranged at the nodes.

The theory of the finite element method is briefly summarized below. Recommended literature of the topic are Zienkiewicz (1973) and Ottosen and Petersson (1992).

2.2.2 Finite Elements

As mentioned above, elements can have various shapes: One-dimensional elements, two-dimensional elements and three-dimensional elements.
The one-dimensional element is the simplest one. This has a cross-sectional area, which can vary along the length but is generally shown schematically as a line segment. Element families used to model a two-dimensional domain are the triangle and the quadrilateral. The most common three-dimensional elements are variations of the two-dimensional elements, the tetrahedron and the parallelepiped. The linear elements in each family have straight sides, while the higher order elements can have either straight or curved sides or both. In certain cases it is required to model curved boundaries, and this is made possible by the addition of nodes along the edges.

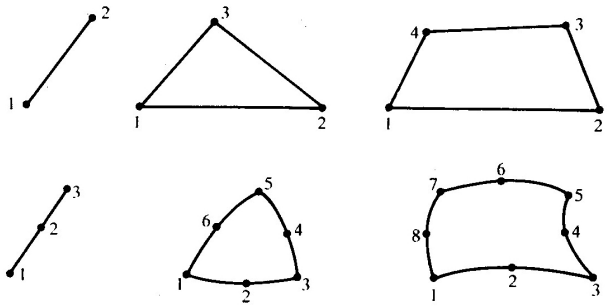

FIGURE 2.2 Shape and node position of some elements used in two-dimensional analysis (from Pande et al, 1990)

2.2.3 Shape Functions

Displacements at any points within the element are related to the displacements of the nodes through so-called shape functions. As an example, the displacements (u, v) at any point within a quadrilateral element mapped into a 2 x 2 unit square element are represented by equation [2-1]:

$$\begin{bmatrix} u \\ v \end{bmatrix} = \begin{bmatrix} N_1 & 0 & N_2 & 0 & N_3 & 0 & N_4 & 0 \\ 0 & N_1 & 0 & N_2 & 0 & N_3 & 0 & N_4 \end{bmatrix} \begin{bmatrix} u_1 \\ v_1 \\ u_2 \\ v_2 \\ u_3 \\ v_3 \\ u_4 \\ v_4 \end{bmatrix} \quad \textbf{[2-1]}$$

where (u_1, v_1,....u_4, v_4) = δ^T are nodal displacements and N_1, N_2, N_3 and N_4 are shape functions associated to the nodes 1, 2, 3 and 4 respectively. The shape functions N_i (i = 1, 2,.....4) are functions of the coordinates of the points whose displacements are required. Thus [2-2]:

$$N_i = N_i\{\xi, \eta\} \quad \textbf{[2-2]}$$

When coordinates of the ith node are substituted, then N_i should be equal to 1 and $N_{j\neq i}$ should be equal to zero. For most commonly used elements, shape functions are determined by intuition and inspection. For higher-order elements, fare more formal mathematical procedures to derive shape functions are necessary. For a three-dimensional case, the technique is the same, except that the number of displacement parameters and shape functions is increased.

2.2.4 Coordinate Transformation

The aim of coordinate transformation is to simplify integration of certain quantities required for calculation of stiffness matrices of the elements. The integration of a function, for example f (ξ, η, ζ) in the three-dimensional case, is carried out over the limits -1 to +1 [2-3]:

$$F = \int_{-1}^{1}\int_{-1}^{1}\int_{-1}^{1} f(\xi, \eta, \zeta)\, d\xi\, d\eta\, d\zeta \qquad \textbf{[2-3]}$$

The shape functions of elements are used for coordinate transformation and the coordinates of a point within the element (x, y, z) are given by [2-4] - [2-6]:

$$x = \sum_{i=1}^{n} N_i x_i \qquad \textbf{[2-4]}$$

$$y = \sum_{i=1}^{n} N_i y_i \qquad \textbf{[2-5]}$$

$$z = \sum_{i=1}^{n} N_i z_i \qquad \textbf{[2-6]}$$

where x_i, y_i and z_i are the coordinates of the nodes of the elements and n is the number of nodes.

An infinitesimal volume of the element, dV, is given by [2-7]:

$$dV = dxdydz = |J|d\xi d\eta d\zeta \qquad \textbf{[2-7]}$$

where the Jacobian matrix is 3 x 3 [2-8]:

$$|J| = \begin{bmatrix} \frac{dx}{d\xi} & \frac{\partial y}{\partial \xi} & \frac{\partial z}{\partial \xi} \\ \frac{\partial x}{\partial \eta} & \frac{\partial y}{\partial \eta} & \frac{\partial z}{\partial \eta} \\ \frac{\partial x}{\partial \zeta} & \frac{\partial y}{\partial \zeta} & \frac{\partial z}{\partial \zeta} \end{bmatrix} \qquad \textbf{[2-8]}$$

The derivatives of the shape functions with respect to a global cartesian coordinate system are given as [2-9]:

$$\begin{bmatrix} \frac{\partial N_i}{\partial x} \\ \frac{\partial N_i}{\partial y} \\ \frac{\partial N_i}{\partial z} \end{bmatrix} = |J|^{-1} \begin{bmatrix} \frac{\partial N_i}{\partial \xi} \\ \frac{\partial N_i}{\partial \eta} \\ \frac{\partial N_i}{\partial \zeta} \end{bmatrix} \qquad \textbf{[2-9]}$$

2.2.5 Strain Displacement Relations

Strains can be written as a function of nodal displacements. For a two-dimensional plane strain (ε_z=0) case the relation between strain and displacement becomes [2-10]:

$$\varepsilon = \begin{bmatrix} \varepsilon_x \\ \varepsilon_y \\ \gamma_{xy} \\ \varepsilon_z \end{bmatrix} = B \begin{bmatrix} u_1 \\ v_1 \\ u_2 \\ v_2 \\ \cdots \\ u_n \\ v_n \end{bmatrix} = B\delta \qquad \textbf{[2-10]}$$

Matrix B consists of n submatrices, B_i (i = 0,....n), of size (4 x 2) whose elements are [2-11]:

$$B_i = \begin{bmatrix} \frac{\partial N_i}{\partial x} & 0 \\ 0 & \frac{\partial N_i}{\partial y} \\ \frac{\partial N_i}{\partial y} & \frac{\partial N_i}{\partial x} \\ 0 & 0 \end{bmatrix} \qquad \textbf{[2-11]}$$

2.2.6 Stress Strain Relations

These relations very often refer to the crux of the finite element analysis and can be expressed as [2-12]:

$$\Delta\sigma = D_T \Delta\varepsilon \qquad \textbf{[2-12]}$$

$\sigma = (\sigma_x, \sigma_y, \tau_{xy}, \sigma_z)^T$ is the vector of stress components and ε represents corresponding components of strains. D_T is a square matrix which are constant in the elastic case. On the other hand, in case of a general nonlinear behaviour, stress or strain is path dependent.

2.2.7 Local Stiffness Matrix

The stiffness equations are derived from the "principle of virtual work" which states that if a structure is in equilibrium, the work done by the external forces through a set of virtual displacements (δ^*) must be equal the work done by internal stresses through the virtual strains (ε^*) caused by the applied virtual displacements [2-13]:

$$(\delta^*)^T F^e = \int_v (\varepsilon^*)^T \sigma dV = \int_v (B\delta^*)^T \sigma dV \qquad \textbf{[2-13]}$$

Then the final result is [2-14]:

$$K^e \Delta\delta^e = \Delta R^e \qquad \textbf{[2-14]}$$

where R^e are the nodal forces along x, y and z axes while δ^e are the associated nodal displacements. The element stiffness matrix K^e is given by [2-15]:

$$K^e = \int_v B^T D_T B dV \qquad \textbf{[2-15]}$$

The size of the various matrices are shown in the following table:

TABLE 2.1. Size of various matrices

	Two-dimensional case	Three-dimensional case
B	4 x 2n	6 x 3n
D_T	4 x 4	6 x 6
B^T	2n x 4	3n x 6
K^e	2n x 2n	3n x 3n

2.2.8 Global Stiffness Matrix

The global stiffness matrix is formed by adding up the stiffness matrices of all elements. The size will correspond to the total number of degrees of freedom for the whole mesh, for example twice the number of nodes in two-dimensional problems and three times the number of nodes in three-dimensional problems. Nodes which are common for different elements, will have contributions to the stiffness from all those elements. The global stiffness equation is given as [2-16]:

$$K\Delta\delta = \Delta R \qquad \textbf{[2-16]}$$

where $\Delta\delta$ is the unknown vector of increments of nodal displacements due to an increment of force ΔR. If the material behaviour is linear elastic equation [2-16] can be written as: $K\delta = R$.

2.2.9 Some Relevant FEM Computer Programs

The DIsplacement ANAlyser Finite Element program (DIANA) is a multipurpose finite element package with special emphasis on advanced linear and nonlinear structural engineering and flow applications. It is owned, maintained and developed by TNO Building and Construction Research in the Netherlands. The program has full 2D and 3D modelling capabilities and a library of 200 elements to meet different kinds of modelling requirements (www.diana.nl, 2001).

Phase^2 is a two-dimensional non-linear finite element program for calculating stresses and displacements around underground openings, and it can be used to solve a wide range of mining and civil engineering problems (Rocscience, 1998-2001). Application of Phase^2 is demonstrated in Chapter 6, Finite Element Modelling.

Another program is ABAQUS developed by Hibbitt, Karlsson and Sorensen, Inc., USA. This program is designed for linear as well as non-linear, three dimensional stress analysis of structures. Normally, joints, rock bolts or other elastic or plastic details are not described distinctly, but through the behaviour of an element (Handbook No.2, 2001)

A fourth program is ANSYS, where both linear and non-linear stress analyses can be performed for isotropic as well as non-isotropic material properties. The program includes a special concrete/rock element which can be used to analyse crack patterns in concrete and rock. It is a powerful tool for determining displacements, stresses, forces, temperature distribution, magnetic fields, fluid flow, pressure distribution and other important design issues (Handbook No.2, 2001).

2.3 Boundary Element Method (BEM)

In this method only the surface of the rock mass to be analysed needs to be discretized. For two-dimensional cases line elements at the boundary represent the problem, while for three-dimensional cases surface elements are required. Compared to FEM, the data preparation is relatively simple, unless there are number of layers of different materials. The matrices of equations are not banded and symmetric as for FEM, but they are fully populated. Even though the number of equations

to be solved is considerably reduced, computation time does not reduce in the same manner.

A well known program used in the past is BESOL (Boundary Element Solutions), which can compute stresses, strains and displacements around excavations of any shape in a variety of geological settings.

But there are problems which are not ideally suited for either the boundary element method or the finite element method. In such cases a combination of finite element and boundary element methods seems to be the most efficient, which is also discussed in Beer and Watson (1992). Basically two approaches to coupling boundary element and finite element regions exist, and the choice of coupling method depends mainly on the software available for the implementation of coupling - if boundary element capabilities are to be added to a finite element program or finite element capabilities to a boundary element program.

2.4 Discrete Element Method (DEM)

2.4.1 Introduction

The Discrete Element Method is based on treating the rock mass as a discontinuous rather than a continuous medium as in the case of FEM and BEM. In the sixties Goodman et al introduced joint elements, and since then numerical computations with geological discontinuities have been developed and applied extensively to rock mechanics (Shi, 1989). The DEM family consists of the Distinct Element Method and the Discontinuous Deformation Analysis. The former was introduced by Cundall. In 1971 he was the first to apply this type of analysis to a stack of rectangular blocks simulating a rock slope (Franklin, 1989). The Discontinuous Deformation Analysis (DDA), whose primary objective was to solve large displacements and deformations of discontinuous materials and block structures, was developed by Shi in the late 1980's. Both methods make use of the equations of dynamic motion which are solved at finite points in time. Meanwhile, there are significant differences related to the formulations and solutions of the equilibrium equations and numerical contacts. The Distinct Element Method's approach is based on Newtons 2. law, $F = ma$, while DDA uses $F = Kd$, inverted to $d = K^{-1}F$, i.e. that the methods are respectively force and displacement based.

2.4.2 The Concept of the Discrete Element Method

In the Discrete Element Method, each body communicates with surrounding bodies via boundary contacts which may change as a function of time (Pande et al, 1990). Distinct from the Finite Element Method, where node points very often are common for various elements, nodes are not common for more than one element in the Discrete Element Method. Generally, the rock mass is represented by elements and the rock joints by the space between the elements. There is no restriction on contacts between elements and nodes may interact with nodes or edges.

The Discrete Element Method can treat nonlinearities caused by large displacement, rotation, slip, separation and material behaviour. The general form of dynamic equilibrium equations for each discrete element is given by [2-17]:

$$[M]\{\ddot{u}\} + [C]\{\dot{u}\} + [K]\{u\} = \{f\} \qquad \textbf{[2-17]}$$

where {u} is the displacement and the superscript dots refers to the derivative with respect on time, [M], [C] and [K] are respectively mass, damping and stiffness matrix while {f} is the applied load.

The interaction of the discrete elements is computed from the relative motion of contacting elements which generate incremental interaction forces. By employing a penalty function approach, the forces are given by [2-18]:

$$\Delta f_n = k_n \Delta u_n + \beta k_n \Delta \dot{u}_n \qquad \textbf{[2-18]}$$

$$\Delta f_s = k_s \Delta u_s + \beta k_s \Delta \dot{u}_s$$

where β is the stiffness proportional damping parameter necessary to damp element-element vibration, Δf_n and Δf_s are incremental components of the contact force normal and tangential to the element-element interaction, k_n and k_s are the

interelement normal and shear stiffness, while Δu_n and Δu_s are the normal and tangential incremental components of the relative displacements between the discrete elements.

The motion of each element is computed by time with changes in loads due to gravity, interaction, etc. and leads to generating of strain rates within the elements from which the incremental stresses are calculated. Depending on the constitutive behaviour of the material, the element will experience elastic or viscoplastic behaviour or may undergo fracturing. A detailed description of the discrete element method is given by Pande et al. (1990).

2.4.3 Some Relevant DEM Computer Programs

UDEC (Universal Distinct Element Code) is a distinct element code and probably the most commonly used program of the DEM family. It is two dimensional and written specifically for analyses of mechanical, thermal and hydrologic behaviour of jointed rock masses. The program requires that the body to be modelled is divided into blocks which are separated from neighboring blocks by joints or interfaces. The blocks may be either rigid or deformable. Deformable blocks are subdivided into triangular finite difference zones for calculation of internal stress and strain. Interfaces may be considered to conform to a standard Mohr-Coulomb slip condition or a displacement weakening model. The boundary conditions can either be static or dynamic, and the blocks are allowed to interact with one another across the interfaces. The program uses an explicit solution procedure, which means that unknown values of the variables relating to each element in the problem are calculated from known values in that element and its immediate neighbors. The equations related to these values are solved locally for each time step. An extension of UDEC is 3DEC (3-Dimensional Distinct Element Code) which allows modelling in three-dimensions (www.itascacg.com, 2002).

DDA (Discontinuous Deformation Analysis) is also a member of the Discrete Element Method family and solves the equilibrium equations in the same manner as the matrix analysis of structures in the finite element method. Chapter 4 presents the theory of DDA and in Chapter 5 some analyses are carried out by using the program.

2.5 Summary

Empirical methods are based on experience, while analytical ones are based on calculation or modelling. Numerical methods belong to the last named and the litera-

ture distinguishes between continuous and discontinuous models, of which the first is most commonly used. In this case, the rock mass is handled as a continuous medium and only a limited number of joints is taken into consideration. On the other hand, in a discontinuous model the purpose for the user is to recreate a model of the actual project, which includes the discontinuities of the rock mass. Thus, the input parameters for the different models are varying. For example, determination of the joint patterns is of crucial significance for discontinuous models, while the choice of material model is most important for continuous models.

The Finite Element Method (FEM) and the Boundary Element Method (BEM) belong to the continuous models, while the Distinct Element Method and the Discontinuous Deformation Analysis (DDA) are members of the discontinuous family. The Distinct Element Method is based on Newtons 2. law $F = ma$, while DDA uses $F = Kd$, inverted to $d = K^{-1}F$, which is the same as for the Finite Element Method. It can be said that the methods are respectively force- and displacement- based.

In Boundary Element Methods only the surface of the rock mass to be analysed needs to be discretized, and they differ from the FEM by the fact that approximations only occur on the boundary of the problem domain since the solution inside the domain always will satisfy the equations of equilibrium and compatibility exactly (Pande et al, 1990).

CHAPTER 3

Existing Mapping Techniques for Discontinuities

3.1 Introduction

In general, the rock mass classifies as a complex building material. Intact rock is intersected by smaller and bigger discontinuities caused by a variety of geological mechanisms acting in sequences or simultaneously or by human activities. The discontinuities vary from a few centimeters to structures which are up to hundreds of kilometres. They have geometrical and mechanical features, which define the total behaviour of the rock mass, and different types of discontinuities may have completely different engineering significance. The discontinuity properties that have greatest influence at the design stage have been listed by Priest (1993) as follows:

1. Orientation
2. Size
3. Frequency
4. Surface geometry
5. Genetic type
6. Infill material

Thorough understanding of the geometrical, mechanical and hydrological properties of the discontinuities is therefore essential.

There are three ways in which a discontinuity can be formed (Anderson, 1995): One by pulling apart and two by shearing (Figure 3.1):

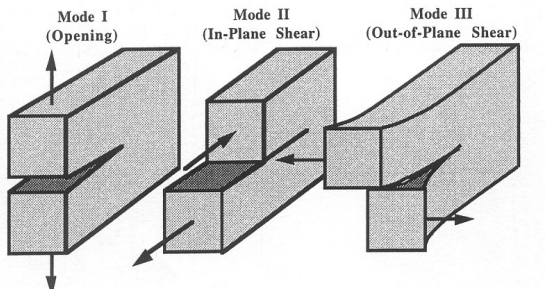

FIGURE 3.1 Mode I, II and III (from Anderson, 1995)

The first mentioned, are discontinuities which have simply been opened and are termed joints. The latter are those in which there have been some lateral movement and are termed shear zones or faults. Stress conditions necessary to induce the three possible types of rock failure are shown in Figure 3.2.

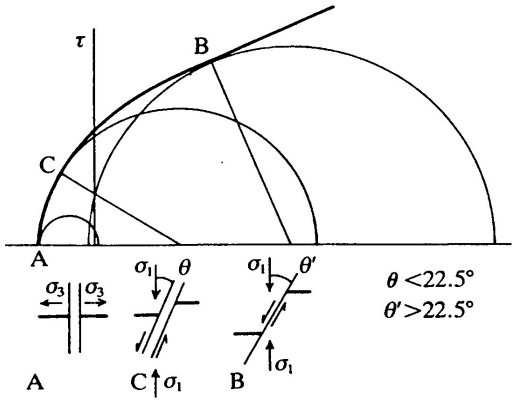

FIGURE 3.2 Stress conditions necessary to induce rock failure - tensile (type A), shear (type B) and hybrid tensile-shear (type C) fractures (from ICS, 2001)

Whether these discontinuities should be allowed for or not, is a primary decision to be made for a particular rock mechanics problem. If the answer is yes, a further question is how, explicitly as in discontinuous modelling or implicitly as in continuous modelling. The detailing level of the discontinuity mapping is usually dependent on the specific engineering problem, but as a rule the mapping process includes three steps: i) Field work - collection of measurement data, ii) Quantification and analysis of geometric parameters and iii) Documentation and presentation of the mapping results, either in report form or as a geometric model.

3.2 Discontinuities

The term discontinuity gives no information concerning the age, geometry or mode of origin of the discontinuities. Thus, in many cases it can be helpful to distinguish between natural discontinuities, which are of geological origin, and artificial discontinuities which are created from human activities such as drilling, blasting and excavation.

Discontinuity is the general term for any mechanical discontinuity in a rock mass having zero or low tensile strength. It is the collective term for most types of joints, weak bedding planes, weak schistocity planes, weakness zones and faults (ISRM, 1978). According to ISRM (1978), the following parameters are needed to completely describe discontinuities and rock masses (Figure 3.3):

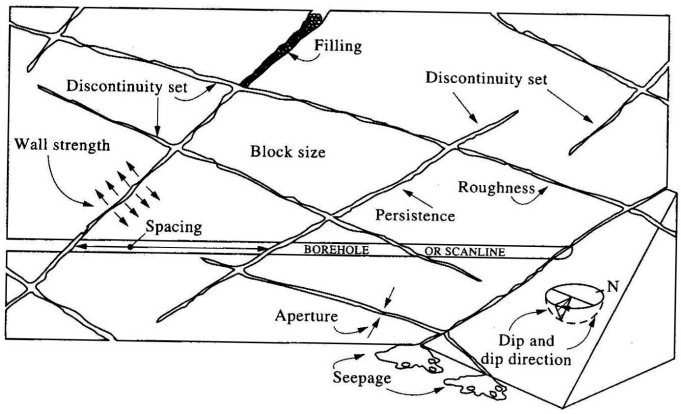

FIGURE 3.3 Primary geometrical properties of discontinuities in rock (from Hudson, 1997)

1. Orientation - attitude of discontinuity in space
2. Spacing - distance between adjacent discontinuities
3. Persistence - discontinuity trace length as observed in an exposure
4. Roughness - inherent surface roughness and waviness related to the mean plane of a discontinuity
5. Wall strength - equivalent compression strength of the adjacent rock walls of discontinuity
6. Aperture - perpendicular distance between adjacent rock walls of a discontinuity, in which the intervening space is air or water filled
7. Filling - material that separates the adjacent rock walls of a discontinuity and that is usually weaker than the parent rock
8. Seepage - waterflow and free moisture visible in individual discontinuities or in the rock mass as a whole
9. Number of sets - the number of joint sets comprising the intersecting joint systems
10. Block size - rock block dimensions resulting from the mutual orientation of intersecting joint sets, and resulting from the spacing of individual sets

Five of the parameters (orientation, spacing, persistence, number of sets and block size) can be considered to be “geometric” parameters. They will define the geometry of the rock mass structure, the size and shape of rock blocks formed and the nature of intact rock bridges in the rock mass. The other five parameters (roughness aperture, filling, wall strength and seepage) may be regarded as “strength” parameters as the properties described can affect the shear strength and stiffness of the discontinuity when undergoing loading.

The two main groups of discontinuities are joints and weakness zones. When joints extend over long distances (> 30 m), they are referred to as major joints. ISRM (1978) uses the following definition “Joint is a discontinuity plane of natural origin along, which it has been no visible displacement”. This is the same definition used by many geologists. Weakness zones are parts of the rock mass where mechanical properties are significantly lower than those of the surrounding rock mass. Weakness zones can be faults, shear zones, thrust zones, weak mineral layers, etc.

3.3 Discontinuity Data Collection

3.3.1 Introduction

A great deal of information about the discontinuities can be obtained by field mapping and measurement of a rock exposure. Depending on the exposures and their orientation, geologists may be able to get enough data to make an estimate of the two- or three-dimensional situation. Unfortunately, it is often the case that no such exposures are available before the construction of a particular project. In this case borehole cores from the drilling process, scans using borehole televiewers or indirect methods, such as geophysical techniques are sources of information.

There is no standardized method for mapping and measuring rock structure geometry. A lot of work has been devoted to providing techniques for measurement and the results differ widely.

3.3.2 Borehole Sampling

A wide range of equipment is available to provide drill cores with diameters between 20 and 150 mm from depths of several hundred meters or more for a variety of rock types. The primary purpose is generally to identify variations in rock types and mineral composition, but the borehole cores also provide information about discontinuities in a relatively undisturbed sample of rock material. Furthermore, the rock cores are very important in connection with laboratory testing to determine mechanical properties of the rock. After drilling, the borehole is often used for water leakage tests (Lugeon tests). Combined, this gives a base for an estimate of the rock mass conditions.

3.3.2.1 Guidelines on Core Logging

In order to avoid too much subjectivity in connection with the logging process, different guidelines are worked out and presented in the literature. Two major sources of information are identified: The driller's report and the core itself.

The driller's report should contain details about the drilling progress, loss of core, bit replacements, colour and loss of drilling fluid, standing water levels and other factors relating to drilling operation (Priest, 1993). Further, it is important to handle the borehole cores with extreme care to minimize the disruption of existing frac-

tures and the creation of new ones. According to Priest (1993), the logging process should be carried out in the following sequence:

1. Remove any protective covering from the core
2. Label the core by borehole number and depth, then photograph it in colour
3. Log the core
4. Remove label, and seal samples for laboratory testing
5. Conduct point load testing or other destructive on-situ tests
6. Split the core for further photography if required
7. Reassemble and re-seal the core as far as possible for future reference

3.3.2.2 Rock Quality Designation

The Rock Quality Designation developed by Deere, is probably the most common method for characterizing the degree of jointing of a borehole core. RQD is defined as the percentage of core bits longer than 0.1 m along the measured length of the core expressed mathematically,

$$RQD = 100 \sum_{i=1}^{n} \frac{x_i}{L} \% \qquad \textbf{[3-1]}$$

where xi = spacing greater than 0.1 m, and n is the number of these intersected by a borehole core or scanline of length L.

TABLE 3.1 Classification of the RQD

Term	RQD
very poor	<25
poor	25-50
fair	50-75
good	75-90
excellent	90-100

RQD is included as a parameter for block size or jointing density in different classification systems for rock masses (Q-system and RMR).

3.3.2.3 Strengths and Limitations of Borehole Sampling

A particular strength with borehole sampling is that it is relatively easy to gather information on discontinuities and at the same time get hold of specimens for laboratory testing. But borehole sampling is relatively expensive. Further, this method is an essentially one-dimensional sample through the three-dimensional rock mass, and therefore the method has obviously limitations.

For example, a borehole core will provide a tremendous amount of information on the occurrence and frequency of discontinuities in the bore hole direction, but will provide little information on the lateral extent of the intersected discontinuities. This problem can of course be solved by using three boreholes in three different directions, but this is very often impossible because of both practical and economical restrictions. A second problem with borehole sampling is that the core can rotate during excavation, and establishment of the true orientation of the sampled discontinuities within the rock mass will in that case demand special sampling and analysis techniques. A third difficulty is that the core is usually of small diameter, which makes it almost impossible to measure the discontinuity size. Other problems can include lack of information in areas because of core loss. Further, filling material and gouge may be washed out from discontinuities, or extraneous matter can be deposited from drilling mud. Nevertheless, core drilling is an important engineering geology tool.

3.3.2.4 Borhole Televiewers

Borehole televiewers make it possible to provide a continuous and detail orientated image of the borehole walls using either acoustic or optic imaging systems, which means that it is possible to localize discontinuities and their orientation in relation to the actual borehole.

An acoustic televiewer (AKTV) produces an acoustic picture, which cover 360 ° of the borehole wall. A rotating piezoelectric unit transmits acoustical pulses, ultrasound, to the borehole wall at the same time as the probe slowly elevates. The amplitude and walking time of the reflected signal is registered digitally, and the result is shown as a picture of the borehole wall on a computer-screen. Roughness will affect both amplitude and walking time because of variations in reflectivity and borehole diameter. Joints which make angles with the borehole between 0 and 90 °, will be observed as a sine curve, while joints perpendicular the borehole will be seen as a horizontal line. By digitalizing the indicated occurrences, the strike, dip

and aperture of the joints can be estimated. In addition, joint frequency for the entire borehole or for defined zones can be defined. The picture is oriented by means of a set of accelerometers and a tri-axial magnetometer, which also can be used for registration of borehole deviation. The instrument can only be used in liquid-filled boreholes because of the acoustic coupling which is necessary for transferring an ultrasonic sound pulse. It can be difficult to distinguish between clean joints and bedding planes, for example in connection with quartz and limestone (Elvebakk and Rønning 2001).

The optical televiewer (OPTV) consists of a video camera which can be lowered down with a velocity of about 1 m/min in a borehole with a diameter of 70-160 mm. A continuous shot of the borehole wall is taken. One picture of each mm downwards the borehole is saved and the picture is divided in 360 or 720 pixels around the circumference, which gives very high resolution and the possibility to register joints with apertures of only 0.5 mm. Figure 3.4 shows the principle of an OPTV. Light emitting diodes (LED) emit small lights, which are reflected from the borehole wall to a hyperbolic mirror, which reflect the rays of light to a video camera. Strike, dip and aperture of the joints can be estimated, and joints and structures with an angle of intersection of 0 to 90 ° represented in the same way as for the AKTV, with sine curves. Orientation of the picture and borehole deviation are determined with accelerometers and a magnetometer. OPTVs can be used in both water filled and dry boreholes, but the former gives the best result. The water must be clear, so it is recommended to wait a little while after drilling before logging. An optical televiewer is a useful inspection tool for feasibility studies for tunnels and rock caverns and in some situations better than traditional core drilling (Rønning 2002).

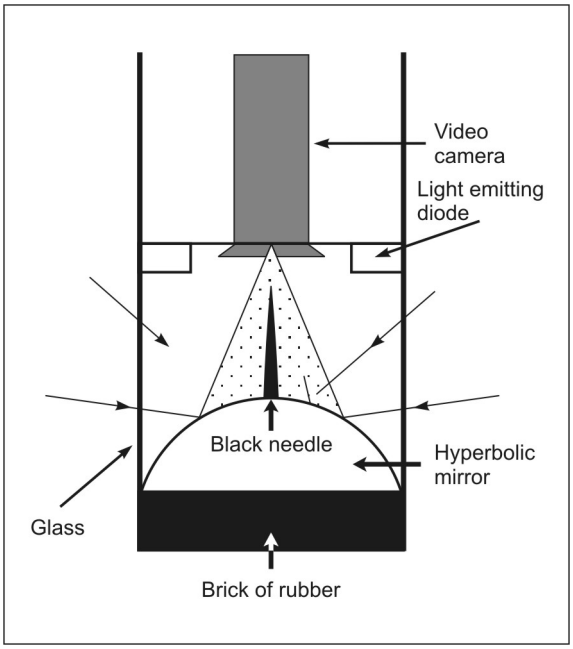

FIGURE 3.4 Principle drawing of an optical televiewer (after Rønning 2002)

3.3.3 Measurements at Exposed Rock Face

Measurements at exposed rock faces are favorable because it gives access to relatively large areas of rock, which enables direct measurement of discontinuity orientation, size and other geometrical features. Geological relations between the various discontinuity groups can also be observed. But disadvantages to this approach exist. An example is that the rock face is often remote from the area of interest and may be subject to blasting damage or degradiation by weathering and vegetation. In the same way as borehole sampling, skilled personnel are needed to take measurements, but equipment and labour costs are small compared to the first mentioned method.

Until the seventies, measurement at exposed surfaces were made in arbitrary, subjective ways derived from geological mapping techniques. This yielded little quantitative data of value for engineering design, so more rigorous statistical sampling and data processing methods have been adopted. Mapping techniques can be divided into three main classes (Villaecusa, 1991):

1. Spot mapping
2. Scanline mapping
3. Area mapping

3.3.3.1 Spot Mapping

This is a technique in which the observer selectively samples only those individual discontinuities that are considered important. Figure 3.5 showes an example of spot mapping. The actual discontinuities as observed in the exposure are shown to the left. The discontinuities depicted to the right are those that have been mapped because the mapping personnel have considered them important.

Thus, the value of the results obtained using spot mapping relies mainly on the judgement of the observer. The repeatability of this method is poor, especially cases when collecting discontinuity information for different engineering purposes. Use of this method is recommended only for preliminary investigations.

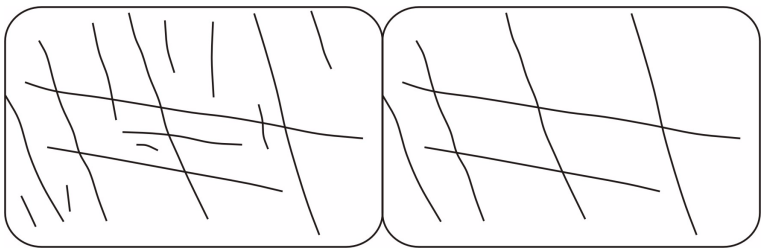

FIGURE 3.5 Spot mapping (after Villaecusa 1991)

3.3.3.2 Scanline Mapping

There is no universally accepted standard for scanline mapping. The purpose of the mapping technique is to involve and sample only those discontinuities that intersect a line set on the surface of the rock mass. Figure 3.6 illustrates the scanline mapping technique.

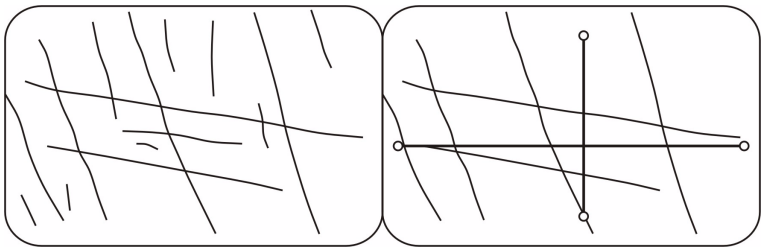

FIGURE 3.6 Scanline mapping (after Villaecusa, 1991)

According to Priest (1993) the following discontinuity parameters should be defined:

1. Intersection distance, d (m)
2. Dip direction (°)
3. Dip angle (°)
4. Semi-trace length (m) below or right of scan
5. Termination
6. Roughness
7. Curvature

Figure 3.7 shows an example of a blank scanline survey logging form.

SCANLINE SURVEY LOGGING FORM | Page | Of

Details of scanline:	**Details of rock face:**	Rock type .....
Label	Location	Excavation method .....
Trend	Dip direction	Condition of exposure
Plunge	Dip angle	
Trimming level .....m	Non-overhanging / Overhanging	Comments
Logged by	Height .....m	
Date logged	Width .....m	

Intersection distance d (m)	Dip Direction (Degrees)	Dip Angle (Degrees)	Semi-trace length *l* (m) above or left of scan	Semi-trace length *l* (m) below or right of scan	Termination I=1, A=2, O=3		Rough-ness *JRC* 1-20	Curv-ature 1-5	Comments (Refer to table of abbreviations and codes)

FIGURE 3.7 Scanline survey logging form (from Priest, 1993)

The scanlines are simply measuring tapes pinned with nails and wire to the rock face along its strike and line of maximum dip. The intention is to impose a linear sampling similar to that of a borehole. Further scanlines should be set up on a second rock face, approximately at right angles to the first, to minimize the sampling orientation bias. Location, orientation and condition of the rock face should be registered at the logging sheet together with the trend and plunge of each scanline. Deviations of the scanline, which are less than about 20 ° from a straight line have shown neglible influence on the sampling system and can be ignored (Priest, 1993). If the deviations are larger, the problem can be solved by splitting the scanline into so called sub-scanlines, and measuring the trend and plunge of each. Photographing of the rock face and scanline, including a scale and appropriate label before commencing the sampling process is recommended (Hudson & Priest, 1979). The length of the scanline is normally extended until a prerequisite number of observations is obtained. Priest (1993) suggests that between 150 and 350 discontinuities should be recorded. Savely (1972) found that at least 60 observations were required to stereo logically define a discontinuity set along a given sample line. Villaescusa (1991) indicates that at least 40 discontinuity observations are required per set to provide a statistical database of the discontinuity set characteristics.

Intersection distance, d, is the distance in metres, rounded to the nearest centimeter, along the scanline to the intersection point with the discontinuity. In cases, where the face is not planar it may be necessary to extrapolate some of the discontinuities to obtain this point. This process can sometimes produce an intersection distance that is out of the sequence, back down the scanline. Meanwhile, such intersections can be re-ordered prior to processing. The intersection distance on a given scanline provides a simple and unambiguous identification for any particular discontinuity in the sample (Priest, 1993). Sometimes it can be difficult to decide whether a given feature is a natural geological discontinuity, or a fracture introduced during blasting and excavation, but as a main rule only those features that form true mechanical breaks of geological origin should be measured. Instead of trying to measure discontinuities in broken or heavily fractured rock, and discontinuities across areas of the face that have been obscured by features as for example vegetation and scree, it should be concentrated on recording the extent of the broken, or obscured zone in addition to describe the nature of the zone.

Orientation is expressed in degrees, as the dip direction and dip angle of the discontinuity measured at the point of intersection with the scanline. If the discontinuity is poorly exposed at this point, it may be necessary to measure the orientation of an exposured surface on the discontinuity some distance from the scanline.

Semi-trace length, l, is the distance from the intersection point on the scanline to the end of the discontinuity trace, which can either be measured directly if the face is accessible, estimated by eye or scaled from the photograph of the rock face when it comes available. There will be two semi-trace lengths associated with each discontinuity: One above and one below a horizontal scanline, one to the left and one to the right of a scanline along the line of maximum dip of the face.

Termination. ISRM (1978) has proposed a termination index T_r which is defined as the percentage of the discontinuity ends terminating in rock (Σr) compared to the total number of terminations ($\Sigma r + \Sigma d + \Sigma x$). The latter is equal to twice the total sample since each trace has two ends [3-2]:

$$T_r = \frac{(\Sigma r) \times 100}{2(\text{no. of discontinuities observed})}\% \qquad \textbf{[3-2]}$$

Σr, Σd and Σx are discontinuities, which extend outside the exposure, discontinuities that terminate in rock in the exposure and those that terminate against other discontinuities in the exposure, respectively. A large value of T_r indicates that a large proportion of discontinuities terminate in intact rock, suggesting that the rock mass contains many intact rock bridges rather than being separated into discrete blocks (Priest, 1993).

Roughness here refers to surface irregularities with a wavelength less than about 100 mm. It can be expressed in terms of Barton's Joint Roughness Coefficient (JRC), and can be measured by taking an impression or profile of the surface, and then digitizing and quantifying the result in the form of a JRC value. For most practical purposes, it is sufficient to assess JRC visually by reference to the example profiles presented.

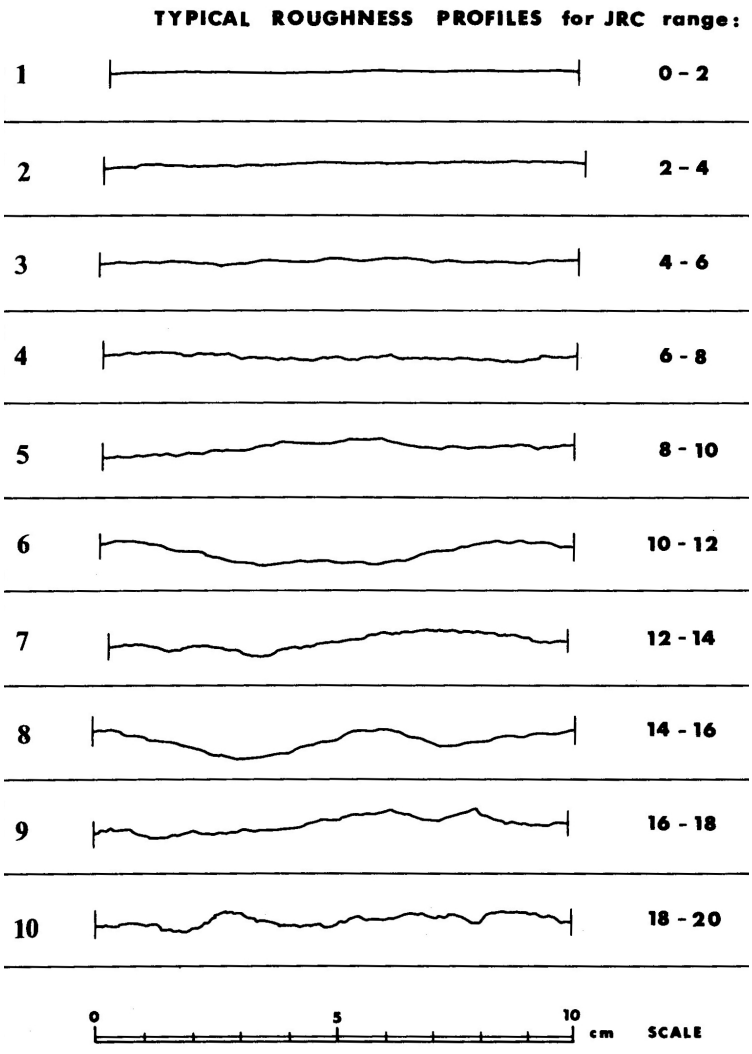

FIGURE 3.8 Roughness profiles and corresponding range of JRC values associated with each one (from ISRM 1978)

Curvature here refers to surface irregularities, with a wavelength greater than about 100 mm, and can be determined by measuring offsets at 100 mm intervals along a straight base line, and then digitizing and quantifying the resulting profile (ISRM, 1978). As with roughness it is often sufficient to assess the curvature visually. A five point scale ranging from 1 = planar to 5 = very curved is satisfactory for most purposes. Alternatively, initial letters of descriptive terms that are appropriate for a particular site, such as "stepped, "undulating" and "planar", can be adopted to provide a direct link with rock mass classification systems (Priest, 1993).

The comments column in Figure 3.7 are used to provide additional qualitative information about each discontinuity in abbreviated form, such as type of discontinuity, broken or obscured rock, nature of infill, aperture, water flow, slickensides and sample locations. In addition, it is noteworthy that the measured discontinuity frequency is expected to vary with the direction of the sampling line relative to the orientation of the discontinuities. Figure 3.9 and Figure 3.10 show variation in discontinuity frequency for a sampling line passing through one and two sets of discontinuities, respectively.

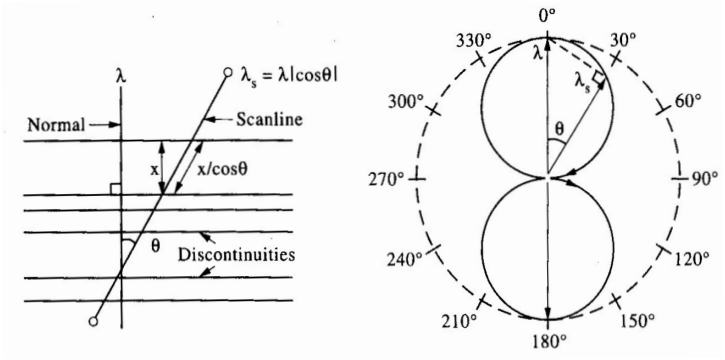

FIGURE 3.9 Variation in discontinuity frequency for a sampling line passing through a single set of discontinuities - two dimensional case (from Hudson, 1997)

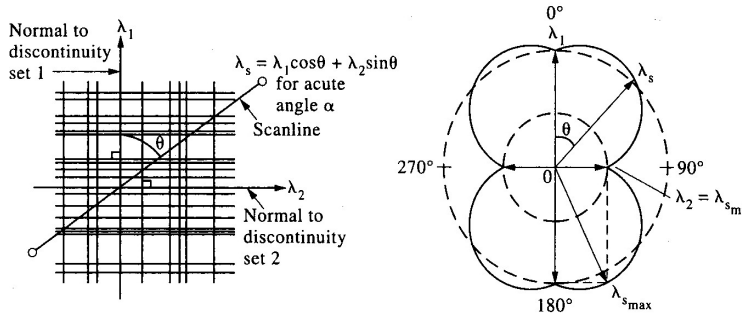

FIGURE 3.10 Variation in discontinuity frequency for a sampling line passing through two sets of discontinuities - two dimensional case (from Hudson, 1997)

3.3.3.3 Area Mapping

The preliminaries and measurement techniques are essentially the same as for scanline mapping, except that all discontinuities that have a portion of their trace length within a defined area of the rock surface are measured, rather than only those that intersect the scanline. Even if this approach reduces the sampling biases for orientation and size created by linear sampling, problems of discontinuity curtailment remain where the rock face is of limited extent.

The sampling area can be defined by setting up a rectangle of measuring tapes pinned to the rock face. In order to minimize the sampling bias effect, the area should be as large as possible such as each side of an edge line intersects between about 30 and 100 discontinuities. If possible, at least two areas of similar dimensions should be set up on adjacent rock faces of different, and preferably orthogonal orientations (Priest, 1993).

According to Pahl (1981) the method requires that three classes of discontinuities are measured:

1. Discontinuities that intersect the area, and have both ends visible in the area are said to be contained within the area.

2. Discontinuities that intersect the area, and have only one end visible in the area are said to dissect the window. The other end is obscured by extending beyond the limits of the area.
3. Discontinuities that intersect the window and have neither ends visible in the area are said to transect the window. Both ends are obscured by extending beyond the limits of the window.

For the purpose of estimating mean trace length, it is only necessary to count the numbers of discontinuities in each of the three classes. The method is best implemented by taking a colour photograph of the face, and then producing a large print. An appropriate area can then be drawn on a transparent overlay, and the discontinuity traces for each observed set can be traced off, using different colour for each set (Priest, 1993). This photographic area sampling method is relatively straightforward and simple, but it holds a number of disadvantages. First, it does not provide any information about discontinuity orientation, frequency, surface geometry or qualitative characteristics as described in the previous section. These properties must be sampled physically at the rock face. The area will usually contain a large number of relatively small discontinuities, which makes it difficult to keep track of which discontinuities that already have been measured, and rendering the process even more laborious than scanline mapping (Mathis, 1987). A second difficulty is that the method can be inaccurate if significant areas of the face are inaccessible, or obscured by loose rock or vegetation cover (Priest, 1993).

3.3.4 Geotechnical Logging Chart

As mentioned introductorily, there is no standardized method for mapping and measuring the rock structure geometry. Most people carry out field mapping using their own method, and have in time developed their own routines. For example, The Norwegian Geotechnical Institute has developed a geotechnical logging chart, which is used as a standard for field mapping underground, which also can be used for logging of drillcores and surface mapping.

In addition to the six Q-system parameters: Rock Quality Designation (RQD), joint set number (J_n), joint roughness number (J_r), joint alteration number (J_a), joint water reduction factor (J_w) and stress reduction factor (SRF), the joint frequency, joint spacing, joint roughness coefficient (JRC), joint wall strength (JCS), permeability, rock strength, rock stress, Schmidt hammer readings, volumetric joint count (J_v), joint length, joint roughness amplitudes, residual friction angle and joint orientation are registered. Incorporating all information in a PC-based spreadsheet, makes it possible to see the variation in the different parameters through the tunnel

or cavern (Bhasin, 1994). Figure 3.11 shows an example of a logging chart from NGI.

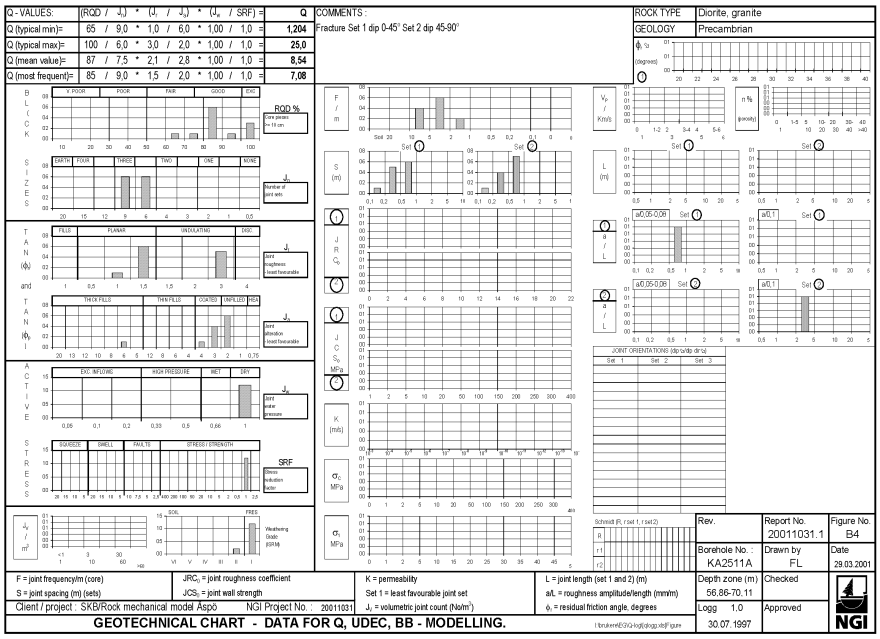

FIGURE 3.11 NGI's Geotechnical Logging Chart (from Grimstad, 2002)

3.3.5 Geophysical Techniques

Geophysical techniques can be used to measure various geophysical properties of the rock mass related to its lithological and geotechnical properties. Most of the methods can only measure discontinuities indirectly.

The main types of geophysical methods used in rock mass investigations are seismic refraction, seismic reflection, crosshole tomography, electric resistivity, electromagnetic radar, and magnetic and gravitational methods. Refraction seismic is most commonly used. If sub-surface investigations by core drilling or excavation of

exploratory adits or shafts are impossible because of e.g. high costs or access problems, refraction seismic can be carried out in order to give useful information about the degree of jointing and configurations of rock bedding.

3.3.6 Semi-automatic Mapping

During the last decades, new techniques and methods like digital photogrammetry, total geodetic station (TS) and laser scanner have been developed as an alternative to the traditional ones. According to Feng (2001) the advantages of these techniques compared with traditional methods are: i) The geometry of the joints are quantified semi-automatically in three dimensions, ii) Measurements are obtained without physically touching the rock face, iii) The accuracy of the measurements is improved comparing with the traditional methods, iv) Both quantitative and spatial analysis is possible and v) It offers a way to digitally record the rock surface in three dimensions, and in visual formats as a database for other applications.

With analytical photogrammetry, a pair of photo hard copies are used to create a stereographic view of the rock face by a stereographic plotter, or stereo comparator. Geometrical parameters of joints, such as orientation, spacing and trace length can then be determined by collecting coordinates of several target points. Digital photogrammetry, is based on the same principle but the procedure is simplified for the user since a computer with a proper software automatically estimates the orientation, spacing and trace length. Beer et al (1999) made use of this method in order to collect realistic input parameters for numerical simulations of a tunnel.

A typical TS instrument consists of four main components, an electronic distance measurement instrument (EDM), an electronic theodolite (ET), a data collector and an on-board microprocessor. Figure 3.12 shows the measuring principle of the TS. The EDM is used to measure the slope distance of a target point P, and the ET measures the horizontal and vertical angles of the point. From the measurements of angles and distances, the horizontal and vertical distances or the coordinate of the target point can be calculated with [3-3]. The results are stored in the data collector, and these raw data can be transferred to a computer for the use of any surveying related applications (Feng, 2001)

$$\left\{ \begin{array}{c} x = S\cos(VA)\cos(HA) \\ Y = S\cos(VA)\sin(HA) \\ Z = S\sin(VA) \end{array} \right\} \quad \text{[3-3]}$$

where S = slope distance, VA = vertical angle and HA = horizontal angle, which is determined with regard to true north, given by a compass or more accurately from measurements of control points with known geodetic coordinates.

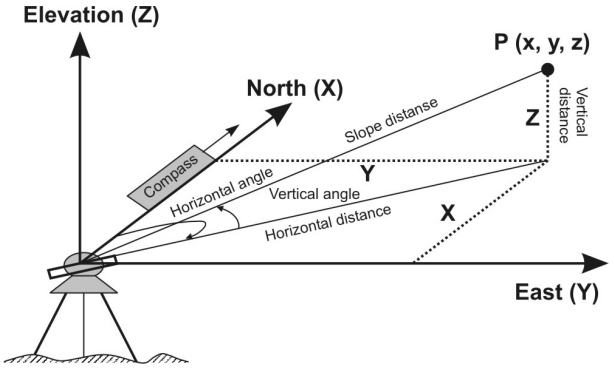

FIGURE 3.12 The measuring principle of the TS (from Feng, 2001)

Feng (2001) makes use of a Laser Radar (LARA) scanning system, which was initially developed for mobile robot navigation and inspection tasks, in order to quantify fracture geometry from exposed rock faces.

The mapping procedure by using the LARA system consist of four steps: i) Control surveying by the TS, ii) Scanning the rock faces by the LARA system, iii) Transforming the laser scanning data to the TS coordinate system and iv) Quantifying discontinuity geometry form the recorded scanning data. Figure 3.13 shows a picture of two major components of LARA: The single-point laser measuring system (the lower-left part), and the mechanical beam deflection system (the upper-left part).

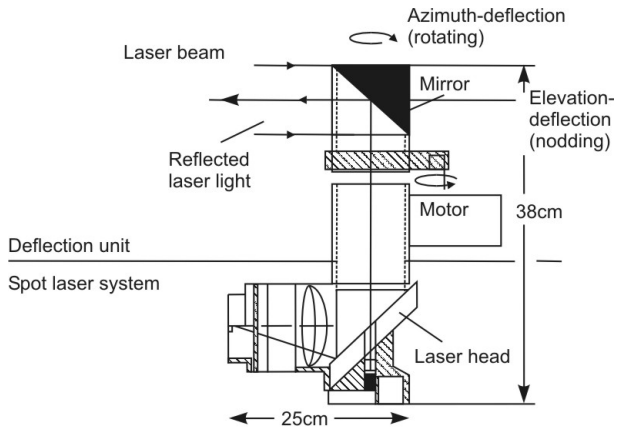

FIGURE 3.13 Major components of the LARA scanning system (from Feng, 2001)

The point-sensor laser measurement system comprises the laser head, the high frequency unit and the signal processing unit for data pre-processing. This part controls the procedure of emitting, receiving and processing of the laser beam. By using the dual frequency AMWC (amplitude-modulated, continuous-wave) method in conjunction with a coaxial transmitter/receiver design, both range and reflectance of a target point can be obtained, and high measurement accuracy (within mm-range) can be achieved. The mechanical beam deflection system consists of a special mirror, and a motor control unit. The mirror is used for deflecting the emitted laser beam generated from the laser head at the bottom, and then collecting the back-scattered laser light cone. The motor control unit controls the mirror to rotate

in the horizontal direction, and nod in the vertical direction, which can make a scanning field overview of 360 ° in azimuth and ± 30 ° in elevation (Feng, 2001).

According to Feng (2001), drawbacks with semi automatic methods are that 3-D measurements are difficult to extract by using image processing techniques: The laser scanner records all parts of a target area with a large amount of data, although only a few percent of the scanned data are needed for discontinuity mapping. For some scanners, the scanning speed is low for scanning the rock face, and it is not easy to filter out unusable information. Further, photogrammetry requires special photographic conditions to obtain a pair of photos for stereoscopic view mapping and some total station methods need a reflector to be put at each target points on the rock face, which cause problems with carrying out measurements on inaccessible or dangerous rock faces.

The use of semi automatic methods are still not widely used in rock mechanics, and the main reasons are probably high equipment costs and lack of knowledge about the methods.

3.4 Application of Statistical Analysis

Most of the methods discussed above are not sufficient for three dimensional characterization of the rock mass structure, and simple statistical techniques in data reduction, presentation and analysis are therefore helpful for estimating an engineering approximation of the jointed rock mass.

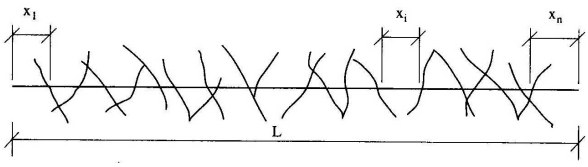

FIGURE 3.14 Sampling line (from Hudson and Harrison, 1997)

Figure 3.14 illustrates a sampling line through a rock mass, which intersects a number of discontinuities. The length of the sampling line is L metres, and the number

of discontinuities it intersects is N. Thus the frequency and mean spacing are given by:

$$\lambda = \frac{N}{L} \; [m^{-1}] \qquad \text{[3-4]}$$

$$\bar{x} = \frac{L}{M} \; [m]$$

Hudson and Harrison (1997), have found that the Poisson process and the associated negative exponential spacing distribution are good theoretical models for discontinuity occurrence (Figure 3.15).

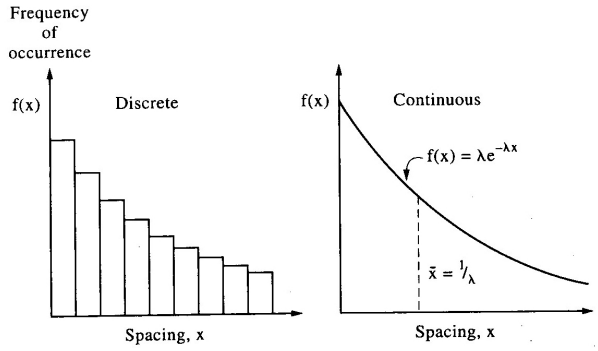

FIGURE 3.15 The negative exponential distribution of discontinuity spacing values (from Hudson and Harrison, 1997)

In case of a infinite number of spacing values and infinitely small class intervals, the histogram tends to be a continuous curve, which can be expressed as the probability density function,

$$f(x) = \lambda e^{-\lambda x} \quad \text{[3-5]}$$

where the mean of the distribution is $1/\lambda$, which is the same as the standard deviation.

3.4.1 Poisson Process

By using the Poisson process, the probability that *k* discontinuities will intersect a scanline interval of length *x* can be determined by:

$$P(k, x) = \frac{e^{-\lambda x}(\lambda x)^k}{k!} \quad \text{[3-6]}$$

3.4.2 The Central Limit Theorem

If we want to know how long a scanline should be in order to determine the discontinuity frequency, or mean spacing, within specified tolerances, it is possible to utilize the central limit theorem. This states that the means of random samples of size N taken from a population of any distribution, that has a mean $\bar{x}$ and a standard deviation σ, will tend to be normally distributed with a mean $\bar{x}$ and a standard deviation of $\sigma/N^{1/2}$. However, in the case of a negative exponential distribution, the standard deviation is equal to the mean: they are both $\bar{x}$ (Hudson and Harrison, 1997). Hence, by using the concept of confidence intervals in the normal distribution, it is possible to determine the scanline length for any desired confidence level.

3.4.3 Sampling Bias and Mean Orientation

The discontinuity frequency, λ_s, along a line subtending an angle θ to the normal of a discontinuity set with frequency λ, is $\lambda_s = \lambda\cos\theta$. If the scanline is rotated to become nearly parallel with the discontinuities, the number of sampled discontinuities per unit length of the scanline will be reduced, and this clearly introduces a sampling bias when λ is being estimated, which can be removed by using a weighting factor. The number of intersected discontinuities, are weighted associated with each set to give an effective number of intersected discontinuities. The weighting factor, w, is calculated from the expression $1/\cos\theta$, where θ is the angle between the normal to the discontinuity, and the scanline for each set. In cases when many discontinuities with different orientations are intersected by a scanline and sampled, Hudson and Harrison (1997), recommend to use the procedure outlined in Figure 3.16 to find the mean dip direction and dip angle. The procedure corrects for oriental sampling bias through the introduction of weighted direction cosines. The first to columns are the dip direction and dip angle as measured, α, β, and the following two columns contain α_n, β_n, the trend and plunge of the normal to each discontinuity. The direction of cosines of each of the normals are then evaluated in the next three columns using the formulae of Figure 3.16.

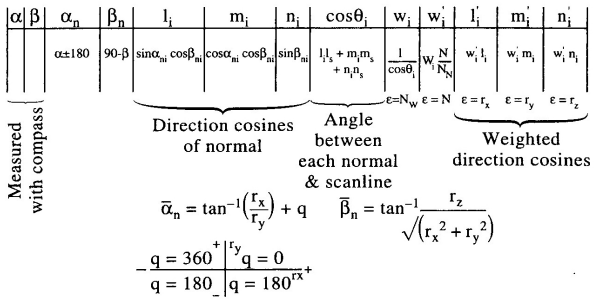

FIGURE 3.16 Evaluation of the mean orientation of a discontinuity set (from Hudson and Harrison, 1997)

By introducing the direction cosines of the scanline l_s, m_s, n_s the corresponding value θ_i can be calculated. The reciprocal of this value is the weighting factor w_i, which is then scaled to w_i' in order to that the overall measured discontinuity frequency is maintained. This procedure ends up in the last three columns, the weighted direction cosines. These values may then be summed, and the mean orientation of the normal computed (Hudson and Harrison, 1997).

3.5 Implementation in modelling

Results from the field mapping process are theoretically the basis for selecting either a continuous or a discontinuous model. According to Brown (1987), a continuous model should be selected if the rock mass is basically free from discontinuities, or if the discontinuities are very closely spaced in comparison to the dimensions of the structure. If slip, rotation and separation of the interfaces between rock blocks dominate, particularly when large deformations may be involved, a discontinuous model is preferable. In other words, in continuous modelling, the joints allowed for implicit, and essential input data for a numerical model are the strength and deformability parameters of the rock mass. Otherwise, if discontinuous modelling is chosen, the joints should be explicitly allowed for, and crucial input data includes joint patterns and strength parameters of the joints. Preparatory work such as field mapping and laboratory testing is therefore vital for obtaining a reliable mode.

The biggest challenge of discontinuous modelling, is undoubtedly how to get sufficient information about the joint patterns, and how to include them in the model. Some program codes have their own pre-processors, which automatically generate lines representing the joints based on input parameters like dip angle, and direction of the joint sets, together with joint spacing and length. However, this is not always adequate and some groups have developed their own systems for generating joints, which may work out in a satisfactory way for some approaches, but give incorrect results for others. It is very important to keep in mind, that the rock mass is a very complex building material, and that the joint patterns are extremely seldom, or never identical in different rock masses. In continuous modelling, the effect of the rock joints is simulated implicitly, and it is therefore very important to select a proper material model for the rock mass, and of course corresponding material parameters. For engineering rock mechanics problems usually the traditional Mohr Coloumb failure criteria, or the empirical Hoek Brown failure criteria are chosen.

Practical use of discontinuous and continuous modelling are demonstrated in Chapter 5 and Chapter 6, respectively, and a further discussion on how to implement the discontinuities in modelling will be given there.

3.6 Summary

Geological field mapping is of great interest in connection with modelling, especially when it comes to discontinuous modelling, since detailed information of the joint patterns is required. A big challenge is therefore to obtain necessary information about the rock mass conditions in the field, and then to implement the observed data into a numerical model. Uncertainty is connected both to the mapping- and implementation part.

In order to completely describe the discontinuities and rock masses, five geometric parameters are needed: i) Orientation, ii) Spacing, iii) Persistence, iv) Number of sets and v) Block size in addition to the "strength" parameters roughness aperture, filling, wall strength and seepage. Desired detailing level of the mapping has very often strict relation to the purpose of the mapping and to the budget of the projects, and there is no standardized method for mapping and measuring the rock structure geometry. The literature distinguishes between mapping connected to boreholes, and mapping at exposured rock faces. As an alternative to the traditional methods, spot-, scanline- and area mapping, new methods like laser scanning and digital photogrammetry have been developed.

It is relatively simple to gather information on discontinuities from borehole sampling, but it should be stressed that this method is an essentially one dimensional sample through the three dimensional rock mass. Difficulties that may arise in connection with borehole sampling, are rotation of the core during excavation and core loss. Further, filling material and gouge may be washed out from discontinuities, or extraneous matter can be deposited from the drilling process. Logging of borehole walls can be done by using a televiewer, acoustical or optical. The latter is preferred, since the acoustical one has problems with separating open joints from mineralized joints.

Exposure mapping seems to be a better characterization technique than borehole core logging, since trace length and termination can be taken. Traditional mapping techniques are spot, scanline and area mapping. Spot mapping is most commonly used, but either scanline or area mapping are recommended in order to remove subjectivity from the results and to allow sampling biases to be corrected. However there is a problem associated with how much data is needed when performing these

mapping techniques, and the detailing level of the mapping has very often relation to the economy of the specific project.

Drawbacks with traditional mapping techniques for exposed rock faces are that important measurements can be missed because of inaccessible or difficult terrain. This kind of problems may in the future be solved by either digital photogrammetry, a total geodetic station or laser-scanning. These methods will also remove human subjectivity. Establishment of a direct relation between the collected data from field measurements, and a pre-processing program generating joint patterns for discontinuous modelling is recommended.

Geophysical techniques, such as seismic refraction, seismic reflection, crosshole tomography, electric resistivity, electric magnetic radar and so called magnetically and gravitational methods, may be an alternative to the traditional methods in some cases.

Results from the field mapping process are usually basis for selecting either a continuous or discontinuous method. However the different methods presented above are so far not good enough for three dimensional, and partial two dimensional joint mapping. This makes it very difficult to get satisfactory information about required input for discontinuous modelling. Utilization of different methods at a specific project combined with statistical techniques, as for example the Poisson process may give reasonable information for simple problems. But for complex problems the existing mapping techniques are not good enough. Uncertainties and shortcomings of the pre-processors which are meant to take care of the implementation of measured discontinuities into a numerical model, cause additional difficulties with the discontinuous modelling process. Different aspects of discontinuous modelling are presented and discussed in Chapter 5.

In continuous modelling the effect of rock joints is simulated implicitly, but it does not mean that any information about discontinuity- orientation, spacing and persistence or number of joint sets or block size is insignificant. These parameters have an influence on the strength parameters values for the model. Required strength parameters are dependent on the selected material Model, usually Mohr-Coulomb or Hoek-Brown. Continuous modelling are presented and discussed in Chapter 6.

CHAPTER 4

Theory of the Discontinuous Deformation Analysis

4.1 Introduction

The Discontinuous Deformation Analysis (DDA) method is a comparatively newly developed technique, which is member of the Discrete Element Method (DEM) family of modelling codes. It was first introduced by Shi and Goodman and further developed by Shi (Shi, 1989). In 1989, Shi published his Ph.D thesis *"Discontinuous Deformation Analysis: A New Numerical Model for the Statics and Dynamics of Block Systems",* where computer programs based on the method and some applications were presented. The first International Conference on DDA was held at Berkeley, California, in 1996. Since that time, lots of improvements and modifications of DDA have been advanced by both academic and practical engineers in order to solve difficult problems.

The formulation of blocks in the DDA method is very similar to the definition of a finite element mesh. A finite element type of mesh is solved, in which all elements are real isolated blocks, bounded by pre-existing discontinuities. The elements or blocks used by the DDA method, can be of any convex or concave shape whereas the Finite Element Method (FEM) uses only elements of standard shape. When blocks are in contact, Coulomb's law applies to the contact interfaces, and the simultaneous equilibrium equations are selected, and solved for each loading or time increment. Large displacements and deformations are accumulation of small displacements and deformations at each step.

4.2 Basic Theory

4.2.1 Block Deformations and Displacement Variables

By adopting first order displacement approximations, the DDA method assumes that each block has constant stress and strains within small time steps. The two-dimensional displacement (u,v), of any point (x,y), in a block i can be represented by:

$$[D_i]= \begin{bmatrix} u_0 & v_0 & r_0 & \varepsilon_x & \varepsilon_y & \gamma_{xy} \end{bmatrix}^T \quad \textbf{[4-1]}$$

where $[D_i]$ is the unknown vector, and u_0, v_0 are rigid body translations for a specific point (x_0, y_0), within the block. r_0 is the rotation angle (given in radians) of the block, with rotation center at (x_0, y_0), and ε_x, ε_y and γ_{xy} are the normal and shear strains in the block. The complete first order approximation of block displacements has the following form:

$$u = a_1 + a_2 x + a_3 y \quad \textbf{[4-2]}$$

$$v = b_1 + b_2 x + b_3 y$$

where (u, v) are the displacements of an arbitrary point (x,y), within block i.

At the center point of gravity (x_0, y_0), the displacements are given by:

$$u_0 = a_1 + a_2 x_0 + a_3 y_0$$

$$v_0 = b_1 + b_2 x_0 + b_3 y_0 \qquad \textbf{[4-3]}$$

The unknown parameters in equation [4-1] can be expressed by subtracting [4-3] from[4-2]:

$$u = a_2(x - x_0) + a_3(y - y_0) + u_0$$

$$v = b_2(x - x_0) + b_3(y - y_0) + v_0 \qquad \textbf{[4-4]}$$

the normal strains ε_x and ε_y, shear strains ε_{xy} and rotation are given by:

$$\varepsilon_x = \frac{\partial u}{\partial x} = a_2$$

$$\varepsilon_y = \frac{\partial v}{\partial y} = b_3 \qquad \textbf{[4-5]}$$

$$\varepsilon_{xy} = \frac{1}{2}\gamma_{xy} = \frac{1}{2}\left(\frac{\partial v}{\partial x} + \frac{\partial u}{\partial y}\right) = \frac{1}{2}(b_2 + a_3)$$

$$r_0 = \frac{1}{2}\left(\frac{\partial v}{\partial x} - \frac{\partial u}{\partial y}\right) = \frac{1}{2}(b_2 - a_3)$$

Solving the last two of the above equations:

$$b_2 = \frac{1}{2}\gamma_{xy} + r_0 \qquad [4\text{-}6]$$

$$a_3 = \frac{1}{2}\gamma_{xy} - r_0$$

Inserted in [4-4]:

$$u = \varepsilon_x(x - x_0) + \left(\frac{1}{2}\gamma_{xy} - r_0\right)(y - y_0) + u_0 \qquad [4\text{-}7]$$

$$v = \left(\frac{1}{2}\gamma_{xy} + r_0\right)(x - x_0) + \varepsilon_y(y - y_0) + v_0$$

which lead to:

$$\begin{bmatrix} u \\ v \end{bmatrix} = \begin{bmatrix} 1 & 0 & -(y-y_0) & (x-x_0) & 0 & (y-y_0)/2 \\ 0 & 1 & (x-x_0) & 0 & (y-y_0) & (x-x_0)/2 \end{bmatrix} \begin{bmatrix} u_0 \\ v_0 \\ r_0 \\ \varepsilon_x \\ \varepsilon_y \\ \gamma_{xy} \end{bmatrix} = [T_i][D_i] \qquad \textbf{[4-8]}$$

where $[T_i]$, is the block deformation matrix. Equation [4-8] expresses the relationship between the deformation and the block shapes. By using equation [4-8] for each time step the block shape is updated.

4.2.2 Simultaneous Equilibrium Equations

Individual blocks are connected to each other, and form a block system through contacts among blocks and displacement constraints on single blocks. By minimizing the total potential energy, Π, Shi (1989), showed that the simultaneous equilibrium equations for a block system consisting of n blocks, can be written on the following matrix form:

$$\begin{bmatrix} K_{11} & K_{12} & K_{13} & \dots & K_{1n} \\ K_{21} & K_{22} & K_{23} & \dots & K_{2n} \\ K_{31} & K_{32} & K_{33} & \dots & K_{3n} \\ \dots & \dots & \dots & \dots & \dots \\ K_{n1} & K_{n2} & K_{n3} & \dots & K_{nn} \end{bmatrix} \begin{bmatrix} D_1 \\ D_2 \\ D_3 \\ \dots \\ D_n \end{bmatrix} = \begin{bmatrix} F_1 \\ F_2 \\ F_3 \\ \dots \\ F_n \end{bmatrix} \qquad \textbf{[4-9]}$$

Since each block has six degrees of freedom (u_0 v_0 r_0 ε_x ε_y γ_{xy}), each element K_{ij} in the coefficient matrix given by [4-9], is a 6 x 6 submatrix. D_i and F_i are both 6 x 1

submatrices, where D_i represents the deformation variables ($d_{1i}\, d_{2i}\, d_{3i}\, d_{4i}\, d_{5i}\, d_{6i}$) of block *i,* and F_i is the loading on block *i* distributed to the six deformation variables. Expressed in a more compact form [4-9] becomes **KD = F**, where **K** is a 6 x 6 stiffness matrix and **D** and **F** are 6 x 1 displacement and force matrices, respectively. The submatrix [K_{ii}], will depend on the material properties of block *i* and [K_{ij}], where *i* different from *j,* is defined by the contacts between block *i* and *j*. The total sum of degrees of freedom for all blocks represents the total number of displacement unknowns. Equation [4-9] has a similar form as these for finite element problems.

The solution of [4-9] is attended with a system of inequalities associated with block kinematics (e.g. no penetration and no tension between blocks), and Coloumb friction for sliding along block interfaces. Briefly, the solution procedure can be described as follow: First, the solution is checked to see how well the constraints are satisfied. If no tension or penetration are found along any contacts, the final displacement variables for a given time step are obtained by an iterative process. On the other hand, if tension or penetration is found the constraints are aligned by selecting new locks and constraining positions. A modified version of ***K*** and ***F*** are formed when a new solution is obtained, and this process is repeated until no tension or penetration are found.

4.2.3 Strain Energy Π_e and Stiffness Matrix of Blocks

In the two dimensional case, the strain energy of a block is given by:

$$\Pi_e = \iint \frac{1}{2}(\varepsilon_x \sigma_x + \varepsilon_y \sigma_y + \gamma_{xy} \tau_{xy}) dx dy = \iint \frac{1}{2} \begin{bmatrix} \varepsilon_x & \varepsilon_y & \gamma_{xy} \end{bmatrix} \begin{bmatrix} \sigma_x \\ \sigma_y \\ \tau_{xy} \end{bmatrix} dx dy \qquad \textbf{[4-10]}$$

where the integration is over the entire area of the *i*-th block. For each displacement step, we assume that the blocks are linearly elastic. For plane strain we have:

$$\begin{bmatrix}\sigma_x\\ \sigma_y\\ \tau_{xy}\end{bmatrix} = \frac{E}{1-\nu^2}\begin{bmatrix}1 & \nu & 0\\ \nu & 1 & 0\\ 0 & 0 & \frac{1-\nu}{2}\end{bmatrix}\begin{bmatrix}\varepsilon_x\\ \varepsilon_y\\ \gamma_{xy}\end{bmatrix} \qquad \textbf{[4-11]}$$

and

$$[E] = \frac{E}{1-\nu^2}\begin{bmatrix}1 & \nu & 0\\ \nu & 1 & 0\\ 0 & 0 & \frac{1-\nu}{2}\end{bmatrix},\ [E_i] = \frac{E}{1-\nu^2}\begin{bmatrix}0&0&0&0&0&0\\ 0&0&0&0&0&0\\ 0&0&0&0&0&0\\ 0&0&0&1&\nu&0\\ 0&0&0&\nu&1&0\\ 0&0&0&0&0&\frac{1-\nu}{2}\end{bmatrix} \qquad \textbf{[4-12]}$$

thus equation [4-10] becomes:

$$\Pi_e = \frac{1}{2}\iint\begin{bmatrix}\varepsilon_x & \varepsilon_y & \gamma_{xy}\end{bmatrix}[E]\begin{bmatrix}\varepsilon_x\\ \varepsilon_y\\ \gamma_{xy}\end{bmatrix}dxdy = \frac{1}{2}\iint[D_i]^T[E_i][D_i]dxdy \qquad \textbf{[4-13]}$$

$$= \frac{S}{2}[D_i]^T([E_i][D_i])$$

where E is Young's modulus, ν is Poisson's ratio, and S is the area of the *i*-th block.

The stiffness matrix is given by minimizing the strain energy Π_e:

$$k_{rs} = \frac{\partial^2 \Pi_e}{\partial d_{ri} \partial d_{si}} = \frac{S}{2} \frac{\partial^2}{\partial d_{ri} \partial d_{si}} ([D_i]^T [E_i][D_i]) , \qquad r , s = 1, ..., 6 \qquad \textbf{[4-14]}$$

k_{rs} forms a 6 x 6 submatrix:

$$S[E_i] \rightarrow [K_{ii}] \qquad \textbf{[4-15]}$$

which is added to $[K_{ij}]$ in the global equation [4-9].

4.2.4 Displacements Constraints

Let (u_m, v_m) and (u,v) represent respectively the assigned and computed displacements at point (x,y) of block *i.* Two stiff springs with stiffness *p,* are then applied to force the displacement (u,v) to be (u_m, v_m). The spring forces are given as:

$$\begin{bmatrix} f_x \\ f_y \end{bmatrix} = \begin{bmatrix} -p(u - u_m) \\ -p(v - v_m) \end{bmatrix} \qquad \textbf{[4-16]}$$

and the strain energy of the spring is:

$$\Pi_m = \frac{p}{2}\left[(u-u_m)^2+(v-v_m)^2\right] = \frac{p}{2}\left[\begin{bmatrix}u-u_m & v-v_m\end{bmatrix}\begin{bmatrix}u-u_m\\ v-v_m\end{bmatrix}\right]$$

$$= \frac{p}{2}\begin{bmatrix}u & v\end{bmatrix}\begin{bmatrix}u\\ v\end{bmatrix} - p\begin{bmatrix}u & v\end{bmatrix}\begin{bmatrix}u_m\\ v_m\end{bmatrix} + \frac{p}{2}\begin{bmatrix}u_m & v_m\end{bmatrix}\begin{bmatrix}u_m\\ v_m\end{bmatrix} \quad \textbf{[4-17]}$$

$$= \frac{p}{2}[D_i]^T[T_i]^T[D_i][T_i] - p[D_i]^T[T_i]^T\begin{bmatrix}u_m\\ v_m\end{bmatrix} + \frac{p}{2}\begin{bmatrix}u_m & v_m\end{bmatrix}\begin{bmatrix}u_m\\ v_m\end{bmatrix}$$

because :

$$\begin{bmatrix}u\\ v\end{bmatrix} = [T_i][D_i] \quad \text{and} \quad \begin{bmatrix}u & v\end{bmatrix} = [D_i]^T[T_i]^T \quad \textbf{[4-18]}$$

The derivatives are computed to minimize Π_m :

$$k_{rs} = \frac{\partial^2 \Pi_m}{\partial d_{ri}\partial d_{si}} = \frac{\partial^2}{\partial d_{ri}\partial d_{si}}\frac{p}{2}[D_i]^T[T_i]^T[D_i][T_i] = p(t_{1r}t_{1s}+t_{2r}t_{2s}),\ r=1,..,6 \quad \textbf{[4-19]}$$

k_{rs} forms a 6 x 6 submatrix:

$$p[T_i]^T[T_i](\quad \rightarrow [K_{ii}]) \qquad \textbf{[4-20]}$$

which is added to the submatrix $[K_{ii}]$ in the global equation [4-9].

Further we minimize Π_m by taking the derivatives at [D] = [0]:

$$f_r = -\frac{\partial}{\partial d_{ri}}\Pi_m(0) = \frac{\partial}{\partial d_{ri}}p[D_i]^T[T_i]^T\begin{bmatrix}u_m\\v_m\end{bmatrix} = p(t_{1r}u_m + t_{2r}v_m) \qquad \textbf{[4-21]}$$

f_r, r =1,.....,6 forms a 6 x 1 submatrix:

$$p[T_i]^T\begin{bmatrix}u_m\\v_m\end{bmatrix} \quad \rightarrow [F_i] \qquad \textbf{[4-22]}$$

which is added to $[F_i]$ in the global equation [4-9].

4.2.5 Point Loading

The potential energy of a point loading (F_x, F_y), acting on point (x, y) is:

$$\Pi_p = -(F_x u + F_y v) = -\begin{bmatrix} u & v \end{bmatrix}\begin{bmatrix} F_x \\ F_y \end{bmatrix} = -[D_i]^T[T_i(x,y)]^T\begin{bmatrix} F_x \\ F_y \end{bmatrix} \quad \textbf{[4-23]}$$

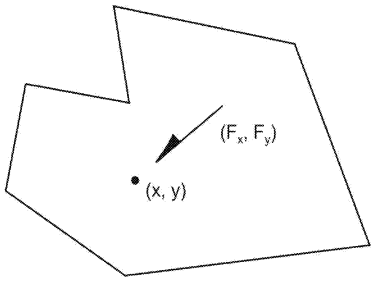

FIGURE 4.1 Point loading (from Shi, 1989)

To minimize Π_p, the derivatives are calculated:

$$f_r = -\frac{\partial}{\partial d_{ri}}\Pi_p(0) = \frac{\partial}{\partial d_{ri}}[D_i]^T[T_i(x,y)]^T\begin{bmatrix} F_x \\ F_y \end{bmatrix} = F_x t_{1r} + F_y t_{2r},\ r = 1, ...,6 \quad \textbf{[4-24]}$$

f_r, r = 1,.....6, forms a 6 x 1 submatrix:

$$\begin{bmatrix} 1 & 0 \\ 0 & 1 \\ -(y-y_o) & (x-x_0) \\ (x-x_0) & 0 \\ 0 & (y-y_0) \\ \frac{(y-y_0)}{2} & \frac{(x-x_0)}{2} \end{bmatrix} \begin{bmatrix} F_x \\ F_y \end{bmatrix} \rightarrow [F_i] \qquad \textbf{[4-25]}$$

which is the product matrix of a 6 x 2 matrix, and a 2 x 1 matrix. The resulting 6 x 1 submatrix is added to the submatrix $[F_i]$ in the global equation [4-9].

4.2.6 Volume Loading

Assume that (f_x, f_y) is a constant body force loading, which acts on the volume of block *i,* and that (x_0, y_0), is center of the gravity of this block, then:

$$x_0 = \frac{S_x}{S}, \quad y_0 = \frac{S_y}{S}, \quad S = \iint dxdy, \quad S_x = \iint x dxdy, \quad S_y = \iint y dxdy \qquad \textbf{[4-26]}$$

and the potential energy of the constant body force (f_x, f_y) is given by:

$$\Pi_v = -\iint (f_x u + f_y v)(dx)dy = -\iint \begin{bmatrix} u & v \end{bmatrix} \begin{bmatrix} f_x \\ f_y \end{bmatrix} dxdy = -[D_i]^T \iint [T_i]^T dxdy \begin{bmatrix} f_x \\ f_y \end{bmatrix} \quad \textbf{[4-27]}$$

where (u,v), is the displacement of any point (x,y) of block i.

$$\iint [T_i]^T (dx)dy = \begin{bmatrix} S & 0 \\ 0 & S \\ -S_y + y_0 S & S_x - x_0 S \\ S_x - x_0 S & 0 \\ 0 & S_y - y_0 S \\ \frac{S_y - y_0 S}{2} & \frac{S_x - x_0 S}{2} \end{bmatrix} = \begin{bmatrix} S & 0 \\ 0 & S \\ 0 & 0 \\ 0 & 0 \\ 0 & 0 \\ 0 & 0 \end{bmatrix} \quad \textbf{[4-28]}$$

The derivatives of Πv are calculated to minimize the potential energy:

$$f_r = -\frac{\partial}{\partial d_{ri}} \Pi_v(0) = -\frac{\partial}{\partial d_{ri}} \left([D_i]^T \begin{bmatrix} f_x S \\ f_y S \\ 0 \\ 0 \\ 0 \\ 0 \end{bmatrix} \right), \quad r = 1,.....,6 \quad \textbf{[4-29]}$$

Each f_r, r=1,....,6 forms a 6 x 1 matrix:

$$\begin{bmatrix} f_x S \\ f_y S \\ 0 \\ 0 \\ 0 \\ 0 \end{bmatrix} \rightarrow [F_i] \qquad \textbf{[4-30]}$$

which is added to $[F_i]$ in the global equation [4-9]. S is the area of block *i* and (x_0, y_0) is the center of gravity.

4.2.7 Initial Stress

The potential energy of the initial constant stresses (σ_{x0} σ_{y0} τ_{xy}), for the *i-th* block is given by equation:

$$\Pi_\sigma = \iint (\varepsilon_x \sigma_{x0} + \varepsilon_y \sigma_{y0} + \gamma_{xy} \tau_{xy}) dx dy$$

$$\Pi_\sigma = S(\varepsilon_x \sigma_{x0} + \varepsilon_y \sigma_{y0} + \gamma_{xy} \tau_{xy}) \qquad \textbf{[4-31]}$$

$$\Pi_\sigma = S[D_i]^T \begin{bmatrix} 0 \\ 0 \\ 0 \\ \sigma_{x0} \\ \sigma_{y0} \\ \tau_{xy} \end{bmatrix}$$

Assuming that :

$$[\sigma_0] = \begin{bmatrix} 0 \\ 0 \\ 0 \\ \sigma_{x0} \\ \sigma_{y0} \\ \tau_{xy} \end{bmatrix} \quad \textbf{[4-32]}$$

equation [4-31] can be written as:

$$\Pi_\sigma = S[D_i]^T[\sigma_0] \quad \textbf{[4-33]}$$

where the integration is over the entire area of the *i-th* block, and S is the area.

Π_0 is minimized by taking the derivatives:

$$f_r = -\frac{\partial \Pi_\sigma}{\partial d_{ri}} = -S\frac{\partial}{\partial d_{ri}}[D_i]^T[\sigma_0], \qquad r = 1,.....6 \quad \textbf{[4-34]}$$

f_r forms a 6 x 1 submatrix:

$$-S[\sigma_0] \rightarrow [F_i] \quad \textbf{[4-35]}$$

The matrix of [4-35] is added to the submatrix $[F_i]$ in equation [4-9].

4.2.8 Block System Kinematics

The concept of contacts in DDA, is very important. If there are no penetrations at all contacts, there are no penetrations for the whole block system. An edge and an angle, are defined to be a contact if the distance from the angle vertex to the edge is less than ρ, and if there is no overlapping when the angle vertex translates to the edge without rotation. ρ is the maximum displacement of points of all blocks. Two angles, are defined to be a contact if the distance between the two angle vertices is less than ρ and if there is no overlapping when two angles are translated without rotation until the vertices coincide (Shi, 1989). There are three types of contacts:

1. Contact between a convex angle less than 180^o and a concave angle greater than 180^o (Figure 4.2). If one of the following conditions is fulfilled: point P_1 passes line P_2P_3 or point P_1 passes line P_3P_4, an interpenetration will occur. P_2P_3 and P_3P_4 are reference lines.

2. Contact between an edge and a convex angle (Figure 4.3). Interpenetration will occur if, and only if, point P_1 passes line P_2P_3, which is the reference line.

3. Contact between two convex angles, Figure 4.4, Figure 4.5 and Figure 4.6, show two thick lines, which are the reference lines. Interpenetration will occur if the two reference lines are passed respectively by the vertices of the other angles simultaneously. The reference lines are chosen according to the following table.

TABLE 5.1

		Two reference lines	
$\alpha \geq 180^o$	$\beta \geq 180^o$	OE_3	OE_2
$\alpha \geq 180^o$	$\beta > 180^o$	OE_3	OE_4
$\alpha > 180^o$	$\beta \geq 180^o$	OE_1	OE_2
$\alpha > 180^o$	$\beta > 180^o$	OE_1	OE_4

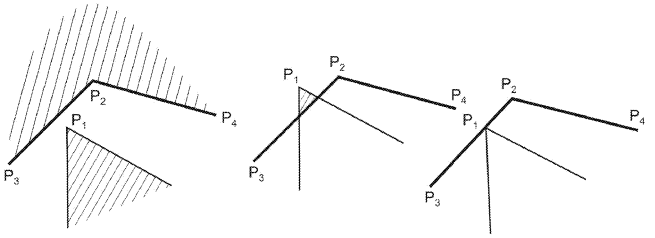

FIGURE 4.2 Two reference lines of a contact between convex and concave angles (from Shi, 1989)

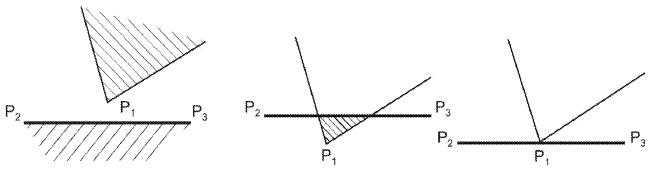

FIGURE 4.3 Reference line of an angle-edge contact (from Shi, 1989)

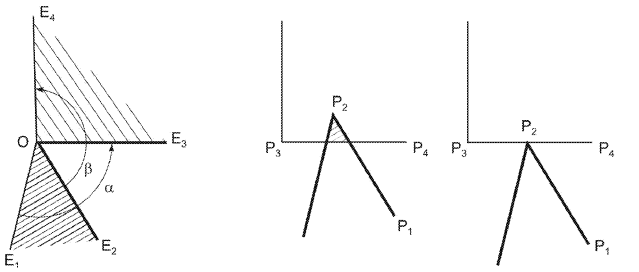

FIGURE 4.4 Two reference lines of an angle-angle contact (from Shi, 1989)

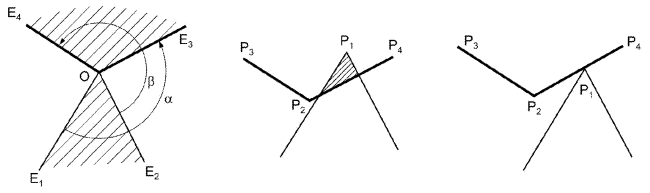

FIGURE 4.5 Two reference lines of an angle-angle contact (from Shi, 1989)

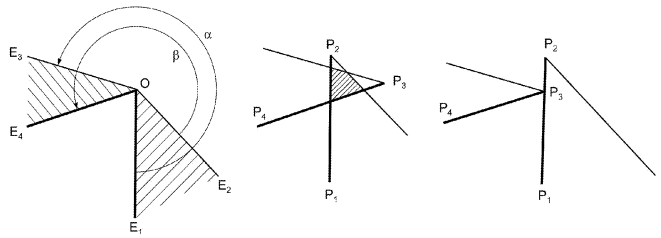

FIGURE 4.6 Two reference lines of an angle-angle contact (from Shi, 1989)

4.2.8.1 Criteria for and Locking of Penetration

Assume that P_1 is a point before deformation which moves to point P'_1 after deformation. P_2P_3 is the reference line and (x_i,y_i) and (u_i,v_i) are respectively the

coordinates and displacement increment of P_i, i = 1, 2, 3. If P_1, P_2 and P_3 rotate anticlockwise, the fact that P'_1 has passed line P_2P_3 is stated by the inequality:

$$\Delta = \begin{vmatrix} 1 & x_1 + u_1 & y_1 + v_1 \\ 1 & x_2 + u_2 & y_2 + v_2 \\ 1 & x_3 + u_3 & y_3 + v_3 \end{vmatrix} < 0 \qquad \textbf{[4-36]}$$

The distance d, from P'_1 to P_2P_3 is:

$$d = \frac{\Delta}{\sqrt{(x_2 - x_3)^2 + (y_2 - y_3)^2}} \qquad \textbf{[4-37]}$$

When contacts are involved the following rules must be taken into consideration:

1. No interpenetration occurs between the two sides
2. No tension force exists between the two sides

If interpenetration takes place at a given position, a stiff spring will be applied as a lock. This starts from the point and lies along the direction normal to the reference line and the application of the lock depends on the three different kind of contacts:

1. Contact between a convex angle less than 180^o and a concave angle greater than 180^o (Figure 4.2). If point P_1 passes through the reference line P_2P_3, a lock between point P_1 and line P_2P_3 is applied. In the same manner a locking device will arise if P_1 passes through the reference line P_2P_4.

2. Contact between an edge and a convex angle (Figure 4.3). The lock is applied when the points passes through the reference line.

3. Contact between two convex angles (Figure 4.4, Figure 4.5 and Figure 4.6). In this case there are two reference lines and if these two are passed by the corresponding points simultaneously, interpenetration will occur. The normal distance from the reference lines to the corresponding points is d_1 and d_2. Assume that $d_1 < d_2$, then the "lock" will be attached between the point and its reference line with distance d_1. For this type of contact, only one stiff spring is applied. the physical meaning of the applying stiff springs is "to push the invaded angle back along the shortest path".

4.2.8.2 The Submatrices of a Normal Contact Spring

Assume there is a spring between point P_1 and the reference line P_2P_3 (Figure 4.3). Denote (x_i, y_i) and (u_i, v_i) as the coordinates and displacement increment of point P_i respectively, i= 1, 2, 3. To push point P_1 back from interpenetration, the distance d should be zero after the displacement increment is applied:

$$d = \frac{\Delta}{l} = \frac{\Delta}{\sqrt{(x_2 - x_3)^2 + (y_2 - y_3)^2}} = 0 \qquad \textbf{[4-38]}$$

where

$$\Delta = \begin{vmatrix} 1 & x_1 + u_1 & y_1 + v_1 \\ 1 & x_2 + u_2 & y_2 + v_2 \\ 1 & x_3 + u_3 & y_3 + v_3 \end{vmatrix} = S_0 + \begin{vmatrix} 1 & u_1 & y_1 \\ 1 & u_2 & y_2 \\ 1 & u_3 & y_3 \end{vmatrix} + \begin{vmatrix} 1 & x_1 & v_1 \\ 1 & x_2 & v_2 \\ 1 & x_3 & v_3 \end{vmatrix}$$

and

$$S_0 = \begin{vmatrix} 1 & x_1 & y_1 \\ 1 & x_2 & y_2 \\ 1 & x_3 & y_3 \end{vmatrix} \qquad \text{[4-39]}$$

If point P_1 belongs to the i-th block and edge P_2P_3 belongs to the j-th block, the displacements of points P_1, P_2 and P_3 can be represented as:

$$\begin{aligned} \begin{pmatrix} u_1 \\ v_1 \end{pmatrix} &= [T_i(x_1,y_1)][D_i] \\ \begin{pmatrix} u_2 \\ v_2 \end{pmatrix} &= [T_j(x_2,y_2)][D_j] \\ \begin{pmatrix} u_3 \\ v_3 \end{pmatrix} &= [T_j(x_3,y_3)][D_j] \end{aligned} \qquad \text{[4-40]}$$

The strain energy of the contact spring is given by:

$$\Pi_k = \frac{p}{2}d^2 \qquad \text{[4-41]}$$

$$= \frac{p}{2}\left(\sum_{r=1}^{6} e_r d_{ri} + \sum_{r=1}^{6} g_r d_{rj} + \frac{S_0}{l}\right)^2$$

where p is the stiffness of the spring and d the interpenetration distance and

$$e_r = \frac{[(y_2 - y_3)t_{1r}(x_1,y_1) + (x_3 - x_2)t_{2r}(x_1,y_1)]}{l}$$

$$g_r = \frac{[(y_3 - y_1)t_{1r}(x_2,y_2) + (x_1 - x_3)t_{2r}(x_2,y_2)]}{l}$$

$$+ \frac{[(y_1 - y_2)t_{1r}(x_3,y_3) + (x_2 - x_1)t_{2r}(x_3,y_3)]}{l}$$

p is a very large number, normally from 10E to 1000E to guarantee that the displacement of the spring is 10^{-3} to 10^{-4} times the total diplacment. If p is large enough, the computation result will be independent of the choices of p.

Minimizing Π_k by taking the derivatives, four 6 x 6 submatrices and two 6 x 1 submatrices are obtained and added to $[K_{ii}]$, $[K_{ij}]$, $[K_{ji}]$, $[K_{jj}]$, $[F_i]$ and $[F_j]$ in the global equation [4-9].

4.3 Summary

As mentioned in Chapter 3, DDA belongs to the DEM family. The method is comparatively new and was first introduced by Shi and Goodman, and further developed by Shi. DDA uses the displacements as unknowns and solves the equilibrium equations, which are established by minimizing the potential energy, in the same manner as the matrix analysis of structures in the Finite Element Method. The number of unknowns is the sum of the degrees of freedom of all blocks, while for FEM the number of unknowns is the sum of the degrees of freedom of all nodes. A lot of new theories and extensions to the DDA method have been advanced by both academic and practical engineers to solve difficult problems during the last years and a long list of computer program based on the theory exist. This is described in Chapter 5.

CHAPTER 5

Discontinuous Modelling - DDA and Gjøvik Olympic Mountain Hall

5.1 Introduction

As mentioned introductorily, DDA was picked out as a representative tool for the discontinuous modelling. This is not a commercial program, but can be distributed by contacting Shi. Part of the work has been carried out at Kyoto University, School of Civil Engineering, Japan, with assistance from Professor Yuzo Ohnishi. The author has mainly made use of programs based on the Kyoto-20020206 source code. A few cases are analysed with Shi's code updated March 2002, compiled with the NDP C compiler. It should be stressed that the main purpose of this chapter is to demonstrate the discontinuous modelling process, to evaluate the applicability of the today's DDA program to solve practical engineering problems, and to get knowledge about the discontinuous modelling process rather than developing new functions.

Gjøvik Olympic Mountain Hall, which was built in connection with the XVII Winter Olympic Games 1994 at Lillehammer, is selected as a case study for the DDA analyses. The reason why Gjøvik Olympic Mountain Hall is used as a case study, is the large amount of available input data from a comprehensive stress and deformation monitoring program performed during and after the excavation. In addition, results from COSHWAN, a finite element program developed at SINTEF Rock and Mineral Engineering, and UDEC calculations are available from SINTEF Civil and Environmental Engineering and the Norwegian Geotechnical Institute (NGI),

respectively. Thus, the basis for verification of the DDA analysis results is both realistic and well suited.

5.2 DDA as a Representative Tool for Discontinuous Modelling

In Norway, the universal distinct element code (UDEC) has for a long time been used as a tool for discontinuous modelling. Several papers and reports, have been published on UDEC modelling of the Gjøvik Olympic Mountain Hall and some other projects. On the other hand, DDA is not well-known among engineering geology and rock mechanics scientists and engineers. This is mainly caused by: i) The program is not yet commercialized and ii) Development of the program is still going on. However, the author hopes that the utilization of DDA in this thesis, will give the reader both information about the method and possibilities to discover strengths and limitations of the DDA method. Modelling a well documented case study as the Gjøvik Olympic Mountain Hall by using the DDA code, could be positive for the further development of the program. Necessary improvements, and where, when and how to use the program can be examined in a proper way.

The main reason for selecting DDA as a representative tool for the discontinuous modelling part was an established co-operation between the SIP Program “Computational Mechanics in Civil Engineering” and existing DDA research environments including Shi.

5.3 Review of Existing Computer Programs Based on the DDA Method

Compared with 1986, when only one DDA computer code existed, today’s engineers have opportunity to use several DDA codes, with various functions and capabilities. The first DDA computer code was a PC-based BASIC language program code, developed by Shi in 1986. In 1989 Shi, completed the first C version, by using the NDP C compiler and afterwards this has been modified and improved several times by Shi and others.

The DDA method has been object for a lot of work by researchers and Ph.D students during the past decade, and some major results are shown in Table 5.1 based on Ma, 1999.

TABLE 5.1 Different versions of DDA programs

Version	Language	Developer	Notes
DDA'86	BASIC	Shi	The first DDA code
DDA'89	C/PC	Shi	The first C DDA code
DDA'92	C/UNIX	Shi	The first X-windows DDA code
DDA'94	C/UNIX	Shi	Cohesion, Tension and Auto Kn
DDA'95	C/UNIX	Shi	Correction of shear lock and rotation problem
DDA'96	C/UNIX	Shi	Joint lines by statistics, material lines, tensile strength, direct equation solver or SOR iteration equation solver, fixed lines
NDDA'92	C/PC	Shyu	The first node based DDA
FBA	C/SUN	Gbara & Pan	The first DDA with good interface, limited functions, 1993
DDA/W	C/Win	Berkeley	The first DDA/Win, less mature, 1996
DDA/W version 1.2	C/Win 95/ NT	Berkeley	Released October 1998
DDA/WT	C/SUN	Ohnishi	Advanced, new functions, great potential
DDA/AJ'94	FORTRAN	Ke	Artificial Joints
DDA/SB'95	FORTRAN	Lin	Sub-Block, breakable block
DDA/API/ Win98/ 2000 Version 2.0	Visual C++/Win	Miki	Based on the DDA'96 developed by Shi. Only DC, DF and DG programs
DDA Kyoto-20020206	Visual C++/Win	Sasaki	Material lines replaced with areas, universal equation for in-situ stress distribution, sequential excavation

5.3.1 DDA Programs

Each of the DDA versions listed above, consists of four DDA programs: i) The line-producing program DDA Lines (DL), ii) The block producing program DDA Cut (DC), iii) The analysis program DDA Forward (DF) and iv) The graphic output program DDA Graph (DG). This section is based on Shi (1989 and 1996)

5.3.1.1 Program DL

Program DL is a pre-processor for program DC, which generates lines representing joints, the boundary of the joint domain, and perimeters of the tunnels. Five tunnel shapes are predefined in the program, and the joints are generated by statistics based on average spacing, average length and average bridge, plus the degree of randomness of each joint set. It is also possible to implement lines directly to define blocks that are not formed by the statistically generated joint lines. Lines defining the outer boundary of the domain, are implemented separately, and DL truncates automatically lines outside the joint domain and those inside the tunnels. All joint lines are defined by line segments, which is defined by a start (x_1,y_1) and end point (x_2,y_2).

5.3.1.2 Program DC

Program DC is a pre-processor for program DF, and divides the analysis domain into generally shaped isolated blocks. Parts of joint lines, which do not contribute to form the finite blocks are deleted automatically by the program after computation of intersection points. The process is called “tree cutting”. Immediately after the identification of the blocks, DC computes, and saves the block areas and block integrals. Coordinates of clockwise-ordered vertices are output numerically and graphically for each block. Fixed points, loading points, measured points and hole points can be defined in the input file, and the program identifies these automatically. Edges shorter than a pre-defined size are eliminated by the DC.

5.3.1.3 Program DF

Program DF is the actual analysis program. Both static and dynamic analyses can be carried out. An input file consisting of physical data like material constants, point loads, body forces, initial stresses and initial velocity is together with blck, the output file of program DC, basis for the analysis process. For each time step, all block contacts are found. A non-zero storage method introduced by Shi 1989, is used to renumber all blocks, and to find all non-zero elements of the coefficient matrix corresponding to the block contacts. The stiffness, loading, mass and contact submatrices are formulated and added to the coefficient, or force matrices of the equilibrium equations.

The locked directions of closing contacts are selected at the beginning of each time step, and a spring is applied in each locked direction to prevent penetration along the spring direction. The submatrices of contact springs are then added to the simultaneous equilibrium equations prior to solving them. Next, a new block system configuration is established. If there is any penetration at a contact with no spring, program DF goes back to the beginning of the time step and applies a contact spring. Further, if a contact spring has a tension higher than the allowable tension calculated from the tensile strength, DF will return to the beginning of the time step and delete this spring. The process above is called an "open-close" iteration. General equilibrium equations are formulated and solved iteratively until there are no penetration and no spring tension higher than the allowable at all contacts, which means that all blocks are in equilibrium with appropriate contact conditions at the end of the time step. New geometries of deformed blocks, block stresses, block velocity and contact forces are saved, and then used at the beginning of the next time step. Thus, incremental displacements and deformations are accumulated to result in relatively large displacements and deformations.

5.3.1.4 Program DG

Program DG is a graphic post-processor, which reads the output file "dgdt" from program DF, and transfers the computed results into graphics. Some DG programs are more advanced than others, but roughly speaking the programs are able to graphically output block deformation and displacements, and the principal stresses in every block. An animation of the analysis progress is also possible in some versions. By looking at the graphic output, the user can intuitively check the computed results. Figure 5.1 shows a flow chart which illustrates how the DDA programs are related to each other.

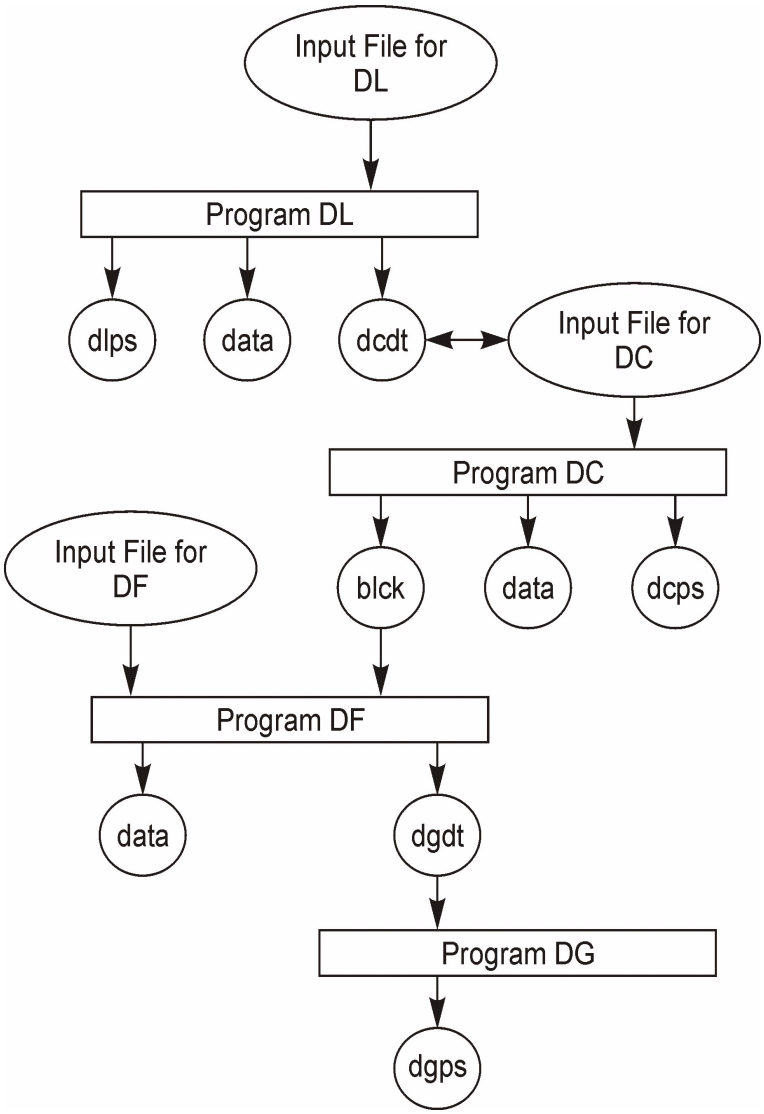

FIGURE 5.1 Flow chart showing how the DDA programs are related (after Shi, 1996)

5.3.2 The Kyoto Version

The Kyoto version is a further development of the DDA/API/Win98/2000 Version 2.0. The programs are converted to Visual C++, and stand out as more user friendly than the original since a window with an action bar appears when the user starts the programs. In addition, some new functions are introduced in the DC and DF programs. No DL program exists in the Kyoto version, and other DL programs, e.g. Shi's code updated March 2002, are not always compatible with program DC for models consisting of more than thousand blocks or for models where the tunnel geometry is directly input instead of using one of the predefined tunnel shapes.

Some modifications and improvements in the programs are introduced with assistance from Mr. Takeshi Sasaki, Senior Manager, Kajima Corporation and Mr. Jianhong Wu, Ph.D. Student, Kyoto University, School of Civil Engineering. In earlier DC programs, so called material lines were used to define the material properties of a specified block. Blocks intersected by a material line were assigned the block material number of the material line. This involves a relatively big amount of input data in cases where the rock mass is heavily jointed, with various rock block sizes, and the user request various material properties for the analysis model. This may for example, be a reduced E-modulus close to the surface influenced by weathering, than for the rest of the model. Material lines are therefore replaced with so called material areas defined by the coordinates, (x_1,y_1), (x_2,y_2), (x_3,y_3) and (x_4,y_4). With this alteration, the input data preparation is less time consuming, and accordingly less expensive. Figure 5.2 shows a simple example where material lines are replaced with material areas.

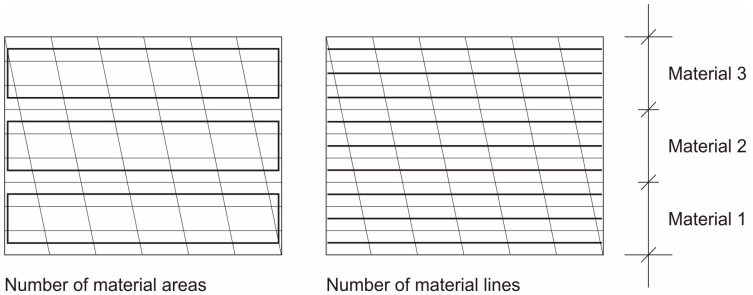

FIGURE 5.2 Material lines replaced with material areas

Further, universal equations for the in-situ stress distribution are included in the DF program. The existing equation system, assume that the initial stress increment in x- and y-directions is constant but not identical, for the entire model. The Kyoto version permits variations of the increment within the model. For example, in some cases it is desirable that the ratio between the horizontal and vertical stresses decreases from the surface to the bottom of the model.

The new universal equations are listed below:

$$\sigma_y = afy + bfy \cdot (ylevel - yg)$$

$$\sigma_x = cfy + (\sigma_y - afy) \cdot fkx \qquad \textbf{[5-1]}$$

where the following parameters must be predefined in the input file (Figure 5.3)

y-level	=	upper y-coordinate of a given area
afy	=	σ_y at a given y-level
bfy	=	the gradient of σ_y
cfy	=	σ_x at a given y-level
fkx	=	ratio between the difference in σ_x/σ_y
yg	=	y-coordinate of the block in which the stresses are calculated

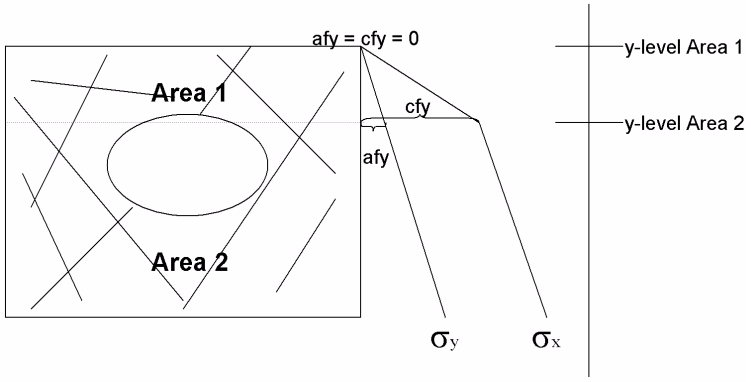

FIGURE 5.3 Illustration of the parameters in Equation 5-1

Finally, a new subroutine is introduced in program DF, which makes it possible to carry out sequential excavation. This functionality is very important for inelastic analysis results because of so-called path dependency. For elastic analyses, sequential excavation has no influence on the results due to the superposition principle.

5.3.3 Latest Developments in DDA

As mentioned introductorily in this thesis, DDA has been subject to a lot of research work during the last years. Since 1996, five international conferences on analysis of discontinuous deformation have taken place and a lot of new modifications and improvements have been presented. A few are listed below.

Granular mechanics has been given a lot of attention over the years. Ohnishi et al, Wang et al and Bray et al (Ma, 1999) introduced a DDA code for rigid disks, DDAD, some years ago. Later elliptic disks and new equation solvers have been introduced (Ma, 1999). Balden et al (2001), make use of a DDA formulation, limited to rigid non-fracturing 2D ore particles, for ball mill simulations, and a preliminary comparison of 3D experimental ball trajectory data is very encouraging. Work

is already in progress to include complex particle geometry, particle deformation and fracturing.

The original DDA makes use of a first order Taylor function to approximate the displacement field within a block. Over the years several approximation schemes have been utilized in order to refine the displacement field, and second and third order Taylor functions and Fourier series functions are therefore introduced (Ma et al, 1996).

Further, Wang et al (1997), introduced a DDA method with finite element mesh in order to study time integration theory, and found that the method is particularly suitable for dynamic analysis. Lin et al (2001) presented a method that couples DDA and the boundary element method in order to solve 2D elastic problems. Existing discontinuities, expected to have significant impact on a given problem, are modelled as a system of blocks by using DDA, while the regions far away from the point of interest are treated as a homogeneous elastic medium by using BEM.

At the 5th International Conference on Analysis of Discontinuous Deformation Analysis in Wuhan, China, October 8-10, 2002, several presentations dealt with the development of a three-dimensional DDA (Shi, Yeung et al and Jang et al).

5.4 Gjøvik Olympic Mountain Hall

Gjøvik Olympic cavern was built in connection with the XVII Winter Olympic Games 1994 at Lillehammer, and is so far the world's largest underground cavern for public use. The main cavern of the complex, which was created primary to house the ice hockey games, has a span of 62 m, a length of 91 m and a height of 25 m. The spectator capacity is currently 5300, and today the cavern is widely used for both sport arrangements and concerts. The cavern is located in Precambrian gneiss, with rock overburden varying from 25 to 50 m, and the excavation was carried out by a five stage sequential mode (Chryssanthakis and Barton, 1994).

A rock engineering program named "Rock Cavern Studium", established between the contractor, consultants and research institutions was responsible for site investigations and tests. In the first phase of the program, activities like engineering geological mapping, in-situ rock stress measurements (overcoring), laboratory testing and numerical analyses by three different methods were carried out.

Since the results so far were satisfactory a program for further investigations was elaborated. Of particular importance was the results from the in-situ rock stress measurements, which revealed relatively high horizontal in-situ stresses. Phase two comprised refraction seismics, core drillings, seismic thomography, stress measurements (hydraulic fracturing) and numerical analyses. Thus, a substantial amount of input data for the modelling process is available. This is unique because numerical analysis is usually used as a part of the pre-investigations when the availability of realistic input parameters are limited. Figure 5.4 shows a picture of the construction of the Gjøvik Olympic Mountain Hall.

5.5 Geology

The Precambrian gneiss at the site, has a composition varying from granitic to quartzdioritic. Due to tectonic effects, the rock has developed a network of microjoints, which are filled or coated with calcite and epidot. The result is a well jointed rock mass, with average rock quality designation (RQD) of about 70%.

The joints are generally rough and well interlocked, and have rather irregular orientations. Foliation is poorly developed but generally strikes approximately E-W with a dip of 35 to 55 ° towards S. The jointing is perhaps more pronounced than in Norwegian basement rocks in general. The spacing of the more persistent jointing is often several meters. The general joint character is one of low persistence, moderate to marked roughness and without clay filling (Barton et al 1994).

FIGURE 5.4 Photo from the construction of the Gjøvik Olympic Mountain Hall (from the research program "Rock Cavern Studium ", 1992)

5.6 Discontinuous Modelling

In discontinuous models the joints are allowed for explicitly. Information about the geometry of the cavern, position in the terrain, jointing, material parameters and the excavation process are collected from various reports and papers performed by the research institutions SINTEF, the Norwegian Geotechnical Institute (NGI) and the consultant company NOTEBY (Bollingmo, 1994, Morseth and Løset, 1994, Hansen and Kristiansen, 1994, Thideman and Dahlø, 1994, Westerdahl et al, 1994, Stjern, 1994). Numerical analysis was carried out by SINTEF and NGI. NGI used the UDEC code, based on the distinct element method, and it is natural to compare the DDA results with the UDEC results, and also make some comments on the UDEC model (Lu, 1994 and Chryssanthakis, 1994).

5.6.1 Implementing measured discontinuities in a numerical model

Setting up a reliable model of the jointed rock mass is quite difficult, and presumably one of the biggest challenges within numerical modelling. It is natural to start the process with field mapping according to one of the techniques listed and discussed in Chapter 3, and then continue processing the results in such a way that they are dexterous for a pre-processor, which is almost without exception a part of the program package.

As an example, necessary parameters for the pre-processor in DDA, program DL, are the number of joint sets, dip angle and direction of each joint set, dip angle and direction of section to be analyzed and average joint spacing, length, bridge and degree of randomness. The dip angle is defined as the angle between a joint plane and a horizontal plane, while the direction is the angle measured clockwise from the north to the horizontal projection of the upward normal vector of the joint plane. The joint bridge is the space between the end points of two adjacent collinear joint lines and can be negative. The degree of randomness may be a number from 0 to 0.5. If 0 is entered, no random pertubation is applied, while full perturbation is applied if 0.5 is entered.

The results from such a software specific pre-processor are not always the best alternative, even though the user has used credible input data according to the field mapping. Some experienced engineers have therefore developed their own methods for generating the joint pattern.

Figure 5.5 shows the joint pattern adopted by NGI in their UDEC analyses of Gjøvik Olympic Mountain Hall. Whether this model reflects a correct picture of the rock mass conditions or not, is a relevant question to be asked. Since the analysis results are in accordance with reality, stable conditions, the model approximation of the rock mass conditions might be considered to be “good enough”. Taking into account the results from the geological investigations from the Gjøvik Olympic Mountain Hall project, without doing too many assumptions, the model approximation of the rock mass conditions would not be “good enough”.

Question marks are especially linked to the use of the joint pattern. In the model the joint pattern appears as quite uniform, even though the geological reports describes the rock mass as normally irregular, rough-walled and with quite large variations in dip and strike. No discontinuities with persistence are presented in the whole model.

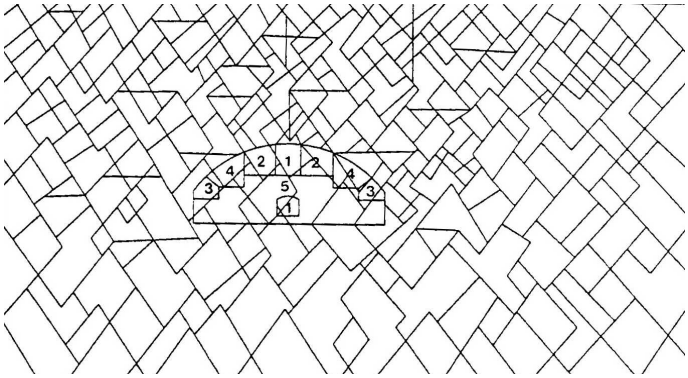

FIGURE 5.5 Joint pattern of the NGI Gjøvik model (from Chryssanthakis, 1994)

The literature mentions several examples of how discontinuous modelling is utilized for stability analyses. In the following some examples are listed and discussed.

An underground cavern, the National Theatre Station, located in oolitic limestone and shales with some igneous intrusive dykes in Norway (Figure 5.6)

An underground cavern located in a rock mass mainly consisting of quartz mica shists with patches of biotite and muscovite shists in the Himalayas (Figure 5.7)

A tunnel close to a rock slope in the Nan-kang formation of Miocene Sedimentary rocks in Taiwan (Figure 5.8)

A powerhouse located in mainly limestone, bioclastic limestone, sandstone and marly shale in China (Figure 5.9)

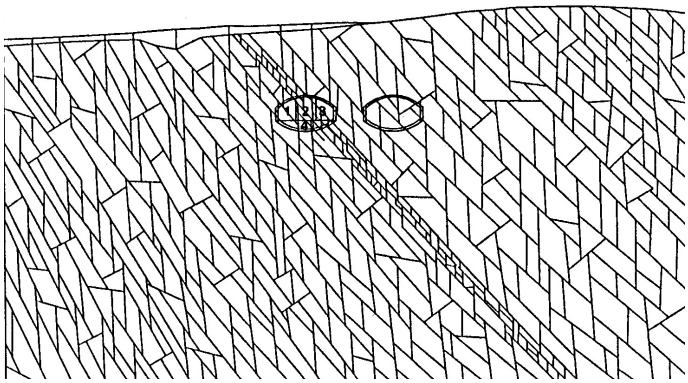

FIGURE 5.6 Numerical model of The National Theatre Station in Norway (from Løset et al, 1995)

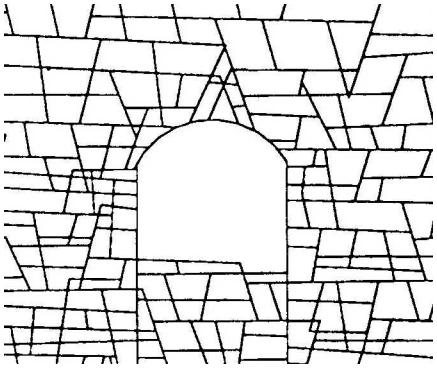

FIGURE 5.7 Numerical model of an underground cavern in the Himalayas (from Bhasin et al, 1998)

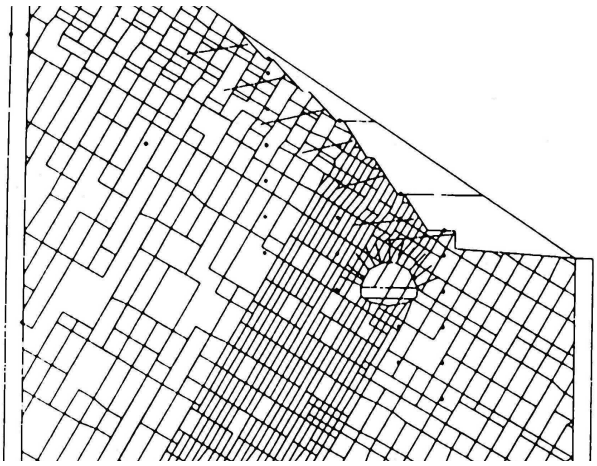

FIGURE 5.8 Numerical model of a tunnel near a rock slope, Nankang formation, Taiwan (from Chen et al, 1995).

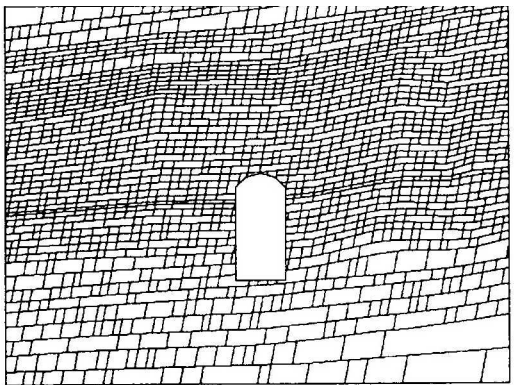

FIGURE 5.9 Numerical model of a Powerhouse, China (Wu et al, 2002)

The examples presented above are from different parts of the world and the rock mass type is varying. However there are some striking similarities between the models: i) The joint pattern is simplified compared to the field situation, ii) Almost all rock blocks have either rectangular or triangular shape and iii) There are small variations in rock block size over large areas and details that may have influence on the results are maybe missed. These similarities may be explained by difficulties connected to i) The field mapping process and ii) The implementation process.

The fact that some experienced engineers have developed their own methods for generating joint patterns for discontinuous numerical modelling, may also be a reason for striking model similarities between different problems to be analysed. Time and cost are usually vital factors for a project, and if an already established method works in a comfortable way it is quite normal to make use of this as a basis for different modelling tasks.

Further, it should be noticed that the analysis results may be different, if the tunnel or cavern in the models above are moved a few meters either to the left, right, up or down, since the number and orientation of the joints that the opening intersects may be changed. Figure 5.10 illustrates an example of to parallel caverns located in a rock mass with identical mechanical properties. The number and orientation of rock blocks intersecting the roof is different for the two caverns, and the analysis results show that the left cavern is stable, while the right tends to collapse.

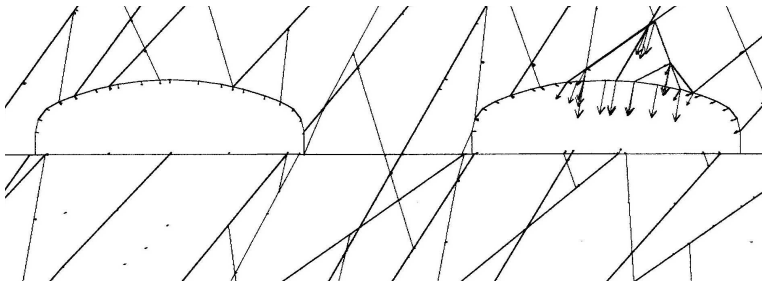

FIGURE 5.10 Two parallel caverns located in a rock mass with identical mechanical properties (from Scheldt, 1998).

The illustrations above show the difficulties and uncertainties of setting up a reliable model of the jointed rock mass. Those who work with discontinuous modelling know that it is impossible to create an actual model of the reality, and that *approximations* must be used. In order to save time and money, it is therefore both tempting to make use of systems for generating joints that are already well known.

The DDA and the different Gjøvik models introduced in this thesis, are not perfect either. The five different models are more or less successful approximations of the jointed rock mass, and setting up a joint model was not at all unproblematic.

Model 1 is introduced in order to control modifications and improvements in program DF. The number of blocks in the model is only 151, which gives relatively short computation time, and it seems quite clear that a model like this one is not suitable for other things than described above, because of an unrealistic presentation of the rock mass conditions. Not all joints are continuous over such an area in reality, and neither is the rock mass so homogenous in the nature. Model 1 was used as basis for Model 2 and 4, to evaluate the influence of joint spacing in the DDA analyses. Common for Model 1, 2 and 4 are two joint sets, and that the size and shape of the blocks in each model are almost identical except for the blocks around the outer boundary edge and for the blocks close to the cavern boundary. Setting up such models are relatively straight forward work, since the user only has to define the number of joint sets, their orientation and of course the spacing between the joints.

In Model 3, one more joint set is added and the line producing program (DL), version 96, is used for generating variations of the orientations in two of the three joint sets. The result is a model with huge variations in block size and increased possibility for numerical calculation problems, which was verified when starting DF. The compatibility of DL (version 96) and DF (Kyoto) is not good, and leads to several computer crashes. Model 3 is perhaps a better approximation than Model 1, 2 and 4, since the shapes of the blocks are somewhat varying, but far from the rock mass conditions described in geological mapping reports from Gjøvik.

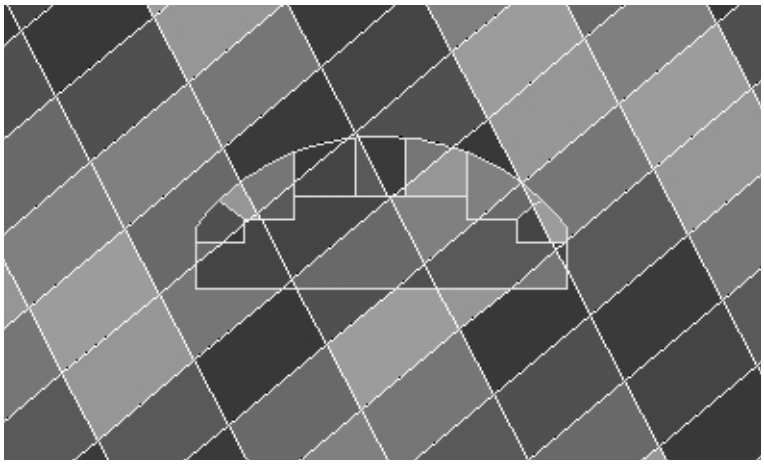

FIGURE 5.11 Model 1 - Gjøvik Olympic Mountain Hall

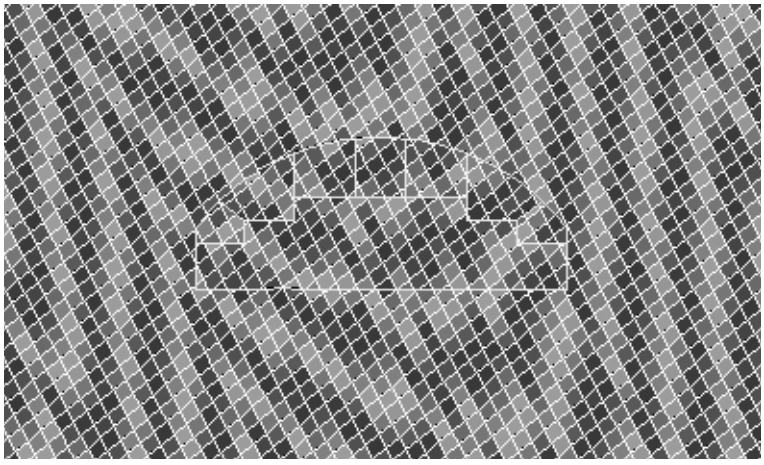

FIGURE 5.12 Model 2 - Gjøvik Olympic Mountain Hall

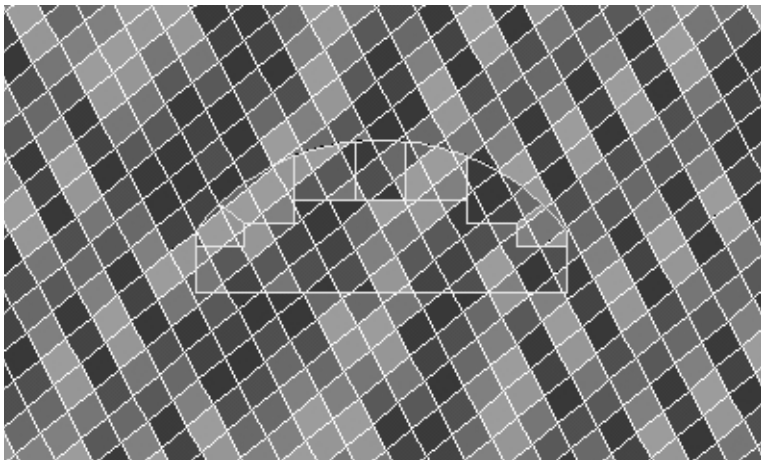

FIGURE 5.13 Model 4 - Gjøvik Olympic Mountain Hall

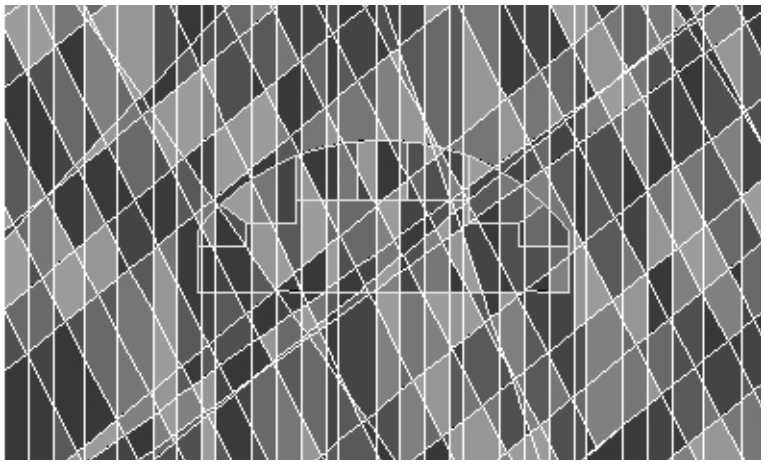

FIGURE 5.14 Model 3 - Gjøvik Olympic Mountain Hall

.

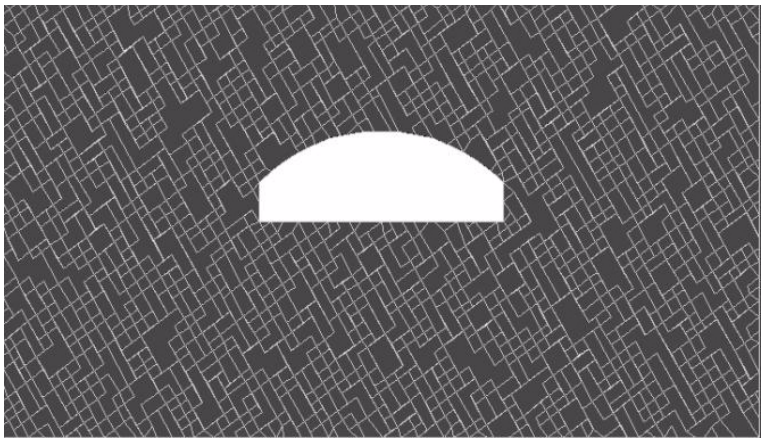

FIGURE 5.15 Model 5 - Gjøvik Olympic Mountain Hall

Model 5 is presumably the best approximation using the pre-processor in DDA and a model that resembles NGI's UDEC model of the Gjøvik Olympic Mountain Hall. Shi's DL program updated in March 2002 is used, and the model shows much less variation in block size than Model 3. Meanwhile, the observant reader will notice that all small blocks have almost the same shape, quadratic, and that the cavern is excavated before the actual analysis starts by using the hole point command in DL

A total number of 27 analysis examples are available in version 96 of DDA, some very simple and others more advanced. However, almost every example with the description "tunnel or tunnels in a blocky rock mass" shows the same geometry or at least a very similar one. But why? Everybody working with engineering geology and rock mechanics knows very well that the rock mass is an extremely complex building material, that varies from place to place depending on the geological history. The reason is evidently that none of today's programs are able to create a correct picture of the jointed rock mass, and every single model is built on approximations.

5.6.2 In-situ Stresses and Boundary Conditions

Both overcoring and hydraulic fracturing showed virgin horizontal stresses of the magnitude of 3.5 - 4.5 MPa in the cavern area, which is quite high considering the moderate rock cover (Hansen and Kristiansen, 1994). The stress profiles adopted in the models, are described as follows: The vertical stress is a result of the weight of overburden and identical for all models. In Model 5, the horizontal stress is twice as the vertical across the whole model, while the other models have horizontal stress like 0 MPa at the surface, 4.5 MPa at the crown of the cavern, and from there to the bottom of the model the ratio between the horizontal and vertical stress is equal to one. The stress profiles used in Model 1 - 4, are identical to the stress profiles which NGI made use of in their UDEC calculations.

The boundary conditions are identical in all cases. A block which defines the outer boundary of the model is equipped with fixed points, that prevent any displacements in x-direction and y-direction.

5.6.3 Intact and Jointed Rock Parameters

The mean values of Young's modulus E and the Poisson's ratio (ν) measured in laboratory tests of the drill cores are 51.2 GPa and 0.21, respectively. Due to the size of specimens, these cannot represent the rock mass. Thus, the corresponding elastic parameters for the rock mass are obtained from Bieniawski's Geomechanics Classification system: E = 30 GPa and ν = 0.21. The degree of rock weathering is taken into account in the modelling, and therefore variation in E from 20 - 40 GPa is introduced. The upper 45 m of the model has E equal to 20 GPa, while the next 25 and 50 m, have 30 GPa and 40 GPa, respectively. The rock density is 2650 kg/m^3.

The joint properties in DDA are friction angle, cohesion and tensile strength. The friction angle of joint set one is 32 °, while the values for the second and third joint set vary between 24 and 30 °. The cohesion is 0.2 and 0.3 MPa respectively and the tensile strength is zero.

5.6.4 Stage Excavation

For all Model 1 - 4 cases, a five stage excavation (Figure 5.16) sequence is applied in accordance with the real excavation. In order to be able to explore if there is any noticeable difference between sequential and immediate excavation the whole cav-

ern is also excavated in one stage in some cases.

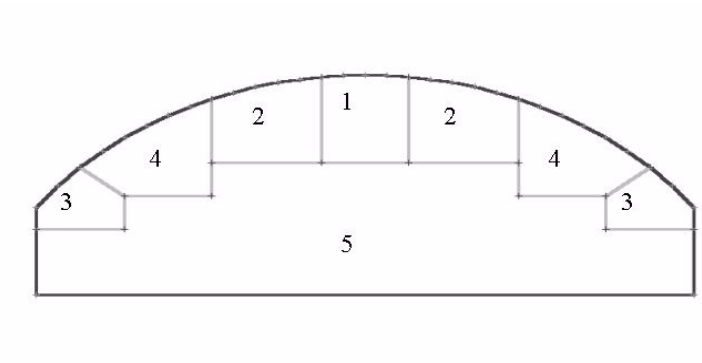

FIGURE 5.16 Cavern construction process

5.7 Analysis Results and Discussion of Results

A total of 5 different geometry models are analysed, with different strength parameters, in-situ stresses and number of time steps, so the total number of cases exceeds fifty. The quality of the analysis results is somewhat varying, which is strictly related to the problems mentioned in section 5.6.1 Implementing measured discontinuities in a numerical model. However, in general the results show agreement with both the reality and the analysis results from the NGI UDEC analyses, in the sense that the large span cavern is stable. An accurate comparison of the analysis results and measured values is not possible, since the applied version of DDA does not quantify the cavern crown subsidence. The results from all cases will not be presented and discussed in detail, but main features and data that might be of interest for further development and improvements will be presented.

Model 1 was used as a test model for controlling the changes and new subroutines introduced in program DF (Kyoto version). The computation was quite fast because of the relatively small amount of rock blocks, and the analyses showed acceptable results with respect to the input. Problems with blocks flying in all directions and into other blocks occurred during some of the first analyses. This is caused by large variation in block size, which leads to calculation problems of the stiffness matrix. The problem was solved through an little change in the source code.

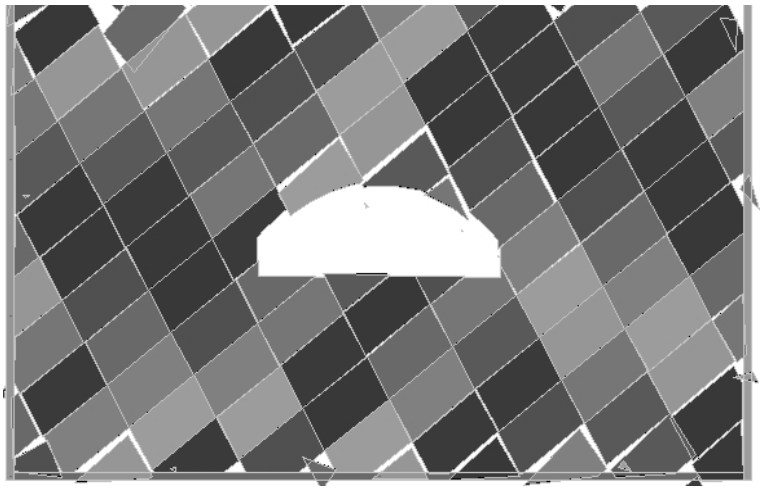

FIGURE 5.17 Flying blocks Model 1

However, the model was not realistic compared with the mapped geology, since the size of the rock blocks compared to the span of the cavern is too big. Model 2 and 4 have exactly the same joint geometry as Model 1, but here the spacings between the joint sets are reduced several times.

The allowable number of time steps before program crash, varies for the different models. As an example, Model 2 with 3616 blocks shows signs of being too large for the portable computer, a Pentium III, 600 MHz and 128 MB, used in this work. It was only possible to go through a very few time steps before the program collapsed. It is of course natural to set up a question mark concerning the model geometry.

The geometry of Model 3, was also unfavourable for the computation, since the different rock blocks vary considerably in size. Thus, the geometry of Models 4 and 5, were mainly made use of in the parameter study, and all cases showed that the large span cavern is stable. Change of friction angle for Model 4 has mostly negligible

influence on the stability. The results are almost identical, except for one case where two-three blocks close to the excavation surface, indicate movements.

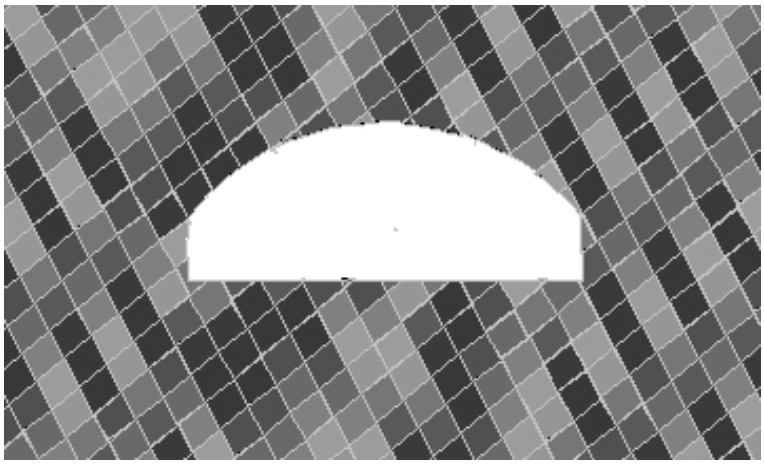

FIGURE 5.18 Analysis result Model 4, friction angle of joint sets 32 and 30 °

This is caused by the orientation of the joint set compared to the magnitude of the friction angle. Sequential excavation, has no influence on the stability. Variation of Poisson's ratio gives different analysis results. This is illustrated in Figure 5.19.

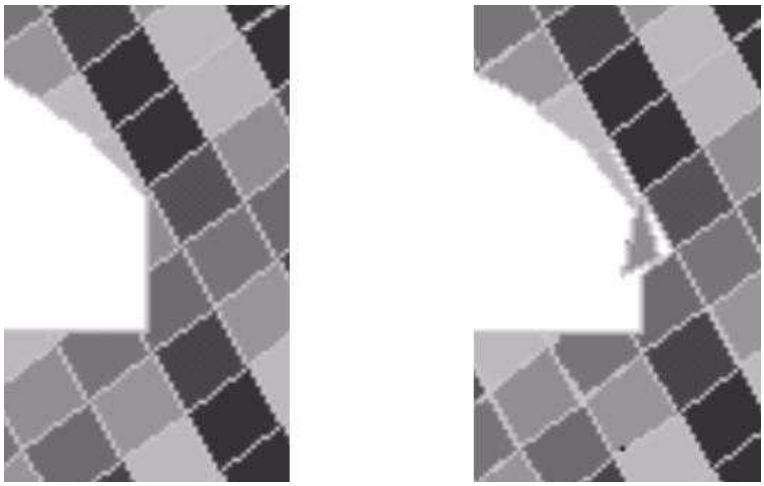

FIGURE 5.19 Block movements Model 4, varying Poisson's ratio left $\nu = 0{,}2$ and right $\nu = 0$

The results from Model 5, do not differ much from the Model 4 results. The influence of changing the friction angle shows exactly the same tendency as for Model 4. While Model 4 has a varying E values, Model 5 has the same value for the whole model, and the model was therefor analysed for different E values. For example changing of the E from 40 to 30 GPa, gives a less stiff rock mass and it is therefore logical to think that the deformation will make the block movements increase. However this is not the situation.

The block geometry seems to have a surprisingly small effect on the calculation results, since both Model 4, which has continuous joints, and Model 5, which has a substantial degree of discontinuous joints, are stable.

The reason for this is mainly favourable tectonic horizontal in-situ stresses, which provide sufficient constraint.

FIGURE 5.20 Model 5 analysis result - 5000 steps

Model 5 is for one parameter combination analysed for both 2500 and 5000 time steps. The block movements for the 5000 step calculation are noticeable compared with the 2500 time step calculation. The situation without any rock support tends to be unstable. The reason why not all cases are calculated for 5000 step, is that the calculation process is fairly time-consuming.

5.8 Strengths and Limitations of Discontinuous Modelling with DDA

DDA is both a computer program and a theory. The modelling procedure for DDA resembles the distinct element modelling procedure with UDEC, while it more closely parallels the finite element method with respect to: i) Minimizing the total potential energy to establish equilibrium equations, ii) Choosing displacements as unknowns of the simultaneous equations and iii) Adding stiffness, mass and loading submatrices to the coefficient matrix of the simultaneous equation. The equilibrium equations are derived by minimizing the total potential energy. The

displacements are the unknowns, and the stiffness, mass and loading submatrices are added to a submatrix in the global equation.

In DDA and discontinuous modelling, the joints are allowed for explicitly. Compared with the nature of the rock mass, this represents a strength. As an example, it is possible to predict potential rock falls or to study details of the local instability. It is however very difficult to create a reliable model of the jointed rock mass, because of limited access to exposured rock faces, especially for underground projects.

From an engineering point of view the introduction of sequential excavation, material areas and universal equations for the in-situ stress definition increases the user-friendliness, and applicability of the program. However, the quality of the results is completely dependent on the input parameters from field and laboratory work.

Both statics and dynamics are taken into consideration in DDA. The only difference is that static computations assume velocity equal to zero in the beginning of each time step, while dynamic computations inherit the velocity of the previous time step.

According to Shyu et al (1997) the major advances of DDA are the “open- close iteration” and “inertia matrix”. Open-close iteration is the algorithm to find the correct contacts of the block system, and to satisfy the convergence criteria of no-tension and no penetration conditions at any points. An accurately-integrated inertia matrix controls the stability of the open-close iteration, and large displacements and deformations are the accumulations of the small increments from each time step. Ma (1999) refers to some other major features as for example topological identification of block systems, simultaneous rigid body movement and deformation, and possibility to implicitly couple DDA with FEM or BEM.

But there are limitations, which have been experienced during this work. If the geometry is defined in such a way that the proportions between the different blocks in a model is considerably large, or if the angle between two joints are approximate zero the computation cracks up.

Other limitations are that stresses and strains are constant within any given block, because of the first order formulations, and that blocks are not allowed to fracture. Further, pore water pressure are not taken into consideration, even if this is an important factor in many types of geotechnical and rock mechanics problems. Further, the post processing possibilities are limited compared to for example UDEC, but of course satisfactory for localizing potential failure blocks.

According to Ma (1999), other limitations are numerical truncations and round-off errors, which are inherent all numerical methods. DDA uses an implicit formulation and guarantees numerical stability regardless of the size of time steps, but it does not guarantee accuracy.

5.9 Summary

The purpose of this chapter is to demonstrate different aspects of discontinuous modelling. The Discontinuous Deformation Analysis (DDA) is used as a representative program tool, and Gjøvik Olympic Mountain Hall is picked out as a case study because of the large amount of available input data from several reports worked out by the research institutions SINTEF and NGI and the consultant Noteby.

Several program versions of DDA exist today, and a number of groups throughout the world are working on DDA development. However, bad compatibility between the different versions is a very huge drawback, and a challenge for the future is therefore to collect all important improvements and developments in one program package. Compared with e.g. UDEC, DDA is so far less user friendly.

The biggest challenge for discontinuous modelling is to create a reliable model of the jointed rock mass. Some programs have their own pre-processor for generating block systems, but the quality of the results is varying and of course dependent on the input parameters. Shi's DL program updated March 2002 seems to give a much better result than the 96 version, but the result is not at all realistic compared with the field situation. This is not only a problem for DDA, but a general problem for discontinuous modelling, and still in a foreseeable future a major weakness that prevent realistic results in practical engineering.

Another element of uncertainty related to the joint pattern is where to locate a construction in relation to the selected joint geometry. Moving a tunnel or cavern a few meters to the left, right, up or down may give totally different analysis results, because of different combinations of orientation and number of joints along the excavation boundary.

A total of five different geometry models of the Gjøvik Olympic Mountain Hall are introduced and analysed for various values of material parameters, and in-situ stress situations. As mentioned above it is very difficult to create a correct model of the jointed rock mass. The normal procedure is then to make approximations, which inevitably will give uncertainties in the results. This procedure is also applied in this work.

Almost all analysis results showed that the large span cavern is stable. This is in accordance with both the reality and the results from the UDEC analyses carried out by the Norwegian Geotechnical Institute. It is very important to note that the main reason for the cavern stability is favourable tectonic horizontal in-situ stresses.

DDA has problems treating models with large numbers of blocks, especially if the size and shape of the blocks vary considerably. This is a usual problem also for other discrete element programs. A flying block phenomena occurred in some parameter combinations. Thus, Model 4 and Model 5 were mainly used in the parameter study. Modifications for the input of rock mass properties and in-situ stresses are accomplished, and sequential excavation were introduced in the Kyoto version in order to make the program more user friendly.

Discontinuous modelling is time consuming and expensive, and the best way to obtain experience is through trial and error. The modelling process requires far more advanced knowledge about: i) The geological field mapping and implementation of measured discontinuities into a numerical model and ii) The in-situ rock stress field. Critical evaluation of the results is absolutely necessary, preferably in combination with field observations.

Further development of both existing mapping techniques and existing methods for implementation of measured discontinuities into a numerical model, is necessary before discontinuous modelling may be used as a realistic practical tool for underground hard rock problems. Shortcomings of today's mapping techniques are discussed in Chapter 3. Supposing the geological field mapping results to be satisfactory for a particular problem, an implementation method which includes a minimum of approximations is manual input of each measured discontinuity. But this is extremely time consuming and usually not of current interest for underground projects because of limited access to exposured rock faces and with that restricted information on discontinuities. Thus, mapping information from random rock exposures combined with statistics are basis for the establishment of a numerical model. Today's combination is not good enough to obtain a correct and realistic model of the jointed rock mass without taking too many approximations into consideration.

CHAPTER 6

Continuous Modelling - Phase^2 and Gjøvik Olympic Mountain Hall

6.1 Introduction

In continuous modelling, the rock mass is treated as a continuous medium, and only a limited number of discontinuities may be included. This is the most commonly used category of numerical modelling, and includes the finite element method (FEM), the finite difference method (FDM) and the boundary element method (BEM). FEM, represented by Phase^2, is selected as a representative tool for the continuous modelling part in this work, and in this chapter different aspects of continuous modelling are demonstrated and discussed.

As in the discontinuous modelling part, the Gjøvik Olympic Mountain Hall is selected as a case study. Geological and technical information about the large span cavern has already been presented in Chapter 5. More than 50 different analyses have been carried out, with different in-situ stress situations and strength and deformability parameter values. Mohr-Coloumb's failure criterion is utilized in about 80% of the analyses, which is the same criterion used in the former FEM analyses carried out by SINTEF Civil and Environmental Engineering. In the remaining cases the rock mass properties are defined by Hoek-Brown parameters. The analysis results have been compared with stress and deformation measurements performed in connection with the construction of the cavern.

6.2 Phase^2

Phase^2 is a two dimensional non-linear finite element program, developed by Rocscience Inc., a geomechanics software development company in Toronto, Canada. The program calculates stresses and displacements around underground openings.

Phase^2 provides an integrated graphical environment for data entry and visualization, and a CAD based modeler allows for point and click geometry input and editing (Figure 6.1). The state of the art automatic mesh generation facilities allow convenient performance of parametric studies, and the graphical data interpreter provides an extensive array of tools for the display of analysis results (Rocscience, 2002).

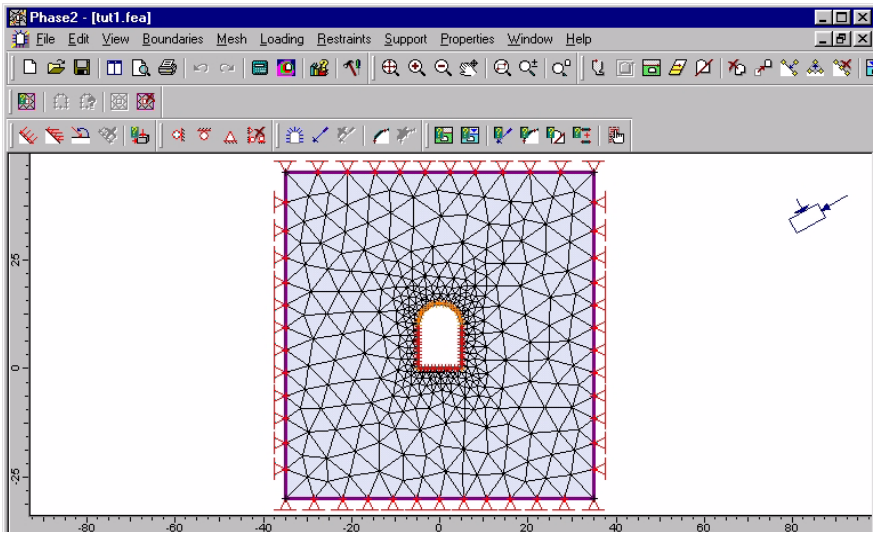

FIGURE 6.1 Picture of Phase^2 layout

6.3 Continuous modelling

6.3.1 Implementing Measured Strength Parameters in Modelling

Chapter 5 illustrates different difficulties of setting up a reliable discontinuous numerical model, and that the final model usually is a result of several approximations from both the field part and the modelling work. Continuous modelling is an alternative to discontinuous modelling, where the joints are taken into consideration implicitly, i.e. the rock mass quality is described by strength and deformability parameters through a failure criterion.

Most geotechnical software has Mohr-Coulomb failure criterion, but in Phase^2 the Hoek-Brown criterion is also available. Required input for the numerical model is dependent on the selected failure criterion, and as mentioned above both Mohr-Coloumb and Hoek-Brown have been utilized in this work.

There is no direct correlation between the two failure criteria, and consequently determination of Hoek-Brown parameters for a rock mass that has been evaluated as a Mohr-Coulomb material and vice versa, is a difficult task, that has been topic for several researchers during the last years. Details about this is beyond the scope of this work, but for those who are interested the paper "A brief history of the development of the Hoek-Brown failure criterion" prepared by Hoek (2002) is recommended.

Based on former work carried out by SINTEF, NGI and Noteby, independent Mohr-Coulomb and Hoek-Brown parameters have been determined. The procedures are listed in section 6.3.1.1 and 6.3.1.2.

6.3.1.1 Mohr-Coulomb Input

In the Mohr Coloumb's failure criterion, the rock mass strength is defined by the cohesive strength, c, and the friction angle, ϕ. The relationship between the major and minor principal stresses σ_1 and σ_3 for the Mohr Coloumb criterion is:

$$\sigma_1 = \sigma_{cm} + k\sigma_3 \qquad \text{(Hoek,2000)} \qquad \textbf{[6-1]}$$

where σ_{cm} is the uniaxial compressive strength for the rock mass and k is the slope of the line relating σ_1 and σ_3.

$$k = \frac{1 + \sin\phi}{1 - \sin\phi} \quad \text{[6-2]}$$

$$\sigma_{cm} = \frac{2c\cos\phi}{1 - \sin\phi} \quad \text{[6-3]}$$

Mohr Coulomb parameters for intact rock can usually be found from laboratory triaxial tests, or direct shear tests. However, for some reasons the tests were not performed, and the cohesion and friction are obtained from a linear fit of the Barton Bandis peak shear strength envelope based on the parameters measured by NGI. For the B-B parameters JRC = 7.5, JCS = 75 MPa, ϕ_r = 27° and i=6°, the resulting M-C parameters are ϕ_r=39.5° and c=0.3 (Lu, 1994).

JRC	joint roughness coefficient
JCS	joint wall strength
ϕ_r	residual friction angle
i	roughness component
c	cohesion

These parameters are for rock joints and are therefore used as the lower bound of the corresponding parameters for the rock mass.

Due to weathering three different rock materials (1-3) are introduced (Figure 6.2). Material 1 has best rock mass quality and material 3, located close to the surface poorest. The mean value of the Young's modulus (E) and Poisson's ratio (ν), measured in laboratory tests of the drill cores are 51.2 GPa and 0.21, respectively.

These values are from small specimens and cannot represent the rock mass. The corresponding elastic parameters for the rock mass, E =30 GPa and ν=0.21, are obtained from Bieniawski's Geomechanics Classification system based on the uniaxial compressive strength, RQD, groundwater condition and joint parameters (Lu, 1994).

Thus, Materials 1 - 3 are assumed to have E values like 40, 30 and 20 GPa, see Figure 6.2. The density of the rock mass is 2650 kg/m^3.

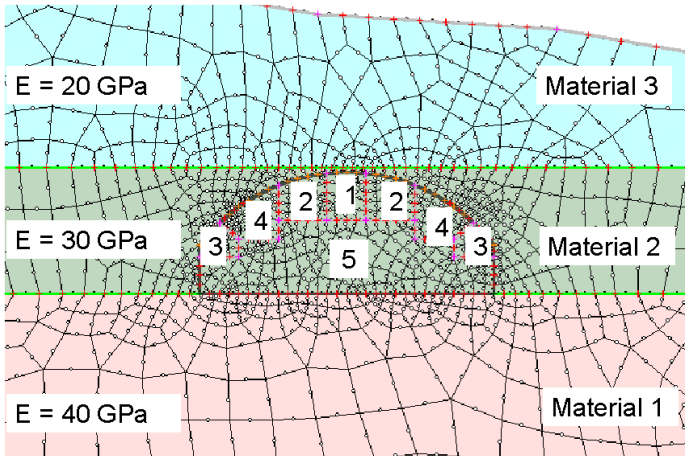

FIGURE 6.2 A section of the Phase^2 model of Gjøvik Olympic Mountain Hall

6.3.1.2 Hoek-Brown Input

The Hoek-Brown criterion is based upon an assessment of the interlocking of rock blocks and the conditions of the rock face. It has been modified over years in order to meet the needs of users who were applying it to problems that were not considered when the criterion was developed (Hoek, 2002). The generalized Hoek-Brown failure criterion for jointed rock mass is defined by (Hoek, 2000):

$$\sigma_1 = \sigma_3 + \sigma_{ci}\left(m_b\frac{\sigma_3}{\sigma_{ci}} + s\right)^a \quad \textbf{[6-4]}$$

where

σ_1, σ_3 = maximum and minimum effective stresses at failure

m_b = Hoek Brown constant for the rock mass

s, a = constants that depend upon the rock mass characteristics

σ_{ci} = uniaxial compressive strength of the intact rock pieces

For intact rock, the failure criterion is simplified to:

$$\sigma_1 = \sigma_3 + \sigma_{ci}\left(m_i\frac{\sigma_3}{\sigma_{ci}} + 1\right)^{0,5} \quad \textbf{[6-5]}$$

Required input parameters for Phase[2] are compressive strength and the constants m_b and s. The former is estimated in the laboratory, while the constants m_b and s may be determined by using the formulas below:

$$m_b = m_i \exp\left(\frac{GSI - 100}{28}\right) \quad \text{[6-6]}$$

$$s = \exp\left(\frac{GSI - 100}{9}\right) \quad \text{GSI >25}$$

$$a = 0.5 \quad \text{GSI>25}$$

$$s = 0 \quad \text{GSI<25}$$

$$a = 0.65 - \frac{GSI}{200} \quad \text{GSI<25}$$

The geological strength index, GSI, and the constant m_i, may be found from a combination of field inspections and tables developed by Hoek and Brown, and based on experience, or by using (Singh and Goel 1999), which assumes that RMR and *Q'* are known:

$$GSI = RMR - 5 \quad \text{for GSI } \geq 18 \text{ or RMR } \geq 23 \quad \text{[6-7]}$$

$$GSI = 9 \ln Q' + 44 \quad \text{for GSI<18}$$

Q' is a modified tunneling quality index, $[RQD/J_n]\cdot[J_r/J_a]$, and RMR is a shortening for the rock mass rating system. RMR was initially developed by Bieniawski and is based on the six parameters:

1. Compressive strength
2. Rock quality designation (RQD)
3. Joint or discontinuity spacing
4. Joint condition
5. Ground water condition
6. Joint orientation.

If the Q value ($[RQD/J_n]\cdot[J_r/J_a]\cdot[J_w/SRF]$) of the rock mass is already known, one of the correlations listed below may be used to determine RMR (Singh and Goel 1999).

$RMR = 9\ln Q + 44$	Bieniawski
$RMR = 5.9\ln Q + 43$	Rutledge and Preston
$RMR = 5.4\ln Q + 55.2$	Moreno
$RMR = 5\ln Q + 60.8$	Cameron-Clarke and Budavari
$RMR = 10.5\ln Q + 41.8$	Abad et al

An interesting question is however which formula will give the most reliable answer for a specific problem to be analysed?

In the case of Gjøvik Olympic Mountain Hall, NGI found a typical best rock mass quality Q=30, while the typical poorest quality was Q=1.1. Thus, the weighted average of Q was 11.6, which is described as a good quality. RMR values calcu-

lated from the formulas above are:

66 57 68 73 68

respectively, and as the reader may see, there are some differences in the results. Average RMR value is 66, and that gives an average GSI value of 61. Quoting a range of GSI from 55 - 65 is however more realistic, because of elements of uncertainty.

GSI, RMR and Q are useful indices for rock mass classification, but all correlations between the different systems should be treated with scepticism, since the basis material are limited, and not representative for all rock types.

Average compressive strength value from the laboratory testing of the quartz dioritic gneiss is 75 MPa, while the constant m_i is estimated to lie in the range of 20 - 30.

6.3.1.3 Mohr-Coulomb versus Hoek-Brown

In Hoek's Practical Rock Engineering, Edition 2000, a spreadsheet for calculation of Hoek-Brown and equivalent Mohr-Coulomb parameters is presented. This is made use of in order to compare calculated results of ϕ and c, with applied parameter values for Mohr-Coulomb, that are estimated independent of the Hoek-Brown input.

The calculation is based on linear regression analysis, and necessary input are uniaxial compressive strength of the intact rock pieces, the Hoek-Brown constant m_i and GSI. ϕ and c are then calculated from [6-2] and [6-3].

According to Hoek (2000), the most critical step in this process is the selection of the range of values of the minor principal stress σ_3. No theoretically correct method for choosing this range exists, but on basis of trial and error, it has been found that the most consistent results are obtained when 8 equally spaced values of σ_3 are used in the range $0<\sigma_3<0.25\sigma_{ci}$.

The following input and output

Hoek-Brown input	Mohr-Coulomb output
σ_{ci} = 75 MPa	ϕ = 43.4°
m_i = 28	c = 4.75
GSI = 60	

show that the calculated friction angle lies within the applied range of analysis values, 40-45°. The cohesion is however more than ten times larger than the value estimated in section 6.3.1.1.

In order to inquire whether the range of σ_3 may explain the "large" cohesion value or not, the range was changed such as $\sigma_{3\ max}$ was 4.5 MPa. The calculated results show ϕ=54.81° and c=1.82 and this means that linear curve fitting results in higher friction and lower cohesion when the maximum value of σ_3 is reduced. The gradient of the curve increases. This calculation method will never result in values that correspond to the estimated and applied Mohr-Coulomb parameters, unless other values of σ_{ci}, m_i and GSI are selected.

An interesting question is therefore if we should rely on measured values from field works for a current project, or on calculations based on experience from selected case studies?

It should be stressed that Mohr-Coulomb and Hoek-Brown are two different and independent failure criteria. Required input for the modelling should therefore be gathered directly from field measurements for the particular problem. Correlations based on experiences from selected studies should be treated with caution since the rock mass is a complex building material, that varies considerably in composition from place to place.

Input:	σ_{ci} =	75	MPa	m_i =	28		GSI =	60	
Output:	m_b =	6,71		s =	0,0117		a =	0,500	
	k =	5,40		**ϕ =**	**43,43** °		**c =**	**4,75 MPa**	
	σ_{cm} =	22,07	MPa	E =	15400,4	MPa			

Calculation:

σ_3	1,00E-10	2,68	5,36	8,24	10,71	13,39	16,06	18,75	*7,52E+01*
$\sigma_{1\ H\&B}$	8,13	40,28	57,91	73,16	84,59	95,89	106,33	116,23	*582,53*
$\sigma_3*\sigma_1$	0,00	107,90	310,25	602,93	906,36	1284,28	1707,64	2179,31	*7098,68*
σ_3^2	0,00	7,17	28,70	67,93	114,80	179,37	257,92	351,56	*1007,45*
σ_3	1,00E-10	2,68	5,36	8,24	10,71	13,39	16,06	18,75	
$\sigma_{1\ M\text{-}C}$	22,07	36,53	50,99	66,57	79,92	94,38	108,78	123,30	

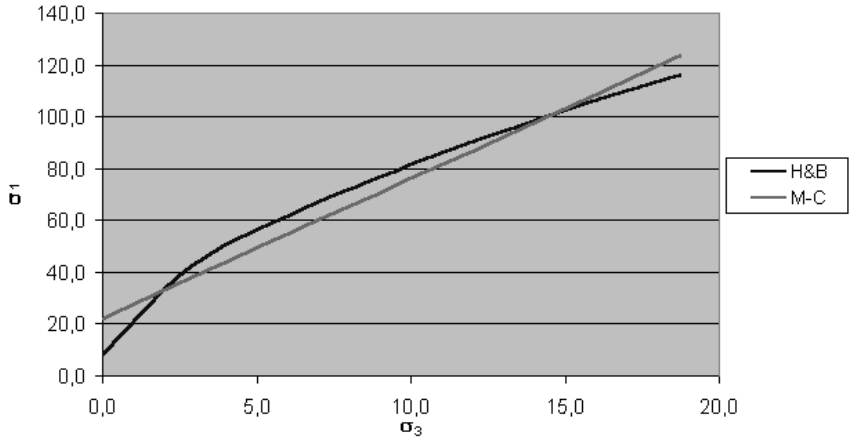

FIGURE 6.3 Spreadsheet for calculation of Hoek-Brown and equivalent Mohr-Coulomb parameters (after Hoek, 2000)

6.3.2 In-situ Rock Stress

In order to study the influence of the in-situ stress, different in-situ horizontal stress conditions are taken into consideration.

The vertical in-situ stress distribution is identical for all analyses and a result of the weight of the overburden $\sigma_v=\rho gh$. The gradient of the in-situ horizontal stress is constant from the surface to the bottom of the models in Group 1. Group 2 represents situations where the horizontal stress increases considerably, compared to the vertical stress, from the surface to the cavern crown level. After that the increase for the horizontal and vertical in-situ stresses are equal.

6.3.3 Finite Element Mesh, Boundary Conditions and Construction Sequence

The cavern is situated relatively close to the surface with uneven topography, and the N-W side higher than the SE-side. The two dimensional model is taken at the caverns central cross section, and to eliminate the influence of the applied boundary conditions and correctly simulate the effect of the ground topography, the finite element mesh stretches to the ground surface and extends in lateral directions three times the cavern span (62 m). The mesh consists of 1171 8-node elements and have 3609 nodes.

The modelling starts with generating the initial stress field, and this is followed by a five stage excavation process. In a couple of cases rock bolts are taken into account in each excavation stage (Figure 6.4). The bolting consists of alternate 6 m fully bonded bolts, and 12 m plain strand cables in a 2.5 by 2.5 m pattern, 5 by 5 m respectively. The former has a diameter of 25 mm and a capacity of 220 kN, while the latter has a diameter of 12.5 mm each and total capacity of 334 kN at yield.

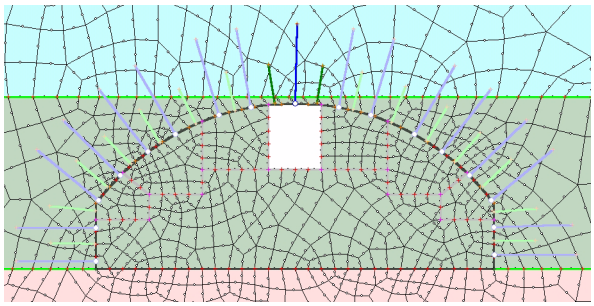

Stage 1

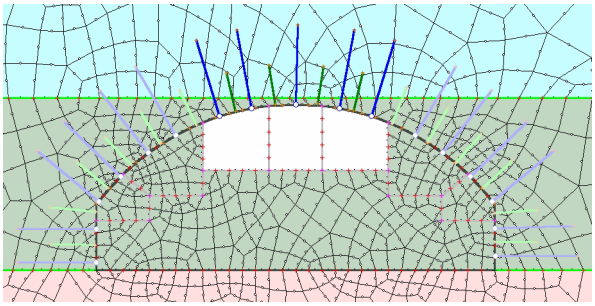

Stage 2

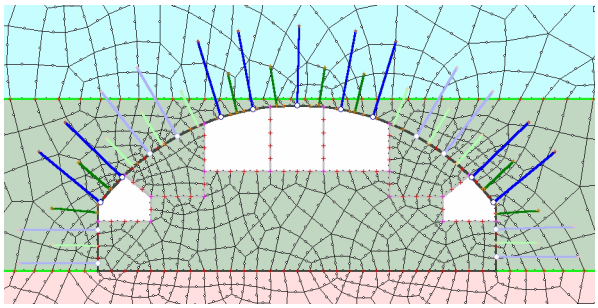

Stage 3

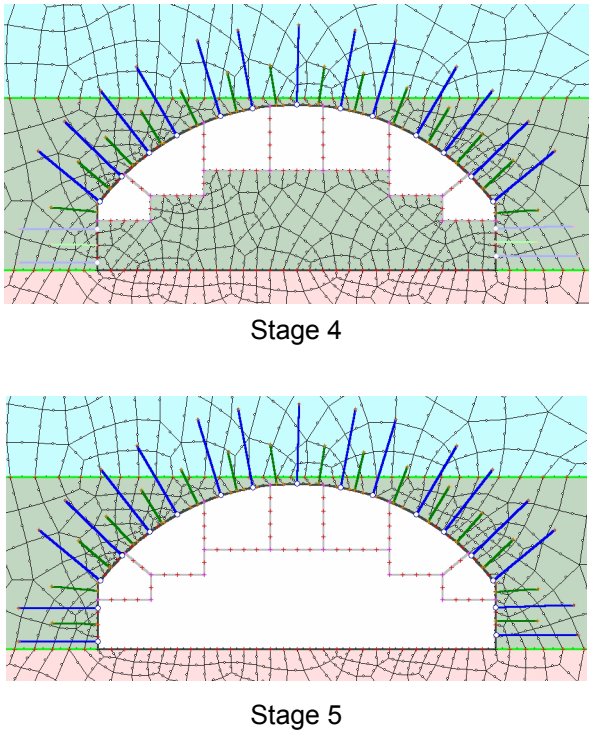

FIGURE 6.4 Sequential excavation with rock bolts

6.4 Analysis Results and Discussion of Results

More than 50 different analyses have been carried out. Appendix A, gives an overview of the different combinations of input parameters. Results from Mohr-Coulomb and Hoek-Brown analyses are presented and discussed separately, compared with the measured values, and then followed by a common summing up.

6.4.1 Mohr-Coulomb Analyses

A total of about 40 cases have been analyzed with varying combinations of input parameters. Upper and lower limit of horizontal in-situ stress conditions are taken into consideration, and rock bolts are included in a couple of cases.

In Group 1, the ratio of vertical and horizontal in-situ stress components is constant from the surface to the bottom of the model, and analyses are carried out for models with stress ratio of 0.5, 1.0, 1.5, 2.0, 2.5, 3.0, 3.75 and 4.0, respectively. Group 2 consists of analyses with varying stress ratio. Selected ratio from surface to the cavern crown level is 1.4, 1.7, 2.1, 2.5, 2.9 and 3.7, respectively, while the ratio is constant and equal to 1.0 for all models, from cavern crown level to the bottom of the model. Both linearly elastic and non-linear analyses are carried out, and for Group 2, the influence of changing the material parameter values is studied.

6.4.1.1 Linearly-elastic Analysis Results

Linearly-elastic analysis results from both Group 1 and 2 are summarized in the following points:

1. Higher horizontal in-situ stress produces less cavern crown subsidence. This agrees with a rule of thumb, which says that high horizontal in-situ stress is necessary to obtain sufficient constraint and stability of a large span cavern. The magnitude of the cavern crown subsidence varies from 0.5 mm to about 4 mm

2. Except for the last excavation stage, the cavern crown subsidence increases during the excavation process, and this is due to the establishment of full span at stage 4.

6.4.1.2 Non-linear Analysis Results

Non-linear analyses require three more input values than the linearly elastic ones. In addition to tensile strength and peak values of friction angle and cohesion, dilation angle and residual values of the friction angle and cohesion are necessary. Main points from the non-linear analysis results are presented below:

1. The existence of high horizontal in-situ stress has opposite influence compared to the linearly-elastic analyses. Higher horizontal in-situ stress results in both higher cavern crown subsidence, floor uplift and deformations. This may be explained by rock mass yielding, which is caused by differential principal

stress, σ_1-σ_3. In the case of Gjøvik Olympic Mountain Hall, the vertical in-situ stress, σ_v, is always σ_3, and the horizontal in-situ stress, σ_h, is always σ_1, in the roof, and $\sigma_h > \sigma_v$. A higher σ_h causes a larger σ_1-σ_3, and consequently higher yielding and larger deformation (Figure 6.5).

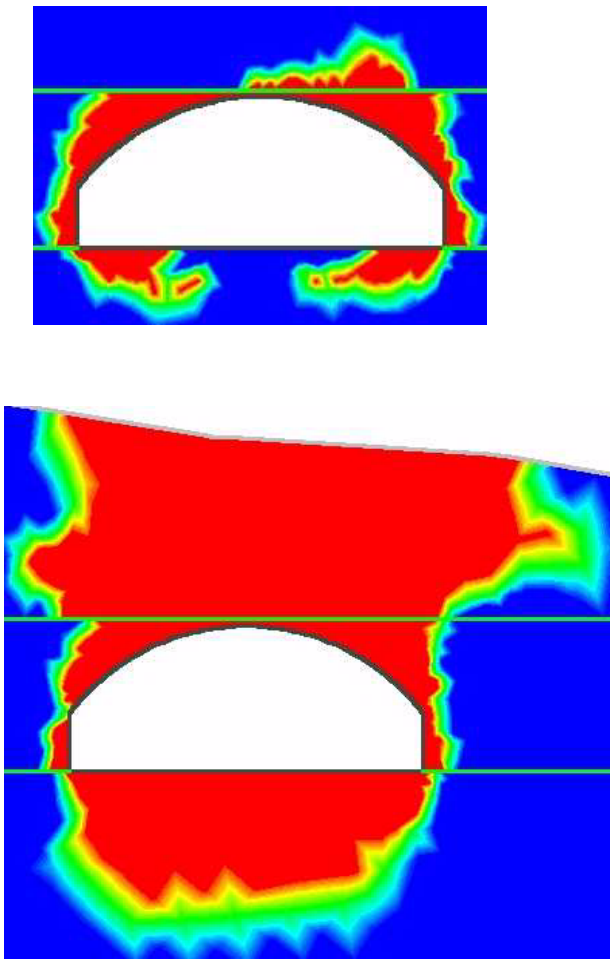

FIGURE 6.5 Yielded elements a) low stress ratio and b) high stress ratio - yielded elements =100% in red areas

2. The calculated cavern crown subsidence for the non-linear analyses vary from 0.5 mm to about 35 mm. This is due to the fact that the cavern crown subsidence is very sensitive to the Mohr-Coulomb parameters, especially for analyses with stress ratio larger than 1.5. The worst case of cavern crown subsidence is represented by one of the cases in Group 2, where the stress ratio is 3.7 from surface to the cavern crown level and 1.0, from here to the bottom. The cavern crown subsidence is reduced with 30% if the friction angle increases with 5°, and the tensile strength with 2 MPa. An increase of the cohesion from 0.5 to 4.5 for the same case, gives a reduction of the cavern crown subsidence of 79%.

3. The cavern crown subsidence increases during the excavation process, which means that the deformation of the rock mass is related to the excavation sequences. The increase is especially noticeable from stage 1 to stage 2, where the span is tripled, and from stage 3 to stage 4, where fully span is established. From stage 4 to 5, the increase is almost negligible, so the deformations are directly connected to the excavation of the top slice.

4. The influence of rock bolts is studied for a couple of cases. Rock bolts are taken into account in each excavation step, and the results show that the effect of rock bolts is stronger for high in-situ horizontal stress cases than for low in-situ stress cases. The reason is that higher σ_h causes higher degree of plastification.

   Far from all bolts show loads, and if loads occur, these are in the parts of the rock bolts close to the excavation surface. As an example, maximum and minimum loads for the case with constant stress ratio 0.5 are 100 and 0 kN, respectively. For a case with constant stress ratio equal to 3, maximum load is increased to 210 kN, while the minimum is close to zero, 0.004 kN, and the total deformation at the cavern crown subsidence is only reduced with 8.5%. The maximum values are registered in one of the fully bonded bolts with length 6 m. Average load of the 12 m long cables is about 30 kN, which is less than 10% of the capacity.

   The majority of the rock bolts show relative low loads, and indicate that the bolts only take care of local stability. Favourable horizontal stresses provide sufficient constraint, and the roof is so-called self-supporting. Figure 6.6 a) and b) show axial forces on the rock bolts for the low and high stress ratio case, respectively.

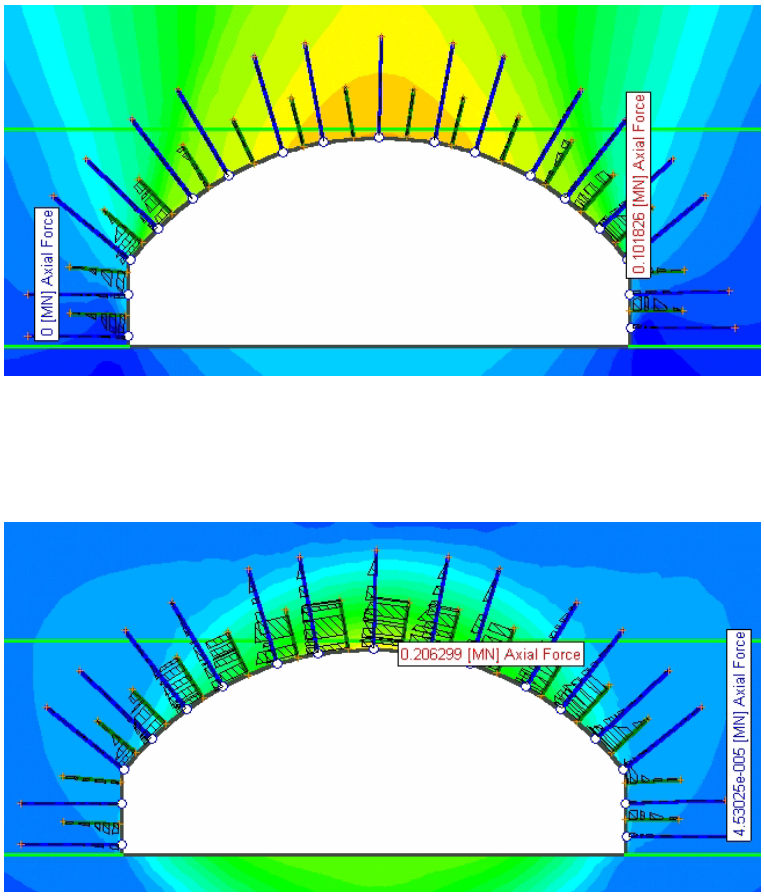

FIGURE 6.6 a) Axial forces on rock bolts - low stress ratio and b) Axial forces in rock bolts - high stress ratio. Minimum and maximum values are shown

Figure 6.7 and Figure 6.8 illustrate graphically, the main analysis results for the Mohr-Coulomb analyses, that are described and discussed above.

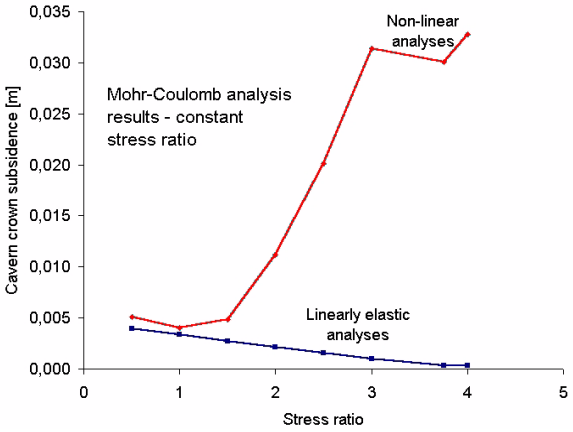

FIGURE 6.7 Stress ratio vs. cavern crown subsidence - Mohr-Coulomb & constant stress ratio

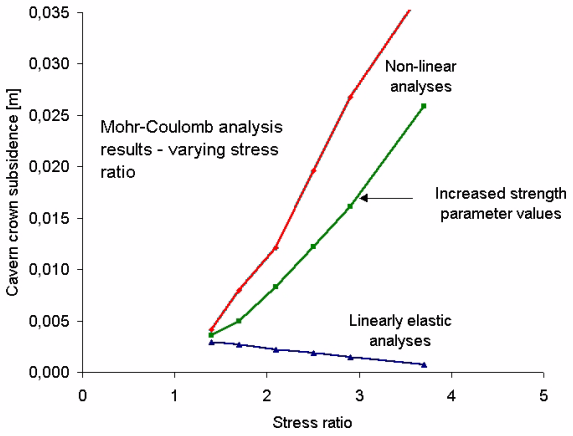

FIGURE 6.8 Stress ratio vs. cavern crown subsidence - Mohr-Coulomb & varying stress ratio

6.4.2 Hoek-Brown Analyses

Only non-linear Hoek-Brown analyses are carried out. The horizontal in-situ stress distribution is equal with the Mohr-Coulomb Group 2 analyses, but the analysis results show opposite trend compared to the non-linear Mohr-Coulomb analyses. Higher horizontal in-situ stress gives lower cavern crown subsidence and deformations, while the floor uplift is almost the same for all stress ratio cases. The magnitude of the cavern crown subsidence lies between 0.5 and 3.5 mm, which is considerably less than for the Mohr-Coulomb models (Figure 6.9).

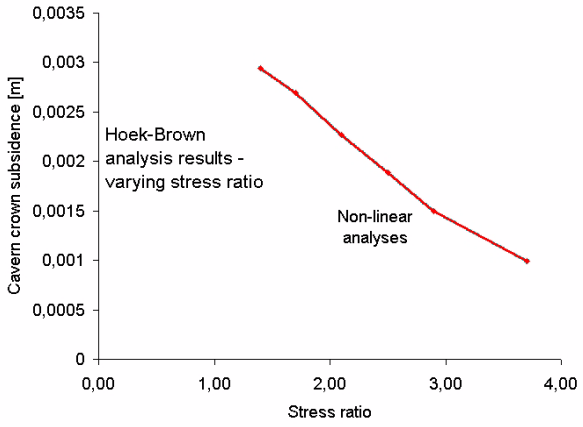

FIGURE 6.9 Stress ratio vs. cavern crown subsidence - Hoek-Brown & varying stress ratio

The difference between Mohr-Coulomb and Hoek-Brown analysis results may be explained by the following:

1. According to the spreadsheet presented in Figure 6.3, the Hoek-Brown material is of better quality than the Mohr-Coulomb material. For σ_3=0, which is the situation on the cavern contour, the Mohr-Coulomb criterion gives uniaxial compressive strength of about 2.25 MPa, while the Hoek-Brown criterion gives a value of about 6 MPa. A plot of the two different failure criterion curves in a σ_1–σ_3 diagram (Figure 6.10) shows that the probability for failure is larger for the Mohr-Coulomb material than for the Hoek-Brown material.

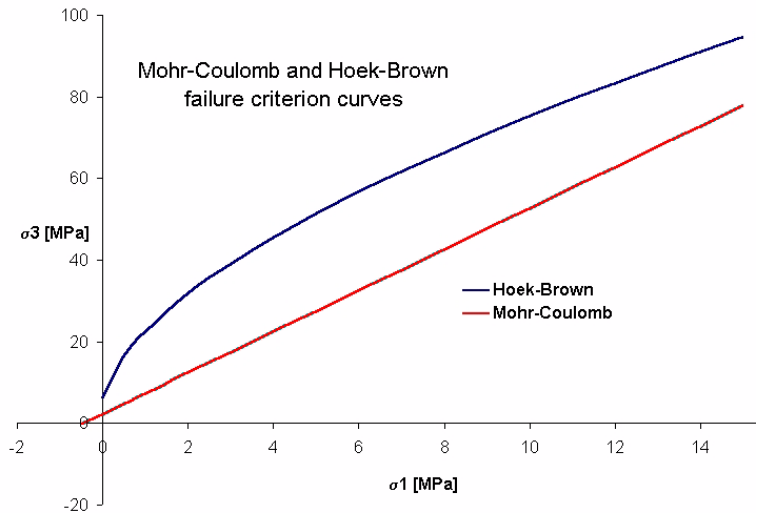

FIGURE 6.10 Mohr-Coulomb and Hoek-Brown failure criterion curves

2. For plastic materials, the strength parameters will only be activated in the analysis if yielding occurs (Rockscience, 2002). If the stress does not go beyond the yield envelope, no yielding and plastic deformation occurs, and the material behaves like a linearly elastic medium. The roof of the cavern behaves like an arch, which is getting more and more convex when increased horizontal forces are applied. This trend will continue until yielding occurs, and subsequently, the Hoek-Brown model will result in large deformations.

Further, the results show that the analyses are sensitive to the dilation parameter, which is a measure of the increase in volume of the material when sheared. As a rule the dilation parameter should lie between zero and m_b. However, a value equivalent to 50% of m_b or higher gives the following message for the last excavation stage: Convergence may not have been established or the problem is unstable. This seems abnormal since all other Hoek-Brown analyses show that the plasticity for the last stage is very limited. Lu (2002) has experienced the similar problem.

6.4.3 Comparison of Analysis Results and Field Measurements

An extensive displacement measurement programme was accomplished in connection with the Gjøvik Olympic Mountain Hall. A total of 10 different multiple position borehole extensometers were installed by SINTEF and NGI, and the total cavern crown subsidence was measured to approximately 8.55 mm.

As illustrated above, the analysis results are sensitive to the horizontal in-situ stress conditions. All linearly elastic Mohr-Coulomb analysis results show cavern crown subsidence less than 8.5 mm. However, the situation is different for the non-linear Mohr-Coulomb analyses. If the stress ratio exceeds 1.8, the cavern crown subsidence is larger than the measured value, otherwise it is less. In-situ stress measurements showed virgin horizontal stresses of magnitude 3.5 - 4.5 MPa in the cavern area (Hansen and Kristiansen 1994), and the vertical stress has a magnitude of 1.2 - 1.8 MPa. Different combinations of these values give stress ratio in the range of 1.9 - 3.75. Thus, the calculated cavern crown subsidence is larger than the measured one for the original Mohr-Coulomb analyses. However, for the analyses with increased strength parameters the calculated cavern crown subsidence agrees with the measured one for a stress ratio of about 2.1.

Further, the analysis results show that the main part of the deformations were obtained during the excavation of the top slice. This agrees with the field observations. The rock bolt models also show good agreement with the real situation at Gjøvik Olympic Mountain Hall, where only three of six operating instrumented roof bolts show load build-up for at least one measuring point along the length of the bolt. Load build-up occurs in the lower part of the rock bolts or close to the rock surface, and the most stressed bolt shows a load of 124 kN, which is 56% of the yielding load (Stjern, 1995).

None of the Hoek-Brown analysis results show larger cavern crown subsidence than the measured value of 8.5 mm. The results is almost identically with the linearly elastic Mohr-Coulomb analysis results, and support a rule of thumb, which says that high horizontal in-situ stress is favourable and in many cases necessary for the cavern global stability.

6.5 Strengths and Limitations of Continuous Modelling with Phase^2

Phase^2 is a user friendly program, that allows both linearly elastic and non-linear analyses. The rock mass is defined by elastic properties and strength parameters, which are dependent on the selected failure criterion. Sequential excavation, multiple materials, support and constant or gravity stress field are available. Point and click geometry input and editing contribute to make the process of setting up a model of the particular problem to be analysed quite simple. Irregularly shaped boundaries may be approximated by the use of either straight elements or elements with curved boundaries, and the size of the elements can be varied. This allows the element grid to be expanded or refined as needed. Further, mixed boundary conditions, for example discontinuous surface loadings, can be handled easily.

Compared to DDA, the computation speed for Phase^2 is very fast and therefore less expensive. The post-processing program, Interpret, gives the user possibility to present analysis results in form of a contour plot directly on the model, including for example stresses, yielded elements, strains or displacements. In addition, data can also be displayed on the model or graphed for user-defined lines, bolts, liners or joints.

6.6 Summary

In continuous modelling, the rock mass is treated like a continuous medium where only a limited number of joints may be included. Phase^2 is picked out as a representative tool. Gjøvik Olympic Mountain Hall is also here used as a case study. More than 50 different analyses have been carried out, using both Mohr-Coulomb and Hoek-Brown failure criteria.

For Mohr-Coulomb, both linearly elastic and non-linear analyses have been carried out. The linearly elastic analysis results show that higher horizontal in-situ stress produces lower cavern crown subsidence. This agrees with a rule of thumb, which says that high horizontal in-situ stress is necessary to obtain sufficient constraint and global stability of a large span cavern. However, for the non-linear analyses higher horizontal in-situ stress results in higher cavern crown subsidence and deformations. This may be explained by rock mass yielding, which is caused by differential principal stresses. If the friction angle is increased, the cavern crown subsidence is reduced (Figure 6.8).

The influence of rock bolts have been studied for a couple of cases. The rock bolts are taken into account in each excavation step, and the results show that the effect of rock bolts is stronger for high in-situ horizontal stress cases, than for low in-situ

stress cases. Not all bolts show loads, and if loads occur, these are in the parts of the bolts close to the excavation surface.

According to the estimated input parameter values, the probability for failure, when the stress anisotropy increases, is larger for the Mohr-Coulomb material than for the Hoek-Brown material. Only non-linear Hoek-Brown analyses have been carried out, and the results show very limited yielding and plastic deformations. The rock mass behaves like a linearly elastic material and higher horizontal in-situ stress produces lower cavern crown subsidence. For some parameter combinations convergence problems occur, even if only slight plastification occurs around the cavern and the utilized dilation parameter value lies within the recommended range. This is abnormal. Lu (2002) has experienced the similar problem.

In comparison with the field measurements, the magnitude of calculated cavern crown subsidence within the stress area of current interest is too high for the Mohr-Coulomb analyses, except for one of the cases with increased strength parameters, and too low for the Hoek-Brown analyses. The rock bolt models in Mohr-Coulomb show good agreement with field measurements and observations.

The biggest challenge for continuous modelling is to select a constitutive law that describes the particular problem in the best way. Different constitutive laws require different strength parameters and may result in different analysis results. For Mohr-Coulomb tensile strength, friction angle and cohesion are required, while Hoek-Brown requires compressive strength and the parameters m and s, that may be calculated from formulas including GSI, and the Hoek-Brown parameter m_i.

It is not easy to get reliable strength parameter values. Some of them may be estimated in the laboratory, but these data are obtained from small specimens representing the intact rock, and additional estimations based on rule of thumbs are therefore necessary. Other may be estimated from rock mass classification systems that are based on several parameters. GSI may be calculated from existing RMR and Q values, but this is only recommended if no GSI value is defined directly from field observations. Thus, the existence of uncertainty and subjectivity may influence on the analysis results.

Generally, continuous modelling is far less time consuming than discontinuous modelling. In Phase^2, input and editing for simple problems are based on a point and click method, and within short time the user will be able to run an analysis. Interpret, the post-processing program, gives the user good possibility to present analysis results in form of a contour plot of for example stresses or deformations directly on the model. Further, data can be displayed on the model or graphed for

user-defined lines, bolts, liners or joints. However, critical evaluation of the results, preferably in combination with field observations and measurements, is absolutely recommended. As for discontinuous modelling, the reliability of the results from continuos modelling are greatly dependent on the input parameters.

URN:NBN:no-3362

CHAPTER 7

Conclusions and Practical Guidelines for Numerical Modelling

7.1 Conclusions

The practical use of continuous and discontinuous modelling is studied for underground hard rock problems. The Gjøvik Olympic Mountain Hall, which was built in connection with the XVII Winter Olympic Games 1994 at Lillehammer, is used as a case study. Phase^2 and the Discontinuous Deformation Analysis (DDA) are used as representative tools for continuous and discontinuous modelling, respectively, and the following conclusions are drawn:

7.1.1 Continuous modelling

- In continuous modelling, the rock mass is treated as a continuous medium and only a very limited number of joints may be included.

- Crucial input are strength and deformability parameters of the rock mass. Required strength parameters are dependent on the selected failure criterion. Usually either Mohr-Coulomb or Hoek-Brown is utilized. In Mohr-Coulomb, the rock mass strength is defined by the cohesive strength, c and the friction angle, ϕ, which can be found from laboratory triaxial tests or direct shear tests. Required Hoek-Brown parameters are the compressive strength of intact rock, and the constants m_b and s. The compressive strength of intact rock may be

determined in the laboratory, while the constants may be estimated from the geological strength index (GSI) or through rock mass classification systems as Q and RMR. Estimating strength properties in the laboratory is relatively straight forward, but a problem is that these values are obtained from small specimens of intact rock. Scale effects and sample representativity must therefore be taken into consideration.

- It is difficult to select a failure criterion which describes the particular problem to be analysed in the best way. Mohr-Coulomb and Hoek-Brown may give different analysis results.

- Good knowledge about the in-situ stresses is necessary to obtain reliable analysis results since the magnitude of especially horizontal in-situ stresses may have crucial influence on the general stability.

- Continuous modelling can give detailed information about the stress and deformation distributions.

- Compared to discontinuous modelling, the computation time is very fast.

7.1.2 Discontinuous modelling

- In discontinuous modelling, the rock mass is modelled as a system of individual rock blocks interacting along their boundaries, and it is therefore possible to predict potential rock falls or to study details of the local instability

- Essential input are joint patterns and strength parameters of the rock joints. It is very difficult to get hold of correct joint patterns from the geological field mapping process because of restricted access to exposured rock faces. Geological mapping techniques that remove subjectivity, for example scanline/area mapping or semi-automatic mapping, are recommended. Today's situation is that no mapping techniques are good enough to give satisfactory information about required input for discontinuous modelling.

- The magnitude of in-situ stresses, particularly the horizontal stresses, is also crucial input for discontinuous modelling.

- The biggest challenge for discontinuous modelling is connected to the implementation of measured discontinuities into a numerical model. The existing preprocessors for generating rock block systems have problems with producing a realistic pictures of the complex rock mass, which is intersected by smaller and bigger discontinuities caused by a variety of geological mechanisms. This is not only a problem for DDA. The universal distinct element code (UDEC) has the same drawback. A couple of unrealistic models utilized for both UDEC and DDA modelling from different parts of the world are presented in Chapter 5.

- Where to locate the planned tunnel or cavern in proportion to the selected joint geometry, is another difficulty of discontinuous modelling. Moving the tunnel or cavern a few meters to the left, right, up or down, may give different analysis results because of different joint orientation and number of rock blocks, which intersect the excavation boundary.

- Discontinuous modelling is fairly time consuming and requires a fast and high capacity computer. The computation time increases with the number of rock blocks, and if the size and shape of the rock blocks are very different, computational problems may arise. As an example, the computation time for a model consisting of about 1500 rock blocks (model 5 in Chapter 5), is two days for 2500 time steps on a portable computer, Pentium III with 600 MHz and 128 MB RAM.

7.1.3 Final Conclusions

- Analysis results from both continuous and discontinuous modelling show that the large span cavern is stable. However, based on the experience from this study, continuous modelling is currently most suitable and therefore recommended for analyses of underground hard rock problems. The main reasons for this statement are the large difficulties connected to the establishment of a reliable numerical model of the jointed rock mass, and that the discontinuous modelling process is very time consuming. Further development of the existing mapping techniques and the procedures for implementation of measured discontinuities are necessary before discontinuous modelling may be used as a realistic practical tool for underground rock mechanics problems.

- The magnitude of in-situ stresses, particularly the horizontal stresses, may have considerable influence on the general stability, and independent of whether con-

tinuous or discontinuous modelling is selected, in-situ stress measurements are recommended in order to estimate a reasonably correct stress level for the particular problem.

- Critical evaluation of all modelling results is strongly recommended. Because of elements of uncertainty connected to the definition of required input parameters, the results should be considered as valuable additional input to field observations, in-situ measurements and experience rather than a precise answer for a given problem. The quality of the predictions will never be better than the input parameters.

- The practical use of numerical modelling within the field of rock mechanics has shown a tremendous growth over the past decades. Constant development of new theories and softwares together with modifications and improvements of existing tools, provide for better and better suitability and user-friendliness. It is however still a long way to go before numerical modelling, particularly discontinuous modelling, may be characterized as a reliable design tool.

7.2 Practical Guidelines for Numerical Modelling

Practical guidelines for the numerical modelling process may be summarized in the following point:

1. Definition of analysis type, material type and parameters and in-situ stresses

   Generally, the decision of either to use continuous or discontinuous modelling should be based on data from the geological field mapping process. If the rock mass is basically free of discontinuities, or if the discontinuities are very closely located in comparison to the dimensions of the problem to be analysed, continuous modelling is preferable. If large deformations including slip, rotation and separation are dominating, as for rock slope stability problems, discontinuous modelling should be selected.

   The problem of selecting correct modelling method is connected to cases laying between the extremities mentioned above. Whether continuous or discontinuous modelling should be selected for a particular problem is primarily dependent on the quality and the amount of required input data. The purpose of the modelling and available economical resources may also have vital importance in some cases.

The quality and amount of required input data have strict relation to the geological field mapping. Due to restricted access to exposured rock faces, the measuring locations may be randomly distributed, and for underground projects often a distance away from the localization of a planned tunnel or cavern. The mapping results are also dependent on the complexity of the rock mass, and the amount of measured data is often limited compared to the dimensions of the problem to be analyzed. Thus, approximations are necessary for the establishment of any numerical model.

In cases where the measured discontinuities show signs of being arbitrary oriented, i.e. no joint patterns are dominating, continuous modelling is strongly recommended since discontinuous modelling will require too many approximations and large uncertainties connected to i) The field mapping process, ii) The implementation of measured discontinuities into a numerical model and ii) The localization of the planned construction in proportions to the joint pattern.

On the other hand, if the discontinuities are easily mapped, e.g. a system dominated by bedding planes without no later tectonic impact, or if the purpose of the modelling is to predict potential rock falls or to study details of i.e. local instability or water flow on joints, discontinuous modelling is recommended.

Occasionally, the user will probably experience situations where both continuous and discontinuous modelling can be used, and in such cases the economy of the project may be vital since discontinuous modelling usually is more time consuming than continuous modelling.

It is important to notify that those cases that are most difficult to map very often coincide with the cases where the models most clearly demonstrate their limitations.

Major input for continuous modelling are strength and deformability parameters of the rock mass, and required strength parameters are dependent on the selected failure criterion. If Mohr-Coulomb is applied, the strength of the rock mass is defined by the cohesive strength, c, and the friction angle, ϕ. These parameters can be found from laboratory tests or direct shear tests. Required Hoek-Brown parameters are the compressive strength of intact rock, and the constants m_b and s, which can be determined from laboratory tests and the geological strength index (GSI), respectively. If no GSI is estimated directly in the field, the rock mass classification systems Q and RMR, may be used in order to determine GSI. Estimating strength properties in the laboratory is relatively simple, but a problem is that these values are obtained from small specimens of intact rock.

Thus, scale effects and sample representativity must be taken into consideration.

Major input for discontinuous modelling are joint patterns and strength parameters of the rock joints. It is very difficult to get hold of correct joint patterns from the geological mapping process because of restricted access to the rock faces. And in order to remove subjectivity e.g. scanline/area mapping or semi-automatic mapping are recommended. The existing pre-processors for the implementation of measured discontinuities into a numerical model are not good enough unless the problem to be analysed has very simple geometry. For more complex problems alternative methods are to directly input the measured discontinuities, which is very time consuming, or to make use of other computer programs as e.g. Autocad or Micro Station to draw the discontinuities and the planned tunnel and cavern. The last mentioned method assumes that a system which automatically reads all coordinates and prepares the data for calculation is established.

In-situ rock stress measurements should be carried out with 3D overcoring or hydraulic fracturing techniques.

2. Pre-processing

The main purpose of the pre-processing is to establish a reliable numerical model of the rock mass, which is ready for calculation. In addition to the parameters listed in the previous paragraph, other specifications to be defined are boundary conditions, location of the problem in proportion to terrain, number of time steps (only for discontinuous modelling), element mesh and refinement (only for continuous modelling), rock support and stage excavation.

3. Model verification and calibration

It is strongly recommended that numerical modelling is used in combination with field observations, in-situ or laboratory measurements and experience. As a concrete example, weathering may be taken into account in the modelling by using varying E-modulus, if different degrees of weathering are observed in the field.

Dependent on when modelling is carried out, before, during or after the construction, the utilization of numerical modelling as a practical tool may be a bit different. Analyses before and after the construction, are often mentioned as

pre- and back- analysis, respectively.

For a pre-analysis, the amount and quality of required input is often limited compared to a backward analysis. A so-called parametric study is therefore useful and necessary in order to establish a reliable numerical model. A good rule is to start with setting up a simple model of the problem to be analysed, and then try to make use of reliable input parameter values within a rational interval. By changing different input parameters, one by one, the analysis results may give indications of critical input parameters, and act as basis for a further choice of investigation methods.

Back-analysis is used in order to obtain more reliable input, and for model verification. A typical situation is a tunnel or cavern, where deformations in the roof are measured by extensometers. The elastic properties and strength parameters in the numerical model may then be changed, in such a way that the calculated deformations fit in with the measured values.

If numerical modelling is carried out during the construction, the modelling process should typically start with setting up a numerical model, based on parametric studies and with parameter values within a rational range. Then the input parameters should be changed and updated, as a consequence of new and useful information during the construction process.

Independent of whether a so-called pre- or back- analysis, or analysis during the construction process are carried out, preliminary analyses and parametric studies are absolutely necessary stages, before a calibrated model may be established, verified and utilized for final analyses. A good rule of thumb, is to update the numerical model according to new knowledge about the rock mass properties, excavation process, etc.

4. Computation

The computation process is automatic. Computation problems may be caused by either code or user errors. Examples of user errors are for example mistakes in using the code and selection of inaccurate or wrong input data. In discontinuous modelling, computation problems may arise if the size of the rock blocks are very different at the same time as the number of rock blocks is large.

5. Post-processing

The amount of data from a numerical computation is usually very large, and so-called post-processors are therefore made use of in order to sort out important information for the user.

6. Analysis results and reporting

Elements of uncertainties will always be connected to the numerical modelling process, so critical evaluation of all modelling results is strongly recommended. As mentioned in section 7.1.3, the analysis results should be considered as valuable additional input to field observations, in-situ measurements and experience rather than a precise answer for a given problem. The quality of the results will never be better than the input parameters.

A final report of the numerical modelling process should present the analysis results in a clear way, and substantiate possible difficulties connected to the different parts of the process if they may have influence on the analysis results.

URN:NBN:no-3362

References

Anderson, T.L (1995): "Fracture Mechanics. Fundamentals and Applications" ISBN 0-8493-4260-0, CRC Press 1995

Balden, V., Scheele, F. and Nurick, G. (2001): "Discontinuous Deformation Analysis in Ball Milling" Proceedings Fourth International Conference on Discontinuous Deformation Analysis, Glasgow, Scotland, UK, pp. 337-348

Barton, N., By., T.L., Chryssanthakis, P., Tunbridge, L., Kristiansen, J., Løset, F. Bhasin, R., Westerdahl, H. and Vik, G. (1994): "Comparison of prediction and performance for a 62 m span sports hall in jointed gneiss" Rock Cavern Stadium, Subtask 2 Rock Engineering and Engineering Geology, Publications, Publication 18

Barton. N. and Bandis, S. (1990): "Review of predictive capabilities of JRC-JCS model in engineering practice" Rock Joints, Barton & Stephanson (eds) © Balkema, Rotterdam, ISBN 90 6191 109 5, pp. 603-610

Beer, G., Opriessnig, G., Golser, H., Fasching, A., and Gaich, A. (1999): "Geotechnical data acquisition, numerical simulation and visualization on site" Proceedings, 9th International Congress on Rock mechanics, Paris, France, ISBN 90 5809 071 X, pp.1333-1338

Beer, G. and Watson, J.O. (1992): "Introduction to Finite and Boundary Element Methods for Engineers", John Wiley & Sons, ISBN 0 471 92813 5

Bhasin, R. (1994): "Technical Note. Rock Mass Characterization for Large caverns in India and Norway Using a New Method of Recording and Presenting Engineering Geological Data" Int. J. Rock Mech. Min. Sci. & Geomech. Abstr. Vol. 31, No1, Elsevier Science Ltd., pp. 87-91

Bhasin, R. and Høeg, K. (1998): "Parametric Study for a Large Cavern in Jointed Rock Using a Distinct Element Model (UDEC-BB)" Int. J. Rock Mech. Min, Sci. Vol. 35, No. 1, Elsevier Science Ltd, pp. 17-29

Bollingmo, P. (1994): "Rock Engineering Programme", Rock Cavern Stadium, Subtask 2 Rock Engineering and Engineering geology, Final Report, pp. 9-10

Brown, E.T. (1987): "Analytical and Computational Methods in Engineering Rock Mechanics" Allen & Unwin, London

Chen, S., Chern, J.C. and Koo, C.Y (1995): "Study on the Performance of Tunnel near Slope by DDA" Proceedings First International Conference on Discontinuous Deformation Analysis, Taiwan, R.O.C, pp.109-123

Chryssanthakis, P., Barton, N., Løset, F. Lorig, L. and Christianson, M. (1997): "Numerical modelling of fibre-reinforced shotcrete in a tunnel by using the discrete element method" Bergmekanikkdagen 1997, Oslo, Norway, ISBN 82-91341-19-2, pp. 26.1-26.12

Chryssanthakis, P. (1994): "Numerical Modelling Using a Discontinum Approach" Rock Cavern Stadium, Subtask 2 Rock Engineering and Engineering geology, Final Report, pp. 67-74

Chryssanthakis, P. and Barton, N. (1994): "Predicting Performance of the 62 m Span Ice Hockey Cavern in Gjøvik" Rock Cavern Stadium, Subtask 2 Rock Engineering and Engineering Geology, Publications, Publication 13

Elvebakk, H. and Rønning, J.S. (2001): "Borhole Inspection. Testing and Comparison of Optical and Acoustical Televiewer" (in Norwegian) NGU Report 2001.001

Feng, Q (2001): "Novel methods for 3-D semi-automatic mapping of fracture geometry at exposured rock faces" Doctoral Thesis, Division of Engineering geology, Department of Civil and Environmental Engineering, Royal Institute of Technology. pp-1-65

Franklin, J.A. and Dusseault, M.B. (1989): "Rock Engineering" McGraw-Hill Publishing Company, ISBN 0-07-021888-9, pp. 205-233

Grimstad, E. (2002): Personal communication and a digital copy of NGI's Geological Logging Chart

Hansen, S.E. and Kristiansen, J. (1994): "In Situ Stress Measurements" Rock Cavern Stadium, Subtask 2 Rock Engineering and Engineering geology, Final Report, pp. 23-31

Hansen, S.E. and Kristiansen, J. (1994): "Displacement Measurements" Rock Cavern Stadium, Subtask 2 Rock Engineering and Engineering geology, Final Report, pp. 95-100

Hoek, E. (2002): "A brief history of the development of the Hoek-Brown failure criterion", downloaded from http://www.rocscience.com

Hoek, E., Carranza-Torres, C. and Corkum, B. (2002): "Hoek-Brown failure criterion - 2002 edition", downloaded from http://www.rocscience.com

Hoek, E. (2000): "Practical Rock Engineering", Chapter 11 Rock mass properties, downloaded from http://www.rockscience.com, Hoek's Corner

Hudson, J.A. and Harrison, J.P. (1997): "Engineering Rock Mechanics, An Introduction to the Principles" Pergamon, ISBN 0 08 043864 4

Hudson, J.A. and Priest, S.D. (1979): "Discontinuities and Rock Mass Geometry" Int. J. Rock Mech. Min. Sci. & Geomech. Abstr. Vol. 16, Pergamon Press Ltd 1979, pp. 339 - 362

ICS (2001): Julius Kruttschnitt Mineral Research Centre (JKMRC)/Itasca/ International Caving Study, Chapter 2 - Rock Mass Classification.

ISRM (1978): "Suggested Methods for the Quantitative Description of Discontinuities in Rock Masses" Int. J. Rock Mech. Min. Sci. & Geomech. Abstr. Vol. 15, Pergamon Press Ltd 1978, pp. 319-360

Jang, H.I. and Lee, C.I. (2002): "Development of a three-dimensional discontinuous deformation analysis technique and its application to toppling failure" Proceedings Fifth International Conference on Analysis of Discontinuous Deformation, Wuhan, China, © Swets & Zeitlinger B.V., Lisse, The Netherlands, ISBN 90 5809 519 3, pp. 225-237

Lin, J.S. and Al-Zahrani, R.M. (2001): "A coupled DDA and Boundary Element Analysis" Proceedings Fourth International Conference on Analysis of Discontinuous Deformation, Glasgow, UK, pp. 379-388

Lu, M. (2002): Personal communication

Lu, M. (1994): "Finite Element Modelling" Rock Cavern Stadium, Subtask 2 Rock Engineering and Engineering geology, Final Report, pp. 61-66

Lu, M., Kjørholt, H. and Ruistuen, H. (1994): "Numerical study of Gjøvik ice-hockey cavern" Computer Methods in Advances in Geomechanics, Siriwardane & Zaman (eds), © Balkema, Rotterdam, ISBN 90 5410 380 9, pp. 2609-2614

Lu, M., Kjørholt, H. and Ruistuen, H. (1992): "Numerical Analysis of the Gjøvik Ice Hockey Cavern" Sintef Report STF36 F92059, Sintef Rock and Mineral Engineering

Løset, F., Backer, L., Kveldsvik, V. and Chryssanthakis, P. (1995): "Practical use of computer based numerical modelling in rock constructions in Norway" (in Norwegian), Bergmekanikkdagen 1995, Oslo, Norway, ISBN 82-91341-06-0, pp. 31.1-31.8

Ma, Y.M. (1999): "Development of discontinuous deformation analysis the first ten years (1986-1996)" Proceedings Third International Conference on Analysis of Discontinuous Deformation, Vail, Colorado, USA, pp. 17-32

Ma, Y.M., Zaman, M. and Zhu, J.H. (1996): "Discontinuous deformation using the third order displacement function" Proceedings First International Forum On Discontinuous Deformation Analysis, June 12-14, 1996, Berkeley, California, USA, pp. 383-394

Mathis, J.I. (1987): "Discontinuity mapping - A comparison between line and area mapping" Proceedings 6th ISRM International Congress on Rock Mechanics, Montreal 1987, Canada, Volume 2, pp. 1111-1114

Morseth, B. and Løset, F. (1994): "Pre investigations - Decision base - Excavation", Rock Cavern Stadium, Subtask 2 Rock Engineering and Engineering geology, Final Report, pp. 11-22

Ottosen, N. & Petterson, H. (1992): "Introduction to the Finite Element Method", Prentice Hall Europe, ISBN 0-13-473877-2

Pahl, P.J. (1981): "Estimating the mean length of discontinuity traces" Int. J. Rock Mech. Min. Sci. & Geomech. Abstr. Vol. 18, Pergamon Press Ltd 1981, pp. 221-228

Palmstrøm, A. and Nilsen, B. (2000): "Handbook No 2, Engineering Geology and Rock Engineering", Norwegian Group for Rock Mechanics (NBG), ISBN 82-91341-33-8

Pande, G.N., Beer, G. and Williams, J.R. (1990): "Numerical Methods in Rock Mechanics" © John Wiley & Sons Ltd., ISBN 0471 92021 5

Priest, S.D. (1993): "Discontinuity Analysis for Rock Engineering" © Chapman & Hall, London, ISBN 0 412 47600 2

Priest, S.D. (1981): "Estimation of Discotninuities Spacing and Trace Length Using Scanline Surveys" Int. J. Rock Mech. Min. Sci. & Geomech. Abstr. Vol. 18, Pergamon Press Ltd 1981, pp. 183-197

Rocscience Inc. (1998-2001): "Phase^2 2D finite element program for calculating stresses and estimating support around underground excavations, User's Guide" Rocscience, Geomechanics Software & Research, Toronto, Canada pp. 173

Rønning, J.S. (2002): "New methods of investigation" (in Norwegian), NIF Kursdager 2002, NTNU, Trondheim

Sasaki, T., Ishii, D., Ohnishi, Y. and Yoshinaka, R. (1995): "Stability analysis of jointed rock foundations by discontinuous deformation analysis" Rock Foundation, Yoshinaka & Kikuchi © Balkema, Rotterdam, ISBN 90 5410 563 3, pp. 337-342

Savely, J.P. (1972): "Orientation and Engineering Properties of Jointing in the Sierrita Pit, Arizona" MS Thesis, University of Arizona, Tucson, USA

Scheldt, T., Lu, M. and Myrvang, A. (2002): "Numerical Analysis of Gjøvik Olympic Cavern: A Comparison of Continuous and Discontinuous Results by using Phase^2 and DDA" Fifth International Conference on Analysis of Discontinuous Deformation Analysis, Wuhan, China, © Swets & Zeitlinger B.V., Lisse, The Netherlands, ISBN 90 5809 519 3, pp. 125-131

Scheldt, T (1998): "Input parameters for numerical modelling in rock mechanics" (in Norwegian), Diploma Thesis, Department of Geology and Mineral Resources Engineering, Norwegian University of Science and Technology

Shi, G.H. (2002): Personal Communication, Fifth International Conference on Analysis of Discontinuous Deformation Analysis, Wuhan, China

Shi, G.H. (1996): "Discontinuous Deformation Analysis" Technical Note, First International Forum On Discontinuous Deformation Analysis, June 12-14, 1996, Berkeley, California, USA

Shi, G.H. (1996): "Discontinuous Deformation Analysis Programs, Version 96, Users Manual", revised by Yeung, M.R.

Shi, G.H. (1989): "Block System Modeling by Discontinuous Deformation Analysis", Department of Civil Engineering, University of California, Berkeley, pp. 205

Shi, G.H. and Goodman, R.E. (1988): "Discontinuous deformation analysis - A new method for computing stress, strain and sliding of block systems" Key Questions in Rock Mechanics, Cundall et al. (eds) © Balkema, Rotterdam, pp. 381 - 393

Shyu, K., Chang, C.T. and Salami, M.R. (1997): "Tunnel Engineering Applications Using Discontinuous Deformation Analysis with Finite Element Mesh" Proceedings Second International Conference on Analysis of Discontinuous Deformation Analysis, Kyoto, Japan, pp. 218-237

Singh, B. and Goel, R.K. (1999): "Rock Mass Classification - A Practical Approach in Civil Engineering" © Elsevier, ISBN 0 08 043013 9, pp. 1-4, 17-22, 34-44, 93-94, 242-247

Stjern, G. (1995): "Practical Performance of Rock Bolts" Doctoral Thesis, Department of Geology and Mineral Resources Engineering, Norwegian Institute of Technology, pp. 97-111

Stjern, G. (1994): "Rock Support Instrumentation", Rock Cavern Stadium, Subtask 2 Rock Engineering and Engineering geology, Final Report, pp. 75 - 81

Thidemann, A. and Dahlø, T.S. (1994): "Engineering Geological Investigations" Rock Cavern Stadium, Subtask 2 Rock Engineering and Engineering geology, Final Report, pp. 33-52

Villaescusa, C. (1991): "A three dimensional model of rock jointing" Doctoral Thesis, Julius Kruttschnitt Mineral Research Centre, Department of Mining and Metallurgical Engineering, University of Queensland, pp. 14-37

Wang, C.P., Sheng, J., Wang, C.Y., Lee, C.L. (1997): "Selection of contact spring stiffness values in the numerical analysis for the system rigid disks" Proceedings Second International Conference on Analysis of Discontinuous Deformation, Kyoto, Japan, pp. 451-458

Westerdahl, H., Kong, F., and Kristiansen, J. (1994): "Geophysical Investigations" Rock Cavern Stadium, Subtask 2 Rock Engineering and Engineering geology, Final Report, pp. 53-60

Wu, A., Ding, X., Sheng, Q. and Fu, J. (2002): "DDA Numerical Modelling for Shui Buya Project in China", distributed on the Fifth International Conference on Analysis of Discontinuous Deformation, Wuhan, China

www.diana.nl (2002): "Welcome to DIANA Analysis BV"

www.itascacg.com (2002): www.itascacg.com/udec.html

www.rockscience.com(2002): www.rockscience.com/roc/software/Phase2.htm

Yeung, M.R., Sun, N. and Jiang, Q.H. (2002): "A study of wedge stability using physical models, block theory and three-dimensional discontinuous deformation analysis" Proceedings Fifth International Conference on Analysis of Discontinuous Deformation, Wuhan, China, © Swets & Zeitlinger B.V., Lisse, The Netherlands, ISBN 90 5809 519 3, pp. 171-180

URN:NBN:no-3362

Appendix A

TABLE 1. Phase^2 analyses, c=constant, v=varying, r=reference value, h=high, l=low

File-name	Linearly elastic	Non-linear	Stress ratio	Strength parameters	Rock bolts
MC1	x	x	c	r + h	x
MC2	x	x	c	r	
MC3	x	x	c	r	
MC4	x	x	c	r	
MC5	x	x	c	r	
MC6	x	x	c	r	x
MC7	x	x	c	r	
MC8	x	x	c	r + h	
MC9	x	x	v	r + h	
MC10	x	x	v	r + h	
MC11	x	x	v	r + h	
MC12	x	x	v	r + h	
MC13	x	x	v	r + h	
MC14	x	x	v	r + h	
HB1		x	v	r +h+l	
HB2		x	v	r+l	
HB3		x	v	r+l	
HB4		x	v	r+l	
HB5		x	v	r+l	
HB6		x	v	r+l	
HB7		x	v	r+l	

URN:NBN:no-3362